PKC GAMMA SENSES/PROTECTS FROM STRESS IN RETINA THROUGH REGULATION OF GAP JUNCTIONS

by

VLADIMIR YEVSEYENKOV

B.S., Kansas State University, 2002
O.D., NOVA Southeastern University, 2009

AN ABSTRACT OF A DISSERTATION

submitted in partial fulfillment of the requirements for the degree

DOCTOR OF PHILOSOPHY

Graduate Group Biochemistry

KANSAS STATE UNIVERSITY
Manhattan, Kansas

2010

Abstract

Exposure to oxidative stress leads to accumulation of reactive oxygen species and this stimulates protective cellular functions as a compensatory response to prevent the spread of apoptotic signal and prevent cell death. The purpose of this dissertation is to understand the importance of PKCγ activation and regulation of the retinal gap junction protein Cx50, and what role PKCγ plays in this neuro-protective effect.

Through electron microscopy we were able to show that PKCγ knockout mice retinas had incomplete cellular organization in the outer plexiform layer (OPL) of the retina, the layer of retina where Cx50 plays an important role in retinal cellular synapses. Electroretinograms confirmed that this structural disorganization also led to loss of functional response to light stimuli in PKCγ knockout mice retinas.

In vivo exposure to 100% hyperbaric oxygen (HBO) caused significant degradation of the retina in knockout mice compared to control mice. Thicknesses of the inner and nuclear and ganglion cell layers were increased, with complete disruption of OPL in PKCγ KO mice retinas. Damage to the outer segments of the photoreceptor layer and ganglion cell layer was significantly more apparent in the central retinas of HBO-treated knockout mice. Cx50 immunolabeling showed significant reduction to HBO treatment of PKCγ control mice retinas, HBO treatment failed to produce reduction of Cx50 immunolabeling in KO mice retinas.

In the R28 retinal cell line, PKCγ enzyme was shown to be activated by phorbol ester (TPA) and hydrogen peroxide. This resulted in translocation to the cellular membrane as confirmed by western blot and confocal microscopy. Suppression of PKCγ by siRNA rendered R28 cells more sensitive to oxidative stress-induced cell apoptosis, the process of apoptosis started earlier, and this resulted in cell death. R28 treatment with phorbol esters and hydrogen peroxide led to reduction in gap junction activity and Cx50 gap junction cell disassembly.

This dissertation shows that PKCγ plays an important role in structural organization of retina and has a neuro-protective effect in response to oxidative stress, in part because of its control of Cx50.

PKC GAMMA SENSES/PROTECTS FROM STRESS IN RETINA THROUGH REGULATION OF GAP JUNCTIONS

by

VLADIMIR YEVSEYENKOV

B.S., Kansas State University, 2002
O.D., NOVA Southeastern University, 2009

A DISSERTATION

submitted in partial fulfillment of the requirements for the degree

DOCTOR OF PHILOSOPHY

Graduate Group Biochemisty

KANSAS STATE UNIVERSITY
Manhattan, Kansas

2010

Approved by:

Major Professor
Dolores J. Takemoto
Department of Biochemistry

Copyright

Abstract

Exposure to oxidative stress leads to accumulation of reactive oxygen species and this stimulates protective cellular functions as a compensatory response to prevent the spread of apoptotic signal and prevent cell death. The purpose of this dissertation is to understand the importance of PKCγ activation and regulation of the retinal gap junction protein Cx50, and what role PKCγ plays in this neuro-protective effect.

Through electron microscopy we were able to show that PKCγ knockout mice retinas had incomplete cellular organization in the outer plexiform layer (OPL) of the retina, the layer of retina where Cx50 plays an important role in retinal cellular synapses. Electroretinograms confirmed that this structural disorganization also led to loss of functional response to light stimuli in PKCγ knockout mice retinas.

In vivo exposure to 100% hyperbaric oxygen (HBO) caused significant degradation of the retina in knockout mice compared to control mice. Thicknesses of the inner and nuclear and ganglion cell layers were increased, with complete disruption of OPL in PKCγ KO mice retinas. Damage to the outer segments of the photoreceptor layer and ganglion cell layer was significantly more apparent in the central retinas of HBO-treated knockout mice. Cx50 immunolabeling showed significant reduction to HBO treatment of PKCγ control mice retinas, HBO treatment failed to produce reduction of Cx50 immunolabeling in KO mice retinas.

In the R28 retinal cell line, PKCγ enzyme was shown to be activated by phorbol ester (TPA) and hydrogen peroxide. This resulted in translocation to the cellular membrane as confirmed by western blot and confocal microscopy. Suppression of PKCγ by siRNA rendered R28 cells more sensitive to oxidative stress-induced cell apoptosis, the process of apoptosis started earlier, and this resulted in cell death. R28 treatment with phorbol esters and hydrogen peroxide led to reduction in gap junction activity and Cx50 gap junction cell disassembly.

This dissertation shows that PKCγ plays an important role in structural organization of retina and has a neuro-protective effect in response to oxidative stress, in part because of its control of Cx50.

Table of Contents

List of Figures

List of Tables

Acknowledgements

I would like to extend my gratitude to my committee members, Dr. John Tomich, Dr. Larry Davis, Dr. Sherry Fleming and Dr. Bruce Schultz for agreeing to be on my committee and all the insightful input throughout this process.

I am grateful to Dr. Vladimir Akoyev, Dr. Michael Barnett, Dr. Thu Annelise Nguyen and Dr. Dingbo Lin, past post-doctoral fellows in Dr. Takemoto's lab, for all the guidance and help in helping me with my projects. It has been a wonderful experience working with Willard Lloyd and Dr. Harriet Davidson at the college of veterinary medicine; I am appreciative for all their help in helping me with electron microscopy and electroretinogram.

Huge regards to all of my fellow Takemoto lab mates, you made this experience not only educational but also exciting and entertaining.

But most importantly I would like to thank Dr. Dolores Takemoto, a person without whom I would still be a confused Russian kid with no purpose and no direction of what I wanted to do with my life. Dr. Takemoto introduced me to the field of eyes and through her passion for the field I fell in love with it. It was through Dr. Takemoto's counsel and guidance that I was able to make the most important decision of my life by deciding to pursue my love for the eyes through clinical approach by becoming an Optometrist. Dr. Takemoto is more than my major professor, she is a role model and a friend, but mostly importantly she is, and will be for the rest of my life my mentor.

Dedication

Dedicated to my two mothers, Galina Evseenkova and Carol Claassen

CHAPTER 1 - Introduction and Literature Review

1.1 Introduction

In my research, I explored the role of Protein Kinase C gamma (PKCγ) and one of its potential downstream targets gap junction protein connexin 50 (Cx50) as a stress sensor in the retina. Thus, to introduce this topic in Chapter 1, I have included a detailed literature review/summary of three major topics that are covered in this dissertation: 1st Structure and function of the eye with special focus on the retina; 2nd Structure and function of protein kinase C with special focus on PKCγ and 3rd Structure and function of Gap Junctions with special focus on Cx50.

Purpose of this literature review is to supplement the research data that is presented in this dissertation. Chapter 2 focuses on the structural aspects of the retina and the effect of lack of PKCγ on retinal structure. In Chapter 3 we show that how oxidative stress (mimicked by hyperbaric oxygen) effects retinal structure of normal wild type (WT) and PKCγ knockout mice. Chapter 4 explores the effect of oxidative damage in R28 retinal cell line. Thus in the literature review we discussed, in detail, the effect of stress on structure and function on each layer in the retina.

It is important to understand the structure and regulation mechanisms of the enzyme before theories can be made on the role that it plays in the cell signaling pathways. In the following literature review, PKCγ structure, assembly and methods of activation are discussed in detail. Role of PKCγ in downstream cell signaling on one of its potential targets, Cx50, is one of the topics of this dissertation. In chapter 3 and 4, role of PKCγ acting as a potential stress sensor enzyme through control of Cx50 is explored. Thus the structure and function of gap junctions with special emphasis on Cx50 has been discussed in detail in the following literature review to supplement this dissertation.

1.2 The Eye: Anatomy and Physiology

The eye is a very complex organ. In order for vision to occur, light rays have to reflect off of an object and then enter the eye through the transparent cornea and lens onto a retina. The point where the image is focused is the center of the visual pathway, which is called the macula or fovea. An image (light) is converted into electric signals which go on to the brain for perception of an actual object.

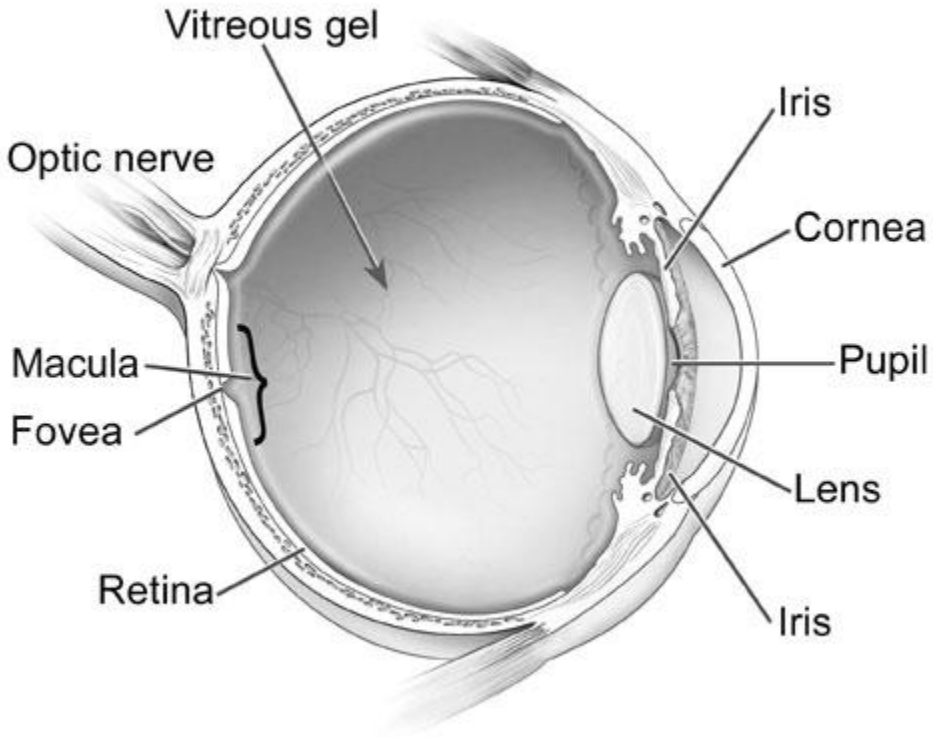

Figure 1-1 Structural Organization of the eye

Image courtesy of the National Eye Institute, National Institutes of Health

The eye ball consists of the three layers (Fig. 1): fibrous tunic, vascular tunic and retina. Cornea and sclera comprise the external layer called the fibrous tunic, and this layer is avascular. The vascular tunic is comprised of: choroid, which is responsible for delivering nutrient to the

retina; ciliary body, that makes aqueous humor which is responsible for keeping eye pressure and delivering nutrients to the lens and cornea; and, iris, that regulates the quantity of light that enters the eye and finally reaches the retina (in the dark, the iris is dilated and in bright conditions the iris is constricted). The innermost layer is the retinal layer, which consists of the retinal pigment epithelium (RPE) which is a non-visual portion, and a visual portion known as neural or sensory retina (Snell, 1998). Primary focus of this thesis is on the retina, as that is where the initial signal transduction pathway that is responsible for vision takes place. Below is the summary of retinal anatomy and physiology, with specific focus on how it is affected under oxidative stress and hypoxic conditions.

1.3 Retina Structure and Function

The retina makes up the innermost layer of the eye. It is an extension of the central nervous system with an intricate histological structure complete with an extensive embryologic origin. The retina extends anteriorly from the optic nerve to the ora serrata, from which it is continuous over the ciliary body with a layer of unpigmented epithelium. It then stretches over the posterior iris with a layer of pigmented epithelium. The external portion of the retina is occupied by photoreceptors (the rods and cones of the eye). Cementing mucopolysaccharide holds these receptors in place so as to produce undistorted retinal images. Externally the retinal pigment epithelium is in contact with the collagen and elastic tissue of Bruch's membrane of the choroids. Internally the retina is next to the vitreous body; the two structures are in intimate contact at the integral limiting membrane of the retina, especially around the ora serrata. Peripherally the neuro-retina ends at the ora serrata, but is continuous with the unpigmented layer of epithelium over the ciliary body. Posteriorly all retinal layers except the nerve fiber layer terminate at the optic disc, being separated from the disc tissues by a layer of glial tissue, the intermediary tissue of Kuhnt (Kolb, 1991).

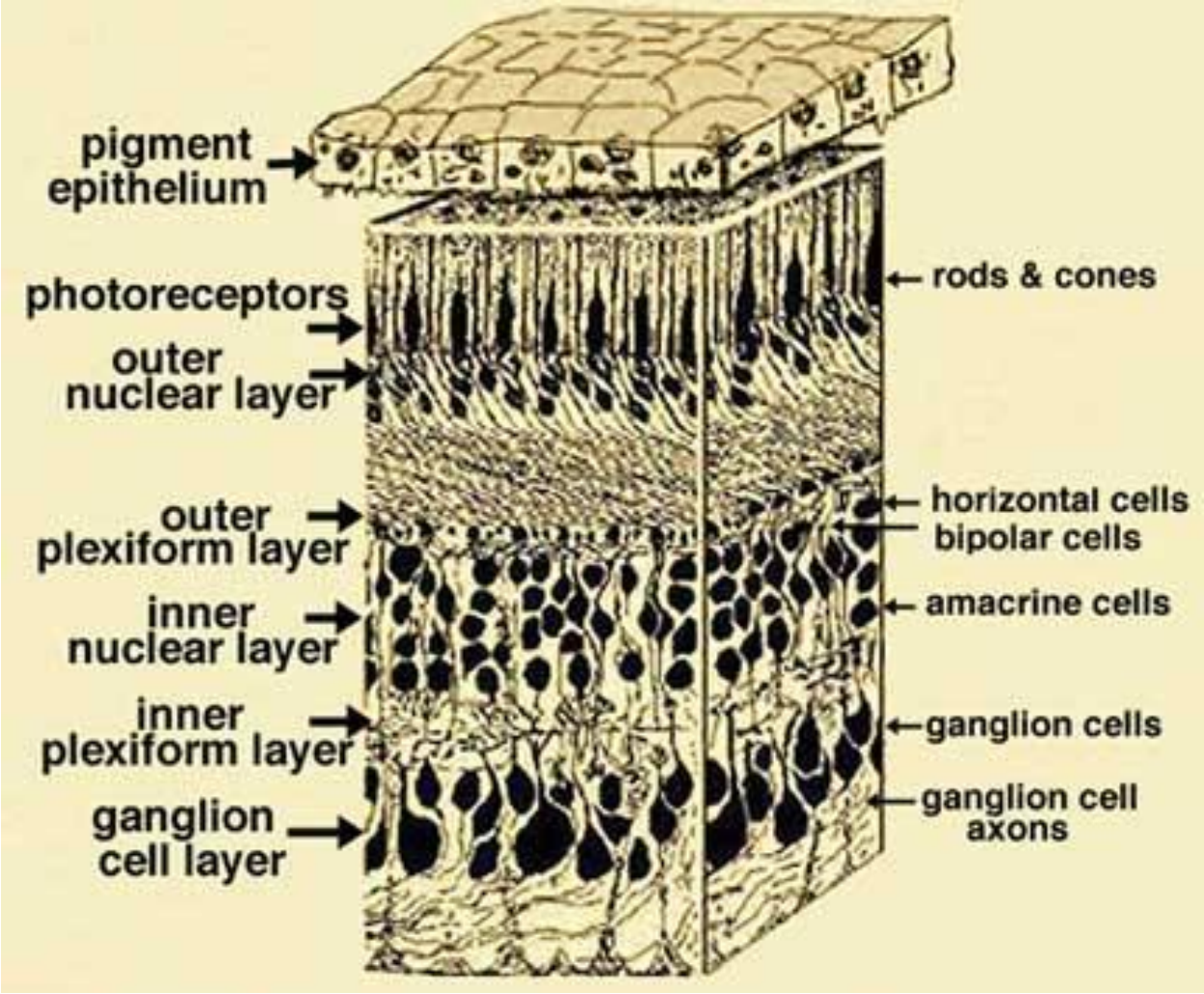

Figure 1-2 Structure of Retina

A. Cross Section of Retina and Retinal layers are shown B. Cells and their synapses of the retina are shown within the layers of the retina. From free public access Wiki Pictures http://ibbiology.pbworks.com/IB-Drawings

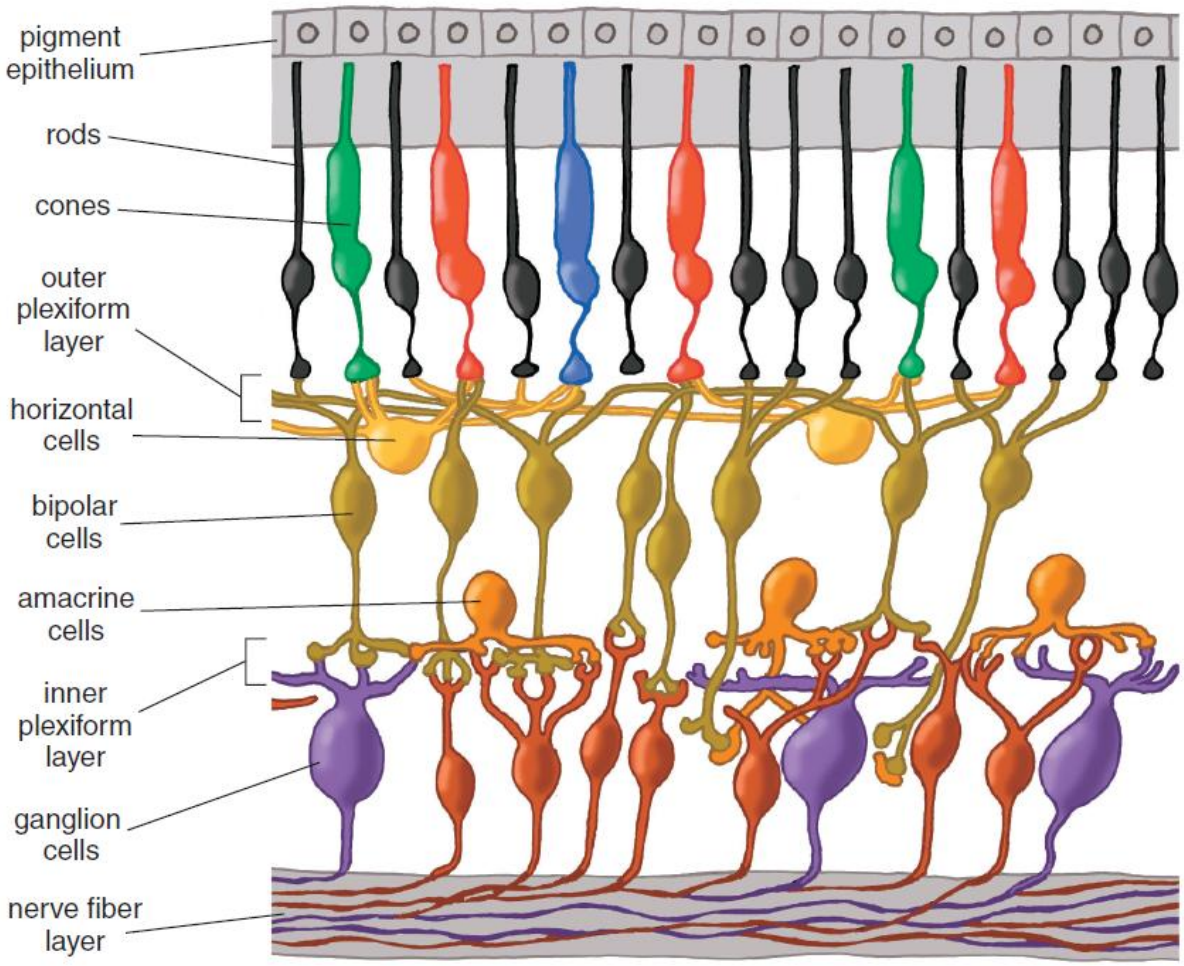

Figure 1-3 Cellular Synapses of the Retina

Figure showing cellular organization and synaptic connection among cells of the retina. Reproduced with permission. Helga Kolb. How the Retina Works. Much of the construction of an image takes place in the retina itself through the use of specialized neural circuits. American Scientist, Volume 91, pages 28-35. © 2003 Sigma Xi, The Scientific Research Society.

1.3.1 Ten Layers of Retina

The vertebrate retina consists of ten distinct layers (Fig. 1.2). The following is a description of each layer in the order that light hits the retina but opposite of how the neuronal signal goes. The most inner layer that separates vitreous and the retina, called the Inner Limiting Membrane (ILM), is formed by astrocytes, the same glial tissue as in brain and spinal cord and

Müller cells, which act as a light gatherer for rods and cones (Reichenbach, 1997). In a study, one day old rats were exposed to hypoxic shock which resulted in cell death and in swelling of Müller cells in the developing retina (Kaur et. al., 1999).

The Nerve Fiber Layer (NFL) is an extension of the Ganglion Cell Layer as it is formed by the axons of the ganglion cells nuclei (Fig 1.2). All the axons then come together in a funnel type fashion and that is what forms the optic nerve. NFL thickness analyses is essential for diagnosis and monitoring of many retinal disorders and it is becoming a standard of care in diagnosis of glaucoma as increased intraocular pressure reduces NFL thickness. This has become possible because technology has made tremendous leaps forward with the development of Optical Coherence Topography (OCT), which can measure NFL thickness in 5 seconds in an in vivo model, (Leung et.al, 2009). NFL thickness also plays a role in monitoring of retinitis pigmentosa (Walia et. al, 2007), and various vascular disorders. NFL thickness is also dependent on the level of hypoxia. As the amount of ocular oxygen perfusion is decreased, the NFL thickness is reduced. This model has been shown, in vivo with patients who suffer from obstructive sleep apnea (Kargi et. al, 2005).

Ganglion Cell Layer (GCL) consists of the cell bodies (nuclei) of the retinal ganglion cells, no neural connections occur in this layer, but it still has been previously shown that nuclei themselves are affected under conditions of stress or hypoxia (Dacey et. al., 1993). In a study of (Kalesnyakas, 2008) cerebral ischemia (was achieved by removal of arteries) in a rat model reduction in the amount of nuclei but not in their size was observed ((Kalesnyakas et. al., 2008).

Neural synapses take place in the plexiform layers of the retina. The inner plexiform layer (IPL) contains the axonal endings of the bipolar cells that pass on the information along through a synapse with the dendrites of the ganglion cells (Kolb and Linberg, 1992). Several types of amacrine cells also make synaptic connections with bipolar cells, e.g. AII amacrine cells link rods and cones, by forming a triad synapse (Kolb and Nelson, 1993). Amacrine cells also play an important role in A17 amacrine cell, making synapses with over 100 rod bipolar cells. Thus it takes part in convergence pathways. Fig. 1.4 show that 1 ganglion cell can receive information from up to 75,000 rods, thus increasing its sensitivity. From Fig. 1.3, it can be deduced that even if one ganglion cell is not functional and not able to synapse, it will still have a tremendous affect on light perception due to this convergence principle.

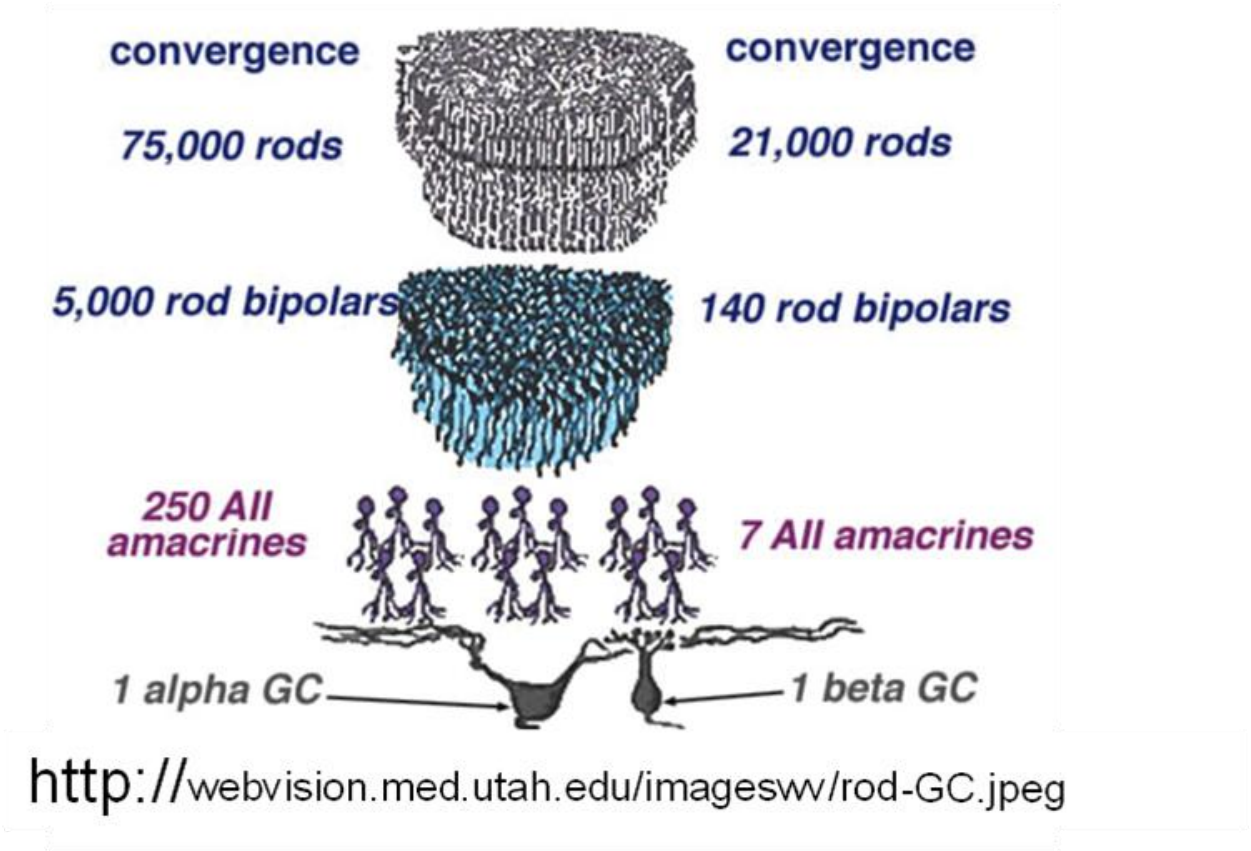

Figure 1-4 Convergence pathway of the retina

Pathways shows that information goes from photoreceptor layer (rods) to the bipolar cells, and it forms a funnel with up to 75,000 rods feeding into 5,000 bipolar cells going into 250 Amacrine cells and all ending up in a Ganglion cell. (Reprinted with permission from Webvision and Dr. Helga Kolb).

The Inner nuclear layer (INL) contains the cell bodies of the Amacrine cells (inner part of INL), Horizontal cells (Outer part of INL) and Bipolar cells, which are the most abundant cells and spread throughout the layer. Bipolar cell apoptosis in a mouse retina model has been shown to be increased under induced activity of hypoxia-inducible factor 1alpha (HIF1alpha) (Chen and Sepko, 2009). In humans, ischemia and hypoxia, where (participants were exposed to SaO_2 (percent O_2) 98% vs. 90% (occur naturally in 4,000 meter altitude), plays an important factor in developing retinal disease. It has been shown that specifically the functional activity of bipolar cells was significantly reduced under ischemia (functional data was measured with multi-focal Electro-Retinogram, mfERG) (Feigle et. al., 2007, Klemp et. al., 2007).

Outer Plexiform Layer (OPL) is a layer where the first neuronal synapses occur. This occurs between dendrites of bipolar cells or horizontal cells with axons of rod and cone spherules (Kolb, 1997). It was shown that structurally, the outer plexiform layer is severely affected under conditions of hypoxia. Electron microscopy showed that it forms membrane-delimited vacuole-like structures in cat retina that results in complete loss of structure in the outer plexiform layer (Negishi, 1972). In rat retina, effects were not as drastic, as it is speculated that deep capillary layers were able to compensate for changes in oxygen demand in the outer plexiform layer (Yu and Cringle, 2002). Human mfERG studies confirmed that bipolar cells are severely affected under hypoxic conditions (Feigle et. al., 2008), thus, reducing their ability to synapse with the photoreceptor layer rendering the outer plexiform layer non-functional.

Nuclei of rods and cones comprise outer nuclear layer and are separated from their cell bodies by a layer called the outer limiting membrane. Cell bodies of rods and cones make up the photoreceptor layer or outer segment layer and that is where the process of vision starts. Rods contain the visual pigment called rhodopsin and are responsible for black/white and night vision. Cones contain three visual pigments: L-cone (500-700 nm, peaks at red color) M-cone (450-630 peaks at green color), S-cone (400-500 peaks at blue color). Beside color vision cones are also responsible for sharpness of vision (Hunt, 2004). Visual pigments absorb light and the information is sent inwards through all the layers discussed above and ends up in the axons of ganglion cells that end up forming the optic nerve which goes into the brain and results in the interpretation of a visual stimulus. Hypoxia has less of an effect on photoreceptor layers (outer layers), than it has on the inner layers as measured in retina by an electro-retinogram (ERG). A-wave of an ERG represents photoreceptors, and B-wave represents bipolar and Müller cells. It was shown that the A-wave was resistant to hypoxia $60 < P_aO_2 < 100$ mm Hg and showed no significant (by 8%) decrease until severe levels of hypoxia were reached P_a0_2 of 25 mmHg. B-wave amplitude was significantly reduced as early as 75 mm Hg $Pa0_2$ (by 7.5%), and B-wave was completely undetectable at 25 mmHg (Kang, 2000). Examination of all the intra-retinal oxygen distribution and oxygen consumption in all retinal layers in a rat model showed that there are three areas of high demand for oxygen: the inner plexiform layer, outer plexiform layer and inner-segment of photoreceptors (Yu et. al., 2007). High demand for oxygen in the plexiform layer reflects a high metabolic demand due to the synapse's that take place in those layers, thus making it more vulnerable to the state of hypoxia. Inner-segments of photoreceptors receive

oxygen from the choroidal capillaries, which are significantly perfused with oxygen, through the Retina Pigment Epithelium layer. Thus it is less affected during the hypoxic state, resulting, in a stable response in functional measurements as measured on ERG.

1.3.2 Macula

The macula is an indentation on the retina found only in primates (called a foveal pit) that is located approximately 2 disc diameters temporal to the disc. It is a highly specialized area, where cone photoreceptors are concentrated at their highest density. It is considered to be a functional and anatomical center of the visual axis. It is an avascular zone that suffers tremendously when ischemia to the retina occurs. Conditions such as diabetic retinopathy can cause macular edema by accumulation of fluid (blood, lipids) from break down of the blood-retina-barrier induced by hydrostatic pressure, oxygen tension, oncotic pressure, osmotic forces, angiogenic factor expression, inflammation and oxidative stress that is caused by diabetes. This results in neo-vascularization (formation of new blood vessels) of the retina. New vessels are fenestrated and leak fluid into the macula, resulting in severe decrease of vision (Ehrlich et. al., 2010). It is very important to understand all the major proteins that are involved in protection and proliferation of damage due to oxidative stress so the visual damage due to diabetic retinopathy can be prevented.

In this project all the retinal studies were done on mouse retinas. Mouse retinas have been used for many years to study physiological pathways that later on are applied to human models. By the end of the third postnatal week, all three vascular layers are fully mature with multiple interconnecting vessels between layers (Stahl et. al., 2010). The major difference between human retina and mice retina is that mice do not have a macula, thus the macula area is rod/cone dominated instead of cone/rod like in humans; mice do possess cones but only lack the L-cone (Jacobs et. al., 2007). This does not prevent using mice models for macular disorders and mouse model have been extensively used in age related macular degeneration, because the vascular level it has proven to be an excellent model for studying structural and vascular changes due to hypoxia related disorders (Ramkumar et. al., 2010).

1.4 ABC Kinase Superfamily

The ABC kinase superfamily belongs to a class of serine/threonine protein kinases that were discovered in the 1970's. They constitute a large phosphorylation dependent family of kinases that are involved in signal transduction associated with cell proliferation, differentiation, and apoptosis (Shoji et. al. 1979, Nishizuka, 1986, Spitaler and Cantrell, 2004). Protein Kinase A (PKA), Protein Kinase B (PKB also called Akt) and Protein Kinase C, make up the ABC protein kinase super family (Newton, 2003). Protein kinases A, B/Akt and C have, in common, a conserved C-terminal kinase (hydrophobic motif) that functions as a substrate binding site and as a location where phosphorylation and dephosphorylation take place (Newton, 2010). All members of the ABC family also have N-terminal regulatory regions (Fig. 1.4) (turn motifs) that function as a targeting mechanism to guide the kinase to appropriate cellular locations e.g. membrane. This also serves a very important role as an auto-inhibitory module, by inhibiting the enzyme until activation by a secondary messenger (Barnett et. al, 2007; Newton, 2003).

Phosphoinositide Dependent Kinase-1 (PDK-1) performs an essential function in cell signaling by providing the activating phosphorylation for an abundance of serine/threonine protein kinases. To initiate activation; all of the ABC kinases need to be phosphorylated by upstream (PDK-1), although this mechanism is still being studied for PKB (Toker, 2000). PDK-1 accesses its binding site at the hydrophobic motif and, once it is bound, it can phosphorylate on the activation loop site (Leslie, 2001).

1.5 Protein Kinase C (PKC)

Protein kinase C (PKC) is a ubiquitous, phospholipids-dependent enzyme that is a well studied member of the ABC superfamily. Since being discovered in 1977, at least ten closely related PKC isozymes have been reported that differ in their structure, biochemical properties, tissue distribution, sub cellular localization, and substrate specificity (Newton, 2001; Goldberg and Steinberg, 1996). PKCs center stage place in signal transduction was secured once it was discovered in the 1980's that PKC can be activated by potent tumor promoting phorbol esters like phorbol 12-myristate 13-acetate (TPA) and that they act as a mediator of the diacylglycerol lipid second messenger signal transduction (Bottaini and Mochly-Rosen, 2007).

1.5.1 PKC – Structure of Isoforms

There are ten different isozymes of PKC that are divided into 3 groups based on the structures of their domains (Mellor, 1998). The PKC family's isozymes are classified as conventional (α, βI, βII, it is an alternative spliced version of βI with the only difference in the last 43 residues at the C-terminus, and the last one is γ), novel (δ, θ, ε and η), and atypical (ζ and ι/λ; an alternative transcript exists for ζ that encodes only the catalytic domain and is referred to as PKM ζ (Gould and Newton, 2009) isozymes (Fig. 1.4).

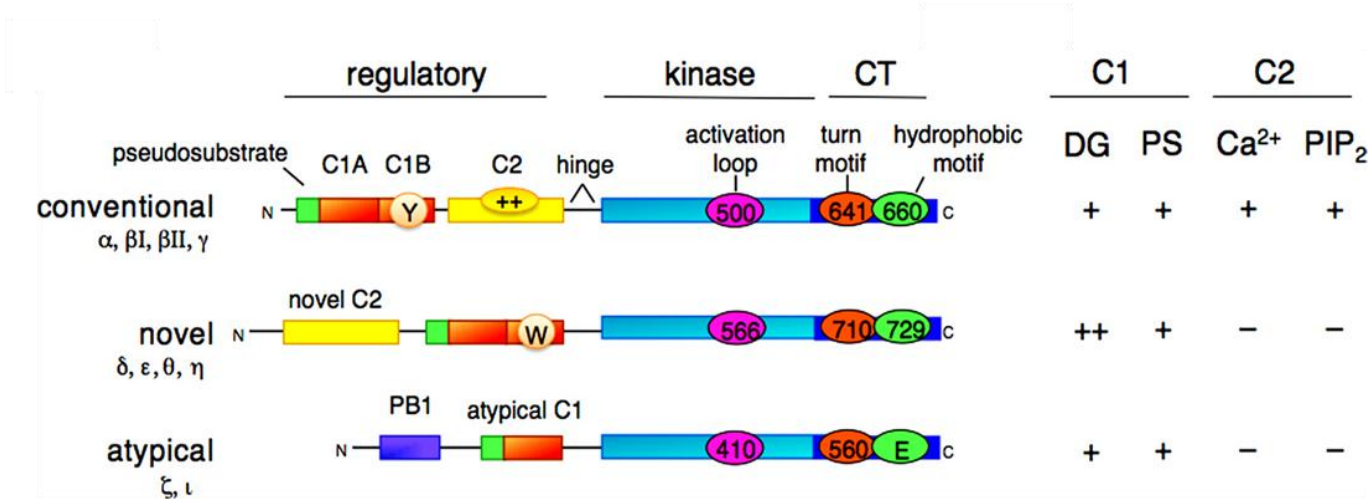

Figure 1-5 Structural schematic showing of domain structures of PKC isozymes. Indicated are pseudosubstrate, C1A domain (orange bar), C1B domain (orange bar), Y – indicates affinity for DAG, W – indicates affinity for DAG, C2 domain (yellow bar), ++ indicates affinity for Calcium, hinge – indicates a hinge connection, kinase – indicating kinase catalytic region, CT – carboxyl terminal tail, green- indicates pseudosubstrate site. Also shown are the 3 priming phosphorylations in the kinase domain, E – indicates Glutamine at phospho acceptor position. A table showing dependence of PKC family members on C1 domain cofactors, DG, and phosphatidylserine (PS) and C2 domain cofactors Ca 2 and PIP2 is at the right (Adapted from Newton AC. (2010) Protein kinase C: poised to signal Am. *J Physiol Endocrinol Metab.* 298(3):E395-402. Copyright©2010 Am Physiol Soc, used with permission granted Aug. 23, 2010).

These three different classes of isozymes all share similarities that are part of the ABC kinase family, such as, all have a conserved kinase core carboxyl terminal to a regulatory moiety. Conventional, novel, and atypical isozymes differ in the ways in which they are activated. Conventional PKC isozymes are Ca^{2+}-dependent (because they have a functional C2 domain, (Fig 1.4.), while novel and atypical isozymes do not require Ca^{2+} for their activation. Conventional PKCs and novel PKCs are both activated by diacylglycerol (DAG) and require phosphatidylserine as a co-factor because as they both possess a C1 domain. The difference is that novel PKCs do not have a functional C2 domain. (Newton, 2009). Atypical PKCs, unlike the other two classes of isozymes, do not respond to either DAG or Ca^{2+}. They rely upon phosphatidylserine as a co-factor, and protein-protein interactions control the function of their isozymes in the cell.

1.5.2 PKC – Domain Structure

PKC is one of a number of signaling enzymes that utilizes two membrane-targeting modules to reversibly regulate their spatial distribution (Newton and Johnson, 1998; Hurley and Misra, 2000). Each module binds membranes with low affinity when both domains are engaged on the membrane.

The C1 region contains one or two copies (depending on the isozyme of PKC) of a cysteine-rich domain, which is about 50 amino-acid residues long (Hurley et al., 1997). Diacyglycerol (DAG) is an important second messenger to this Cys-rich region. Both DAG and phorbol ester (PE), analogues of DAG, are activators of PKC, however, atypical PKCs contain a single copy of the domain which does not bind phorbol esters (Steinberg, 2008). The N-terminal region of PKC, known as C1, has been shown to bind DAG and PE in a phospholipid and zinc-dependent fashion (Zhang et al., 1995; Hommel et al., 1994). The DAG/PE binding domain binds two zinc ions which are coordinated by His and Cys residues at opposite ends of the primary sequence to help stabilize the domain (Zhang et al., 1995). Binding of the phorbol esters to the C1 domain allows for membrane-targeting by altering the hydrophobicity promoting hydrophobic interactions of the surface of the C1 domain. Binding of phorbol esters allows for membrane-targeting without inducing significant conformational changes.

The C2 domain is a Ca^2+-dependent membrane-targeting module found in many cellular proteins involved in signal transduction or membrane trafficking (Nalefski and Falke, 1996). C2 domains are unique among membrane targeting domains in that they show a wide range of lipid selectivity for the major components of cell membranes, including phosphatidylserine and phosphatidylcholine. This C2 domain is about 116 amino-acids in length, with significant homology to the C2-domains found in many proteins. All C2 domains share a tertiary structure that consists of eight anti-parallel β-strands that are connected by loops formed by sequences at the opposite ends of the primary structure to form a pocket like structure (Steinberg, 2009). The C2 domain is thought to be involved in calcium-dependent phospholipid binding and in membrane targeting processes such as sub cellular localization (Ponting, 1996, Gallegos and Newton, 2008).

The Ca^2+-binding motif is present in phospholipases, protein kinases C, and synaptotagmins (among others). Some do not appear to contain Ca^2+-binding sites (Newton, 2009). Particular C2s appear to bind phospholipids, inositol polyphosphates, and intracellular proteins. Unusual occurrences happen in perforin, synaptotagmin and PLC C2s which are permuted in sequence with respect to N- and C-terminal beta strands. C2 domains were detected by SMART using one or both of two profiles. The 3D structure of the C2 domain of synaptotagmin was reported to have the domain that forms an eight-stranded beta sandwich constructed around a conserved 4-stranded motif, designated a C2 key (Bottaini and Mochly-Rosen, 2007). Calcium binds in a cup-shaped depression formed by the N- and C-terminal loops of the C2-key motif. Structural analyses of several C2 domains have shown them to consist of similar ternary structures in which three Ca^{2+}-binding loops are located at the end of an 8 stranded antiparallel beta sandwich. (Ponting, 1996; Nalefski and Falke, 1996)

Eukaryotic protein kinases such as PKC enzymes belong to a very extensive family of proteins which share a conserved catalytic core common with all serine/threonine and tyrosine protein kinases. As could be seen in Fig 1.4. the catalytic domains for all three PKC isoforms are very similar, with about 40% overall sequence identity (Knighton et. al 1991). In the N-terminal extremity of the catalytic domain there is a structural hallmark of protein kinases and nucleotide binding proteins, a glycine-rich stretch of residues in the vicinity of a lysine residue, which has been shown to be involved in ATP binding. In the central part of the catalytic domain there is a conserved aspartic acid residue which is important for the catalytic activity of the

enzyme. In the past few years, determination of the exact crystal structures of kinase domains have been reported using PKCβII which was part of a complex with 2-methyl-1*H*-indol-3yl-BIM-1, PKCθ which was complexed with staurosporine, and PKCι bound to BIM-1. (Grodsky et al., 2006; Newton, 2010). The C-terminal lobe is made of α-helixes and contains the activation loop segment that positions magnesium and peptide substrates (Steinberg, 2008).

It was discovered in the mid-1980s that the regulatory region sequence of PKC resembled that of a substrate except an Ala occupied the phospho acceptor position (House and Kemp, 1987). It was found that peptides based on this sequence were effective competitive inhibitors of PKC and peptides modified to have a Ser at this phospho acceptor position were relatively good substrates of the enzyme (House and Kemp, 1987). Further studies supported the hypothesis that the inactive conformation was maintained because this pseudo-substrate occupied the substrate-binding cavity of PKC, which keeps it allosterically regulated (Makowske and Rosen, 1989). The activation of PKC is accompanied by the release of the pseudosubstrate sequence from the kinase core (Orr et al., 1992). Studies suggest that engaging of the membrane-targeting modules on the membrane provides the energy to release the pseudo-substrate domain or module from the kinase core (Johnson et al., 2000).

1.5.3 PKC Processing and Activation

Protein kinase C, a multimodal protein, uses phosphorylation and binding of co-factors to induce conformational changes that regulate inter and intra domain interactions. All of the PKCs needs to be phosphorylated before they can, in turn go, on and phosphorylate their own substrates. They all have a threonine residue (Fig 1.4.) in their activation loop. In the case of PKC [conventional] it is Thr500 (Fig.1.4) that gets phosphorylated by PDK-1 (Taylor, 1994, Dutil and Newton, 2000). PDK-1 phosphorylation is very tightly controlled mechanism for different type of enzymes, all of PDK-1 substrates need to be in the right place and in the right conformation for it to be activated by PDK-1 (LeGood et. al., 1998). PDK-1 is the first and rate limiting step in activation of several enzymes, one of how the which is PKC (Toker, 2000). Below is a detailed discussion on how process of activation and processing takes place for one of the targets of PDK-1 which is the conventional PKC type enzyme (Fig. 1.5).

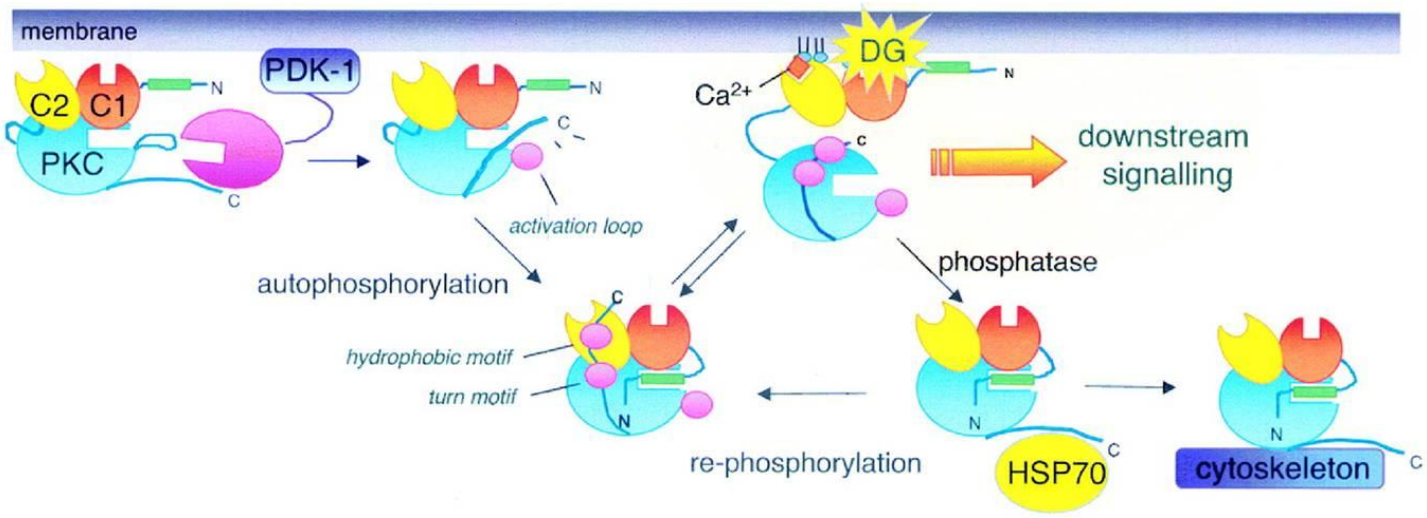

Figure 1-6 Model showing PKC activation

Freshly synthesized PKC at membrane with C2 and C1 and pseudosubstrate (green color) associates with the membrane in an open conformation in which the pseudosubstrate is released from the substrate-binding cavity (shown as a rectangular indent in a cyan circle), and in which the C-terminus is exposed to allow PDK-1 to bind (far left). PDK-1 phosphorylates the activation loop segment and is released from its docking site on the C-terminus. The liberated C-terminus accesses the substrate-binding site and is autophosphorylated by an intramolecular mechanism. The phosphorylated enzyme is released into the cytosol (shown in the middle of the diagram), where it is maintained in an inactive conformation by the bound pseudosubstrate. Generation of Ca^{2}+ and diacylglycerol targets PKC to the membrane. Engagement of the C1 and C2 domains on the membrane provides the energy to release the pseudosubstrate from the substrate-binding cavity, allowing downstream signaling. In this active conformation, PKC is rapidly dephosphorylated. The molecular chaperone Hsp70 binds the dephosphorylated turn motif and stabilizes PKC, allowing it to become rephosphorylated and to re-enter the pool of signaling-competent PKC. In the absence of Hsp70 binding, or as a result of chronic activation, dephosphorylated PKC accumulates in a detergent-insoluble cell fraction, where it is eventually degraded. (Adapted from Newton AC. (2010) Protein kinase C: poised to signal Am. *J Physiol Endocrinol Metab.* 298(3):E395-402. Copyright©2010 Am Physiol Soc, used with permission granted Aug. 23, 2010).

For PDK-1 to phosphorylate conventional PKC, two requirements need to be met, PKC needs to be at the membrane and be in an "open" conformation, which means that the pseudo-substrate is not in the substrate binding cavity. When PKC is freshly synthesized it stays at the membrane and already is in the "open" conformation due to the energy that is provided through association of C1 and C2 domains with the membrane (Sonnenburg, 2001 and Dutil, 2000). As a result when PKC is synthesized it is already in the position and conformation to be phosphorylated at its activation loop by PDK-1. PDK-1 attaches to the PKC at the unphosphorylated hydrophobic motif of the C-terminus (Balendran, 2009) (Fig. 2), phosphorylates the activation loop at position Thr 500 for conventional PKC and, after that, PDK-1 is released. The exact process of release of PDK-1 is still under investigation, but it is because of this step that phosphorylation by PDK-1 is considered a rate-limiting step in PKC activation (Gao, 2001). This newly acquired phosphate at the activation site changes the conformation of the PKC by uncovering the entrance to the substrate binding cavity and this exposes sites on the C-terminus for the phosphorylation.

Following phosphorylation at the activation loop by PDK 1, the active site is opened and PKC autophosphorylation takes place at the turn motif and hydrophobic motif (Behn-Krappa, 1999). Conformational changes follow this phosphorylation and the C-terminus is moved away from the substrate-binding cavity, exposing it for pseudosubstrate binding. The pseudosubstrate binds to the substrate binding cavity, causing auto-inhibition of the PKC and rendering it inactive until further activation by second messengers. This conformation of PKC is called the "closed" conformation. As a result of this change in conformation, PKC loses its binding to the membrane and localizes into the cytosol. At this point PKC is called the "Mature" primed species and this is the form in which a large majority of PKC's are present. In this form PKC is inactive due to the pseudosubstrate auto-inhibiting the PKC, but it is catalytically active and is "primed" for activation by the second messengers (Newton, 2003).

Translocation to the plasma membrane is the key step in activation of mature phosphorylated auto-inhibited PKC. Several second messengers have been identified that help facilitate that: phosphatidyl serine (PS), calcium and diacylglycerol (DAG) (Oancea 1998; Newton, 1995). When calcium levels increase in the cell, calcium brings PKC to the membrane through its binding to the C2 domain. That interaction, in turn, dramatically increases the possibility of the C1 domain to interact with DAG, so calcium and DAG act as synergists in

activating the enzyme. DAG has a very high affinity for the C1 domain of the PKC, thus the energy that is produced causes the release of the pseudosubstrate from the substrate binding cavity, rendering PKC back into the open conformation and allowing for PKC to bind its substrates (Newton, 2010).

PKC's have been shown to have the ability to interact with numerous targets such as plasma membrane, Golgi, cytoskeleton, mitochondria and cell nuclei. As result of all these interactions, PKC plays an important role in differentiation, cell growth, apoptosis, gene expression, muscle contraction, metabolism, and endocytosis to name a few. The rest of this thesis will focus on PKC γ and its regulation by external stress, with major focus on the ability of PKC γ to control gap junction activity in response to external stimuli.

1.5.4 PKC – Distribution in the Eye

PKCs are found in the bow and cortex region of the lens (Gonzales et. al., 1993), in retina (Fugisawa et. al., 1992), in cornea (Bazan et. al., 1987) and in retinal and lens epithelial cells in culture (Wagner et. al., 2002). In lens tissues PKCγ has been detected in rat lens epithelium and cortex but PKCα was present in epithelial cells only (Saleh et al., 2001). In retina it was shown that PKC antisera preferentially react with rod-bipolar cells (Negishi et al., 1988). Antibodies against PKCα are currently used as a marker for rod bipolar cells. It is also localized to cone bipolar cells with axon terminals ramifying near the middle of the inner plexiform layer (IPL), rod bipolar cells located in the Inner Nuclear Layer (INL), Outer Plexiform Layer (OPL) and Inner Plexiform Layer (IPL) (Behrens et. al., 2007; Semkova et. al., 2010). Antisera staining against PKC beta was localized to rod bipolar cells, one class of cone bipolar cell, and numerous amacrine and displaced amacrine cells (Osborne et. al., 1992). PKCε is found in rod bipolar cells, cone bipolar cells and a few amacrine and ganglion cells. PKCζ is found in rod bipolar cells and all of the ganglion cells (Fyk-Kolodziej et. al., 2002). PKCγ isozyme which from this point will be the main focus of this dissertation is localized mainly in the brain, spinal cord (where it is expressed in Purkinje cells of the cerebellum and hippocampal pyramidal cells (Mellar et. al., 2000). In retina PKCγ has been previously shown to have been localized to inner plexiform layer as shown by immunoreactivity with ganglion cells and amacrine cells. (Osborne et al., 1992; Wood et. al., 1997).

1.5.5 PKCγ Isozyme Structure and Regulation

Protein Kinase C γ Amino Acid Sequence for Mouse

```
        1 maglgpgggd seggprplfc rkgalrqkvv hevkshkfta
rffkqptfcs hctdfiwgig
       61 kqglqcqvcs fvvhrrchef vtfecpgagk gpqtddprnk
hkfrlhsyss ptfcdhcgsl
      121 lyglvhqgmk csccemnvhr rcvrsvpslc gvdhterrgr
lqleirapts deihitvgea
      181 rnlipmdpng lsdpyvklkl ipdprnltkq ktktvkatln
pvwnetfvfn lkpgdverrl
      241 svevwdwdrt srndfmgams fgvsellkap vdgwyklinq
eegeyynvpv adadncsllq
      301 kfeacnyple lyervrmgps sspipspsps ptdskrcffg
aspgrlhisd fsflmvlgkg
      361 sfgkvmlaer rgsdelyaik ilkkdvivqd ddvdctlvek
rvlalggrgp ggrphfltql
      421 hstfqtpdrl yfvmeyvtgg dlmyhiqqlg kfkephaafy
aaeiaiglff lhnqgiiyrd
      481 lkldnvmlda eghikitdfg mckenvfpgs ttrtfcgtpd
yiapeiiayq pygksvdwws
      541 fgvllyemla gqppfdgede eelfqaimeq tvtypkslsr
eavaickgfl tkhpgkrlgs
      601 gpdgeptira hgffrwidwe rlerleiapp frprpcgrsg
enfdkfftra apaltppdrl
      661 vlasidqadf qgftyvnpdf vhpdarspts pvpvpvm
```

Figure 1-7 Amino Acid Sequence of mouse PKCγ

C1A, C1B, and C2 domains were highlighted in color and underlined C1A: 36-85, C1B: 101-150, C2: 170-260, Kinase Domain: *351-614*, Potential Auto-Phosphorylation sites: T648, 655, and 674, Putative Caveolin-1 Binding Regions: 539-546 (wsfgvlly), 673-680 (ftyvnpdf). Putative 14-3-3 Binding regions: 104-109 (rlhsys), 144-148 (rsvps). (NCBI access No. P05967).

PKCγ is a classic isoform of the Protein Kinase C family which follows the process of activation as described above for the other classical PKCs, but it differs from other PKC's because it does not require a calcium signal to be activated. This is because the C1B domain of

PKCγ is exposed when it is in its inactive state (Lin et. al., 2005). The C1B domain of PKCγ (Fig. 1.6) has seven Cysteine residues, that contain an alpha helix, five short beta sheets and two zinc ions that form zinc fingers (Fig. 1.7).

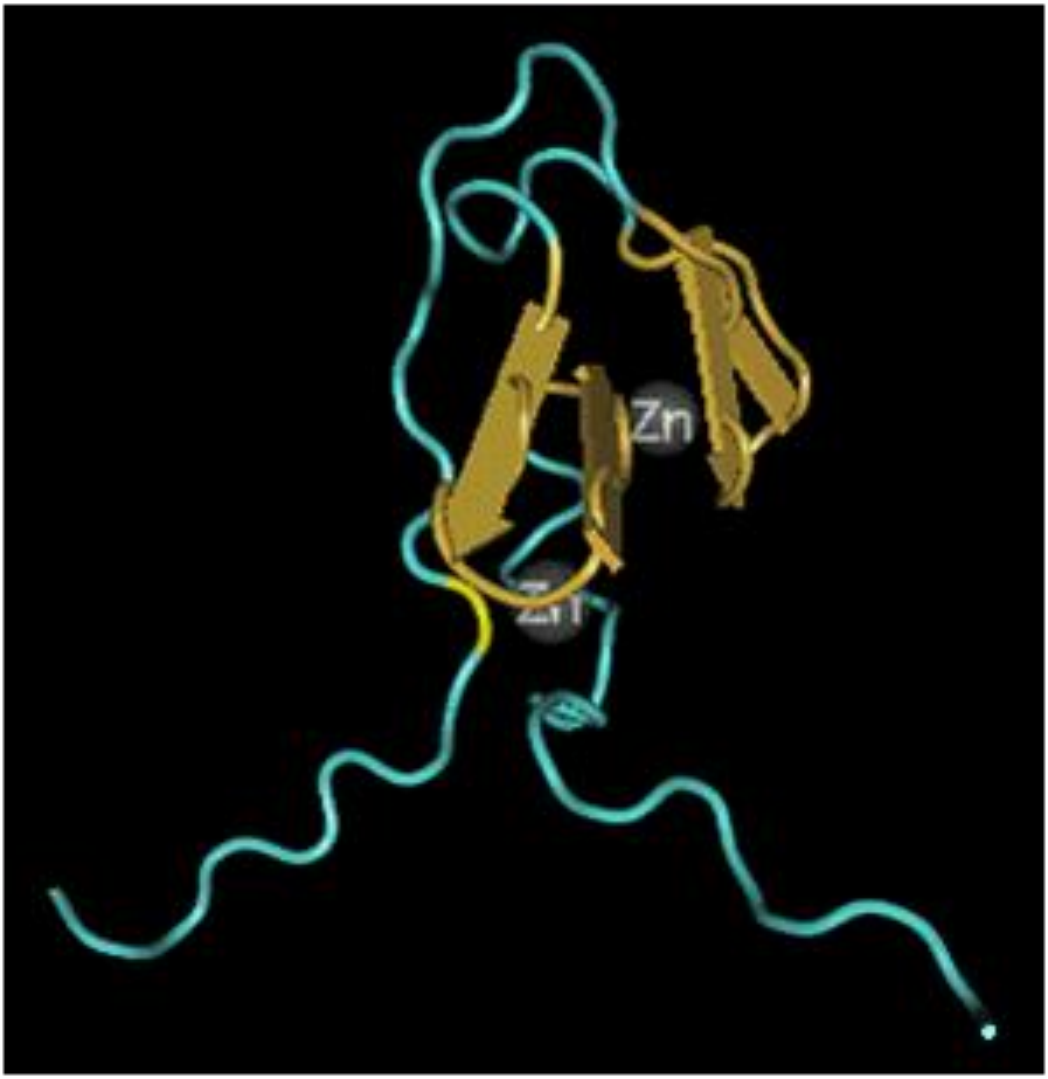

Figure 1-8 NMR structure of C1B region of PKCγ

Showing an alpha helix, five short beta sheets and two zinc ions that form zinc fingers (Reprinted from *Biochemistry.* Sep 2;36(35):10709-17. Xu RX. et al. NMR structure of a protein kinase C-gamma phorbol-binding domain and study of protein-lipid micelle interactions. Page 10713. Copyright (1997), with permission from American Chemical Society, license agreement number 2491480759849).

For PKCγ to be activated it needs to translocate to the membrane where it can be phosphorylated by PDK-1. The process of translocation can be achieved by changing the conformation of the C1B domain so association with the docking protein will be disrupted allowing for PKCγ to be released from the cytoplasm and go to the membrane. This can be achieved as discussed through binding diacylglycerol (DAG), which is a product of phospholipase C. When equilibrium cellular levels of DAG are increased, DAG binds at the C1 domain of PKCγ and changes the conformation of PKCγ, separating it from the docking protein 14-3-3ε, and allowing it to translocate to the membrane (Ananthanarayanan et al., 2003). There are many different ways that PKCγ can be activated (separating from docking protein) besides by DAG. Below is a brief description of several of the ways this can be achieved.

Phorbol-12-Myristate-13-Acetate (TPA) is a phorbol ester that mimics the effects of DAG, and has been used to study PKCγ activation in a multitude of systems: lens tissue (Lin et. al., 2006), live mouse brain tissue (Niikura et. al., 2007), NN lens epithelial cells in culture, (Lin et. al., 2005) just to name a few. TPA is widely used because its activation is superior to DAG, because DAG's ability to recruit PKCγ is short lived as it is rapidly metabolized once in the cell. TPA is not metabolized, thus results in constant activation of PKCγ (Zhang et. al., 1995).

Phosphatidylserine (PS) is an aminophospholipid that has an affinity for the C1 domain of PKCγ. Its affinity is significantly lower than that of DAG, but still it has the ability to recruit PKCγ to the membrane in the absence of DAG and calcium (Sanchez-Bautista et. al., 2009).

Increasing the equilibrium concentration of calcium ions increases the affinity of the C2 domain for anionic lipids (which are present in the membrane), thus recruiting PKCγ to the membrane (Newton, 1993).

Insulin-like Growth Factor 1 (IGF-1) has been shown to have the ability to increase the cellular concentration of DAG through stimulation of PLC and by increasing calcium concentration in the cell (Neri et. al., 1999; Kojima et. al., 1990). IGF-I is known to activate IGF-I receptors in oocytes, thus triggering a cascade that involves the activation of MAPK pathways, which have the ability to affect connexins which are downstream PKCγ targets (Warn-Cramer, 1996). In N/N1003A rabbit lens epithelial cells, IGF-1 induced PKCγ translocation to the membrane. It is proposed that IGF-1 is able to achieve PKCγ translocation through increasing DAG concentration, thus, DAG acts as a second messenger in the IGF-1 system (Nguyen et al., 2003).

PKCγ can be activated by separation from the docking proteins also called receptors for activated C kinase (RACK) or scaffolding proteins such as 14-3-3ε. These proteins bind PKC isozymes and put them in an autoinhibited state (Mochly-Rosen and Gordon, 1998). Scaffolding proteins that bind and inhibit PKC gamma also include 14-3-3 ε, which specifically binds PKC PKCγ at 104-109 (rlhsys), 144-148 (rsvps) (Fig. 1.6) at the C1B region and inhibits the enzyme. By generating synthetic peptides of C1B5 that bind PKC gamma at the exact place where 14-3-3ε does, thus introducing competition for the active site spot, it was shown that PKCγs enzyme activity increases, and translocation to the membrane increases (Nguyen et. al., 2004).

Oxidative stress plays a major role in Protein Kinase C family activation and translocation and, understanding the signal transduction pathway that is activated after exposure to hypoxia is one of the leading research topics that science faces today. It is proposed that when six cysteine residues and 2 histidine residues at the C1B domain of PKCγ (Fig. 1.7) are oxidized due to the oxidative stress, it releases zinc, thus disrupting zinc fingers and, in the process, alters the shape of the C1B domain, thus allowing PKC gamma to unbind from the docking protein and translocate to the membrane (Lin et. al., 2005). N/N1003A lens epithelial cells were treated with H_2O_2 (simulated oxidative stress) which caused an increase in PKCγ activity, and affected gap junctions, a known downstream target of PKCγ (Lin and Takemoto, 2005). H_2O_2 induced activation of PKCγ and increased phosphorylation of gap junctions in rat lenses as well (Lin et al., 2004).

Vascular endothelial growth factor (VEGF) is a major growth factor that gets released in response to oxidative stress. Hypoxia mediates VEGF expression by enhancing the stability of VEGF mRNA transcript through mitogen-activated protein kinase and Akt pathways and through increasing the binding of active hypoxia inducible factor (HIF)-1a to the hypoxic response element of the VEGF promoter (Riddle et. al., 2009). VEGF activates PKC via Src-dependent Phospho-Lipase D 1 (PLD1) stimulation. Using specific PKCγ siRNA to reduce signals resulted in suppression of hypoxia-induced retinal neovascularization (Zhang et. al, 2010). VEGF has long been known to be an important mediator in vascular pathological retinal angiogenesis. It is the most potent growth factor in stimulating retinal angiogenesis under hypoxic conditions (Kermorvant-Duchemin et. al., 2010).

Oxidative stress is caused by the imbalance of reactive oxygen species (ROS) production and rate of degeneration. When ROS accumulates in tissues, oxidative stress rises and cells go

into apoptosis (Barnett et. al., 2007). One of the downstream targets of Protein Kinase C gamma is gap junctions. Activated PKCγ closes gap junction channels, thus stopping intercellular transmission of apoptotic signals (Lin and Takemoto, 2005). Below is a discussion of gap junctions with specific focus on retinal gap junctions and their regulation by PKCγ, and, the resulting effects on protective/survival mechanism of the cell.

1.6 Gap Junctions

Coupling by gap junction channels is a fundamental mechanism for cell-to-cell communication in higher organisms and is the most direct form of intercellular communication (Decrock et. al., 2009). Electrical synaptic transmission via gap junctions is a primary mode of cellular communication in retina and the central nervous system. Gap junctions in retina form a low-resistance pathway for direct electrical signaling among all five cell types that have gap junctions (Meier and Dermietzel, 2006).

Gap junctions are specialized regions of cell-to-cell contact constructed of hexameric oligomers, called connexons, joined end-to-end non-covalently between adjacent cells to form a functional channel, which can pass small molecules (less than 1,000 Daltons) from cell to cell (Lin et. al., 2007). Channel hexamers aggregate into clusters of up to 10,000 membrane channels to form gap junction's plaques. The exact process of functional gap junction plaque formation is still under investigation (Saleh and Takemoto, 2000). A variety of metabolites and signaling molecules that keep signal transduction are able to pass through gap junctions, for example: ions (K^+ and Ca^{2+}), amino acids, nucleotides, small peptides, sugars, cAMP, and inositol triphosphate (Mese et. al., 2007).

The family of connexin genes currently contains 20 genes from mouse and 21 genes from human, with 19 of those genes occurring both in the mouse and human genome. Two different nomenclature classifications exist for connexins; the first one is based on molecular weight and origin of a particular Connexin. For example, a mouse connexin with a molecular weight of 43,036 Da protein, would be called mCx43; if it is from human, than hCx43. In cases where weight is similar, nomenclature established a decimal point, e.g. Cx30 and Cx30.3. A more recent nomenclature that was proposed is based on structural gene similarities, homology and

sequence, as well as the length of connexin cytoplasmic domains. According to this classification, Connexins are divided into α (Cx33, Cx37, Cx38, Cx40, Cx43, Cx46, Cx50, and Cx56), β (Cx26, Cx30, Cx31.1, and Cx32), γ (Cx 29, Cx 45, Cx30.3, Cx 47), δ (Cx40.1, Cx36), and ε (Cx23) (Rackauskas et. al., 2010).

1.6.1 Gap Junction Structure

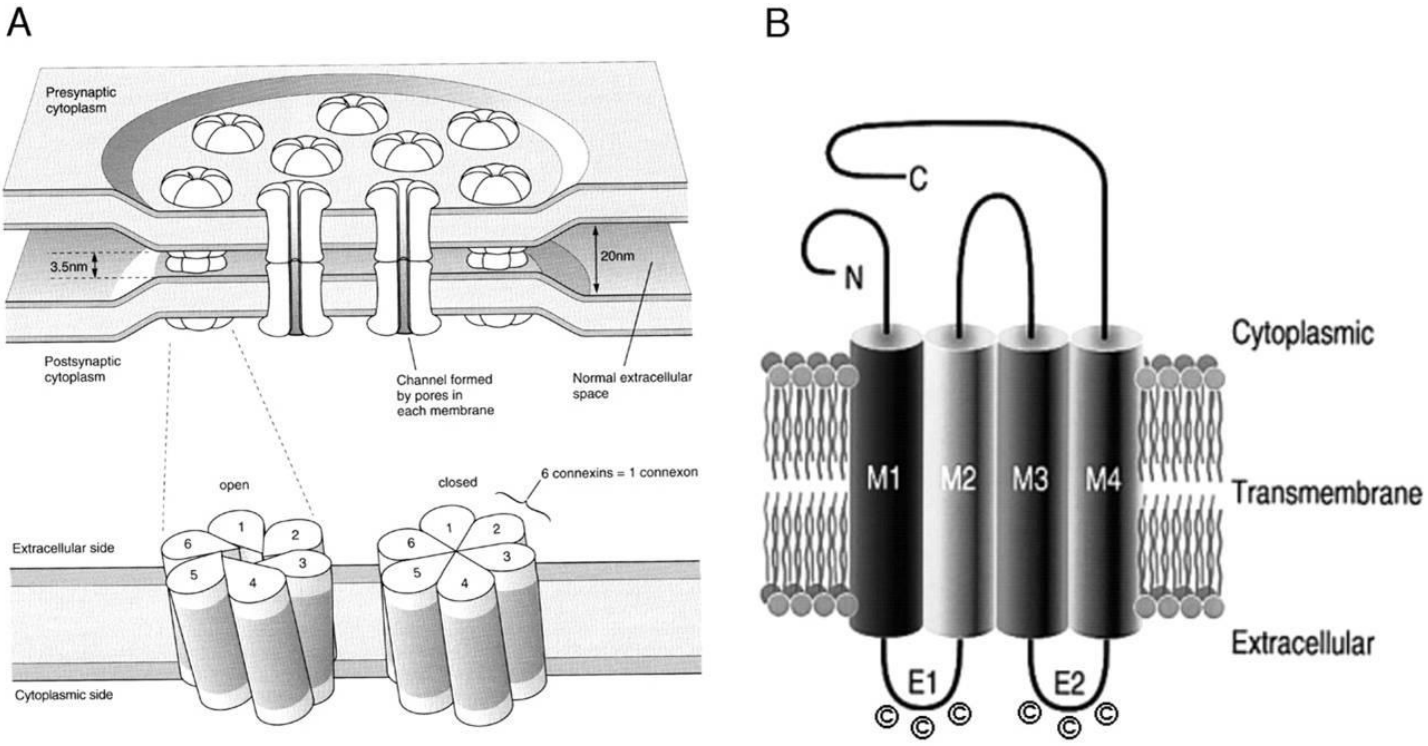

Figure 1-9 Schematic of Gap Junction Structure

A) Schematic drawing of Gap Junction consisting of 6 individual connexins forming 1 connexon. Shown in closed and open conformation. B) Schematic drawing of each individual connexin which has four transmembrane domains (M1 to M4), two extracellular loop domains (E1 and E2), a cytoplasmic loop domain (CL) and cytoplasmic N-terminal (N) and C-terminal (C) tails (Reprinted from *Cardiovascular Research* May 1;62(2):228-32. Söhl and Willecke. Gap junctions and the connexin protein family. Page 229, Copyright (2004), with permission from Oxford University Press, license agreement number 2491431364323).

All of the members of the connexin family share a basic structure (Fig. 1.8B), and consist of 4 hydrophobic transmembrane domains, two extracellular loops (E1 and E2), one intracellular loop and carboxyl and amino termini in the cytoplasm. Four transmembrane domains (M1-M4) share a conservative sequence, with the M3 domain being known as a hydrophilic face that lines the pore of a gap junction channel. Two extracellular loops also share a conserved sequence of the three cysteine residues in both of the loops (Fig. 1-8B). These cysteine residues form disulfide bond and are responsible for docking of the 2 connexons (Bloomfield and Volgyi, 2009). The cytoplasmic portion consists of one loop plus the C and N termini are where the differences in connexin sequences occur, while the ends determine what differentiates each connexins function and regulatory properties. The carboxyl-terminal cytosolic tail-terminus has a number of regulatory binding sites that influence gating and signal propagation. Connexins are called phospho-proteins (besides Cx26) as they contain both serines and threonines on the C-terminus, and, these are phosphorylated. Either activating or inhibiting can occur, depending on the signal (Saez et. al., 2003).

1.6.2 Gap Junction – Synthesis

Connexin synthesis, assembly, and trafficking follow a general secretory pathway for membrane proteins: after transcription of Cx mRNA, it is synthesized at the ribosome of the endoplasmic reticulum and cotranslationally inserted into the ER membrane. Folding of the connexin protein chain into a functional structure (Fig. 1.8B), occurs during integration into the ER membrane, after gap junction hemi-channels are delivered to the plasma membrane, by the interaction of extracellular loops among neighboring cells (Salameh, 2006). Connexin genes are relatively conserved in structure: first exon (exon 1) contains 5'-untranslated (UTR) sequences, which are separated by an intron from a large second exon (exon 2) that contains the complete coding region as well as all remaining untranslated sequences (3'-UTR) (Salameh, 2006).

1.6.3 Gap Junction – Regulation

Expression and functional ability can be regulated by intrinsic and extrinsic factors at many different steps of gap junction synthesis e.g. transcriptional control, RNA processing control, RNA transport and localization control, translational control, mRNA degradation

control, and protein activity control. Transcriptional control is achieved through the basal promoter site that is located within 300 bp from the transcriptional initiation site in exon 1. Located within this region are the binding sites for transcription factors such as Sp1/Sp3 (GC box recognition), AP-1 (activator protein), TATA box binding proteins, GATA4 (cardiac-specific factor), hepatic nuclear factors (HNF-1). Connexin mRNA levels have been shown to be increased, due to different treatments, e.g. cAMP has been shown to induce elevation of Cx43 transcript levels in hepatoma cells through increasing binding at AP-1 site (Geimonen et. al., 1996). Phorbol ester (TPA) was able to induce transcriptional up-regulation of Cx26 in human immortalized MCF-10 mammary epithelial cells (Li et al., 1998). Translational regulation has been shown to be achieved through ribosomal entry sites for Cx43 and Cx26. It was achieved through microRNA, which are negative regulators of translation (Saez et.al, 2003).

Gap junction regulation is highly voltage dependent. There are two distinct voltage-dependent gating mechanisms that can close GJ channels and hemichannels . First, is a fast-gating mechanism that is sensitive to V_j, closes channels and hemichannels to a sub-conductance state, and is localized to the N-terminal domain. The second is a slow-gating mechanism which completely closes gap junctions, leaving no conductance, and is sensitive to Vj, Vi-o or Vm, and is highly sensitive to extracellular calcium ions (Harris and Locke, 2009). Connexin 50 voltage gating is of the latter kind. It was shown that Cx50 gap junctional gating occurs by the gating of a single hemichannel on the positive side of transjunctional potential. The peak calcium ion sensitivity to completely shut down gating in connexin 50 was 200 nM (Beahm and Hall, 2002).

Cytoplasmic changes in acidification, also lead to closure of gap junctions. The regulatory sites for pH are located on the C-terminus and which acts as a ball and in case of Cx43 acts in what is defined as a “ball and chain mechanism”, when the carboxyl end in response to pH, folds over an open channel, thus blocking it (Morley et. al., 1996). Cytoplasmic acidification of oocytes with sodium acetate blocked Cx50 hemichannels (Zampighi et. al., 1999). Currently the exact mechanism of this block is not known and structure/function studies are ongoing.

The major component of connexin regulation is achieved through phosphorylation; all connexins besides connexin 26 are phosphoproteins, which means they are regulated through phosphorylation (Lampe and Lau, 2004). Connexin phosphorylation plays an important role in regulation of intercellular communication, trafficking, assembly, membrane insertion, channel

gating, and degradation. Several of the kinases have been identified that are involved in connexin phosphorylation, including, mitogen activated protein kinase (MAPK also knows as ERK1/2), shown to phosphorylate Cx43, which is the most extensively studied connexin, on Ser-255, S279 and S282 and resulting in decreased cell communication (Lampe and Lau, 2004). Cdc2 is a cyclin dependent serine kinase that is active during mitosis, Cdc2 kinase moves to the plasma membrane at the beginning of mitosis where it phosphorylates Cx43 at S255 and S262 and inhibits Cx43 gap junction communication. PKA is a cAMP responsive protein kinase that can lead to phosphorylation of Cx43 at S364, S365, S369, and S373. Phosphorylation by PKA increases gap junctional communication, stabilizes gap junctions, and facilitate the assembly of new gap junctions (Solan and Lampe, 2005). CK1 is a serine/threonine kinase that can phosphorylate Cx43 at S325, S328, and S330 promoting gap junction assembly (Cooper and Lampe, 2002). Src is an oncogenic kinase, which activates MAPK, cdc2 and PKA, thus affecting gap junctions. It also can directly phosphorylate 2 tyrosine residues (Y247, Y265) on Cx43, leading to inhibition of gap junction activity (Puhajaa et. al., 2007).

PKC, and the specific isoform PKCγ, were shown to inhibit Cx43 gap junctions by phosphorylation at S368 (Lampe et. al., 2000). PKCγ phosphorylation of Cx43 leads to decreased dye transfer of gap junctions and decreased number of functional gap junctions' plaques (Lin et. al., 2005). While Cx43 is found in most cells and is well studied, Cx50, which is another probable PKCγ target, is not as well understood and its regulation and role in signal transduction pathway will be the primary focus of the rest of this dissertation.

1.6.4 Gap Junctions - Connexin 50

The Connexin 50 is found both in human genome (hCx50), located on a 1q21.1 chromosome, and the mouse genome (mCx50), and located on chromosome 3. It is part of a α8 (alpha) group of the connexin family and also can be found in the literature under the following names: GJA8, CAE, CAE1 and CZP1 (Rutkowski et. al., 2008). Cx50 plays a significant role in cellular communication in the variety of eye tissues. Cx50 has been shown to be located in the non-pigmented epithelium (NPE) at apical and basoloateral membranes of the ciliary body (Wolosin et. al., 1997). In the lens Cx50 is readily expressed in lens epithelial cells alongside Cx43, but, unlike Cx43, Cx50 also takes part in the differentiation of fiber cells that takes place in the bow cortex of the lens (Gong et. al., 2007). Cx50 is widely found alongside Cx46 in both differentiating and mature lens fiber cells, but, unlike Cx46, which is found both in cortical and nuclear fibers, Cx50 is found only in the cortical fiber cells (Baldo et. al., 2001). Cx50 has a wide presence in retina, unlike Cx43 (the most studied connexin) which is not present in the neural retina at all. It is expressed in retinal fibrae circulares, musculi ciliaris, astrocytes, and filamentous processes sheathing the photoreceptors (Schütte 1998, Huang 2005, Massey 2003). Cx50 is also very tissue specific for the A-type horizontal cells. Immunocytochemistry shows that it is localized in the outer plexiform layer below rod bipolar cell dendrites in the outer plexiform layer (O'Brien et. al., 2006).

Cx50 regulation has been reported to have a key role in early postnatal lens development, and is one of the three gap junctions alongside Cx43 and Cx46, whose proper function is key in normal lens development, thus preventing cataract development (Gong et. al., 2007). It has been shown that Cx50 is involved in inhibition of fiber progenitor cells during cell proliferation cycle, resulting in the initiation and promotion of lens cell differentiation (Shi et. al., 2010). The C-terminus of Cx50 forms an alpha-helical structure, and its integrity is reported to be crucial to normal cell differentiation (Banks et. al., 2007). Mutation of Val 365 to Gln at the C-terminus (Fig. 1.9) destabilizes the alpha helix of Cx50 and stops lens cell differentiation (Shi et.al, 2010). Multiple mutations (Fig. 1.9) in the extracellular domains: D47A (E1 Loop), S50P (E1 Loop), V64A (E1 Loop), V64A (E1 Loop), R205G (E2 Loop) results in lack of ability for Cx50 proteins to form gap junctions, highlighting the importance of extracellular domains for docking of gap

junctions. This, resulted in a dense nuclear cataract, smaller lenses, vacuole formation and posterior rupture (DeRosa, 2009). N-terminus mutations of Cx50, G22R resulted in formation of a nuclear cataract, and decreased Cx50 ability for voltage-dependent gating, unitary conductance, and sensitivity to regulation by polyamines, and permeability (Xia et al., 2006).

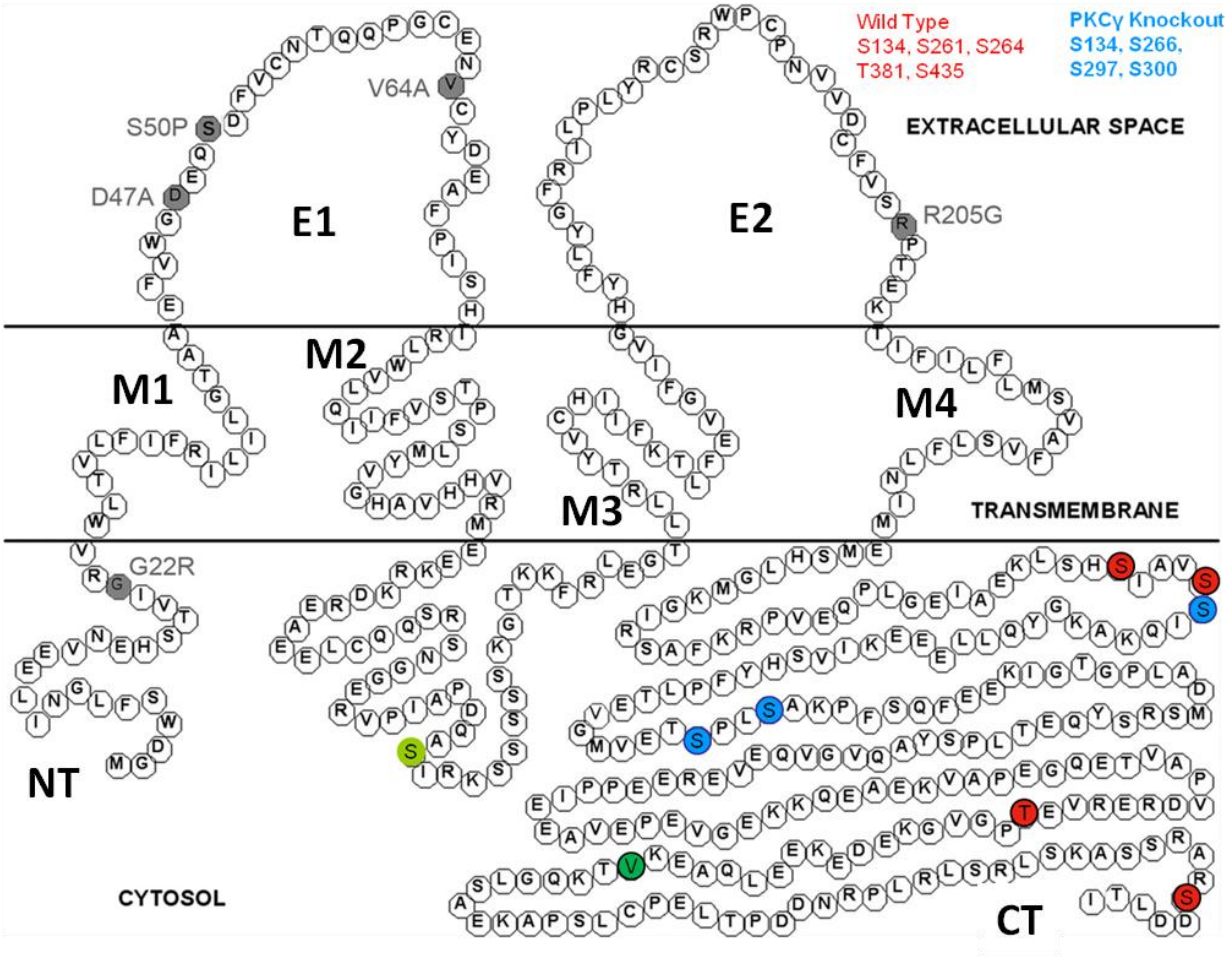

Figure 1-10 Amino Acid Structure and cellular localization of mouse Cx50

Grey - Mutation sites resulting in cataract, Red – possible phosphorylation sites for PKC gamma as proposed through structural studies of Cx43 and how PKCγ might control it, Blue – other phosphorylation sites (MAPK, ERK). V (Valine 365) (green) – its role in the C-terminus responsible for helix formation and differentiation. (Adapted from *Experimental Cell Research* Apr 1;315(6):1063-7. Delarosa et.al. The cataract causing Cx50-S50P mutant inhibits Cx43 and intercellular communication in the lens epithelium. Page 1064, Copyright (2009), with permission from Elsevier, license agreement number 2491440620225).

Phosphorylation of Cx50 also plays a major role in regulation of gap junction activity. Below is a table of all known phosphorylation sites of Cx50.

Phosphorylation Sites	Observed Peptide	Enzyme
S115 singly S118 singly	110–125 114–124 108–127	Trypsin Glu-C Lys-C
S115 þ S118 doubly	110–125	Trypsin
S134	126–136	Trypsin
S258 þ 261 doubly	245–269	Trypsin
S265	258–269	Trypsin, Lys-C
S266	258–269 257–278	Trypsin, Lys-C Glu-C
S266 þ S261 doubly	258–269	Trypsin, Lys-C
S297	281–310 296–309	Trypsin, Lys-C Glu-C
S300	281–310 296–309	Trypsin, Lys-C Glu-C
S297 þ S300 doubly	281–310 296–309	Trypsin, Lys-C Glu-C
T326	311–356	Lys-C
S364	357–378 360–369	Trypsin, Lys-C Glu-C
T404	398–407 403–414	Lys-C Glu-C
T404 þ S410 doubly	408–425 407–414	Trypsin, Lys-C Glu-C
S410 þ S424 þ S427 triply	401–425 403–414	Trypsin Glu-C
S430	408–428	Lys-C
S435	426–432	Trypsin
S430 þ S431 þ S435 triply	426–440	Trypsin

Table 1-1 Phosphorylation Sites of Cx50

Adapted from *Experimental Cell Research* Dec;89(6):898-904. Wang and Schey. Phosphorylation and truncation sites of bovine lens connexin 46 and connexin 50. Page 901, Copyright (2009), with permission from Elsevier, license agreement number 2491441155227).

It has been previously shown that treatment of Cx50 with MAPK and ERK 1/2 specifically increased Cx50 coupling, but not Cx46, and this caused increased levels of lens opacities. When the Cx50 C-terminus was truncated, MAPK/ERK was not able to increase gap

junction coupling (Shakespeare et. al., 2009). This suggests that the C-terminal phosphorylation of Cx50 by MAPK, leads to increased propagation of cellular signals and results in reduction of developmental cell defects. The exact location where MAPK affects Cx50 is still under investigation. Due to Cx43 and Cx50 being in the same family with similar structural alpha helical c-termini, we can suggest several probable sites where phosphorylation of Cx50 can take place (Fig. 1.9).

Connexin 50 is also able to be regulated by PKCs; oxidative and phorbol ester activation of PKCγ was able to disrupt Cx50 gap junctions in dye activity assay in lens epithelial cell line (Lin et al., 2004). It is proposed that this was done through phosphorylation of Cx50. Studies using mouse lens membrane fractions, showed that phosphorylation of Cx50 both on serine and threonine was increased after treatment with hydrogen peroxide (oxidative stress), as detected by reaction with anti- phosphoserine and phospho threonine antibodies (Zampighi et. al., 2003). Treatment with phorbol ester also decreased the formation of gap junctional plaques as detected by electron microscopy using Cx50 antibody gold complexes (Zampighi et. al., 2003).

1.7 Model for PKCγ being as a neuroprotective stress sensor kinase.

Neural tissues e.g. brain and retina are very susceptible to oxidative damage. We propose that PKCγ has evolved into having "stress sensor" kinase functions. The PKCγ C1B region is highly sensitive to oxidative signals and reactive oxygen species. Upon activation PKCγ translocates to the plasma membrane and inhibits gap junctions (Fig. 1.10). Gap junctions have been called both "Good Samaritans" and "Executioners", terms which refer to their ability to pass both necessary metabolites and apoptotic signals from cell to cell (Kistler et al., 1995; Le and Musil, 1998). It is our theory that PKC gamma dependent inhibition of the spread of apoptotic signals that result from accumulation of ROS, is due to the ability of PKC gamma to shut down gap junctions by a phosphorylation dependent mechanism. We have previously shown in our lab, through use of a PKC gamma knockout mice model, that oxidative stress treatment by H_2O_2 resulted in increased lens opacification (cataract) in PKCγ knockout mice compared to controls. Biochemical analyses of lens membrane proteins in the PKCγ knockout and control models also showed that H_2O_2 activation of endogenous PKCγ resulted in phosphorylation of Cx50 and subsequent inhibition of gap junctions in the lenses of control mice,

but not in the knockout mice (Lin et. al., 2006). The purpose of this dissertation is to evaluate PKC gamma dependent neuro-protective effects on a structural and functional level in a PKC gamma knock-out mouse retina model.

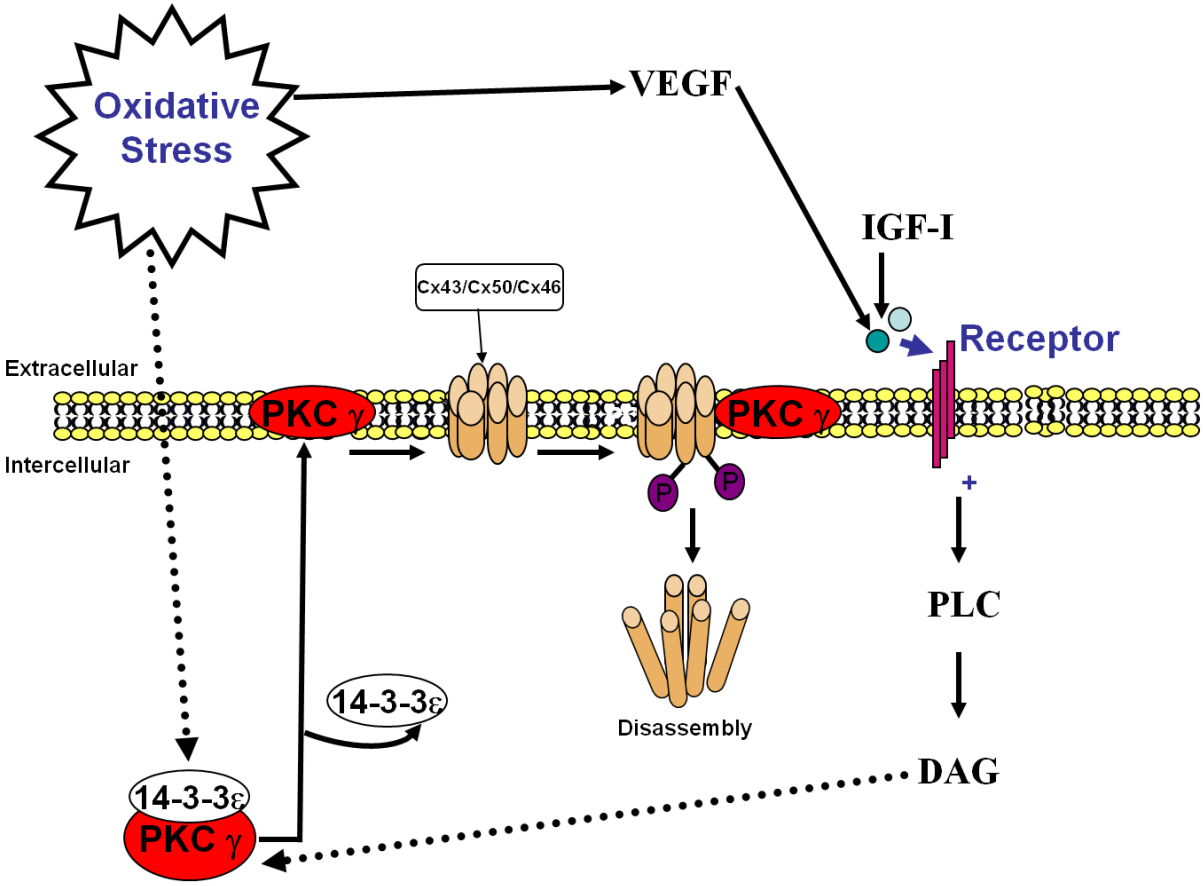

Figure 1-11 Model of Neuro-protection from Oxidative Stress

14-3-3ε docking protein separates from PKCγ, due to breakage of disulfide bonds in the C1B domain; PKCγ translocates to the membrane, where it phosphorylates gap junctions making them inactive, and in some cases leading to disassembly. Oxidative stress also can activate VEGF, which is a possible pathway of activation of PKC gamma through Phospho-Lipase C and Diacyl Glycerol. (Figure is from Takemoto lab, put together with permission from D.J. Takemoto).

CHAPTER 2 - Structure and Electrophysiology of the Retina is Altered in PKCγ Knockout Mice

2.1 Introduction

Protein Kinase C (PKC) belongs to a class of serine/threonine protein kinases and consists of at least eleven isoforms (Newton, 2001; Goldberg and Steinberg, 1996). All the isoforms are divided into three groups. All of the PKC family members have unique activation cascade: conventional PKCs are activated by diacylglycerol (DAG) and calcium, novel PKCs are activated by DAG but not by calcium, and atypical PKCs are not activated by either DAG or calcium. In this chapter the main focus will be on PKCγ, which belongs to the conventional PKCs (Newton, 2001). Some of the major functions of PKCs are receptor desensitization, modulating membrane structure events, regulating transcription, mediating immune response and phosphorylating growth factor receptors, ion channels, structural proteins and gap junction connexin proteins (Newton, 2010). Besides being an integral part of signal transduction pathways, PKC isoenzymes play an important role in control of cellular proliferation and differentiation in a variety of cells (Clemens et. al., 1992). PKCγ also has been shown to have an effect on nerve damage. In peripheral nerves PKCγ translocates to sites of nerve damage thus reducing pain sensitivity (Ohsawa et al., 2001; Mao et al., 1995). Presence of PKCγ in brain tissue (neuronal tissue) has been shown to prevent brain ischemia. Missense mutations (H101Y, G118D, S119P, G128D, or F643L) in PKCγ cause dominant non-episodic cerebella ataxia in humans (Adachi, 2008), signifying that PKCγ -related and polyglutamine-related neurodegeneration might have a similar neuronal cell damage and death in hereditary ataxia (Asai, 2009). Since oxidative damage is known to be involved in neurodegeneration (Seki, 2005), proteins that respond to oxidative stress would be critical for the health of neural tissues. PKC gamma has also been recently shown to be playing an important part in retinal neovascularization, which it does through Vascular Endothelial Growth Factors (VEGF). It was shown that VEGF activates PKC gamma via Src-dependent PLD1 stimulation and that using PKCγ siRNA to reduce the signaling, resulted in suppression of hypoxia-induced retinal neovascularization (Zhang et al, 2010). VEGF has long been known to be an important mediator in vascular pathological retinal angiogenesis and it is the most potent growth factor in

stimulating retinal angiogenesis under hypoxic conditions (Gariano et. al., 2005, Kermorvant-Duchemin et. al., 2010). Thus, PKC gamma could be an essential protein in progression of several diseases, including atherosclerosis, cancer, and a leading cause of blindness in the United States, diabetic retinopathy (Campochiaro et. al., 2000, Duda et. al, 2006).

PKCs are found in the bow and cortex region of the lens (Gonzales et. al., 1993), in retina (Fugisawa et. al., 1992), cornea (Bazan et. al., 1987) and retinal and lens epithelial cells in culture (Wagner et. al., 2002). In retina it was shown that PKC antiserum preferentially reacts with rod bipolar cells (Negishi et al., 1988). Antibodies against PKCα are currently used as a marker for rod bipolar cells, which are located in the Inner Nuclear Layer (INL), Outer Plexiform Layer (OPL) and Inner Plexiform Layer (IPL) (Greferath et al., 1990). Antisera against PKC β antibodies have immunoreactivity with amacrine, terminal processes in IPL and in the ganglion cell layer (GCL) (Osborne et al., 1992). PKCγ has been previously shown to have immunoreactivity with amacrine cells in the inner plexiform layer (Osborne et al., 1992; O'Brian et. al., 2006).

The goal of this study is to determine the structural effects on the retina when PKCγ is knocked out. As the structural effects are determined, functional approach could be taken to determine the exact nature of PKC gamma functional role in the retina. This enzyme could control gap junctions in retina as is reported to occur in lens (Saleh and Takemoto, 2000). PKCγ is located in the OPL, IPL, and ganglion layers. Cx50 is a major retinal gap junction that is primarily localized in the outer plexiform layer. Although levels of Cx50 are not changed in the PKCγ knockout mice, a loss of PKCγ could alter retinal structure or function in these regions, in part because of altered control of gap junctions in retina.

2.2 Materials and Methods

2.2.1 Animals

*C*ontrol, 6 week old mice (B6129pf2/j100903) and 6 week old PKCγ knock-out mice (B6;129p-Prkcctm1St1) were purchased from Jackson Laboratory (Bar Harbor, MA). Mice were euthanized using CO_2, followed by cervical dislocation. This is as IACUC approved and is consistent with the recommendations of the Panel on Euthanasia of the American Veterinary Medical Association. All experiments conformed to the ARVO Statement for Use of Animals in Ophthalmic and Vision Research and were performed under an institutionally approved animal protocol.

2.2.2 Western Blot

Mouse retina tissues were collected within 5 min of sacrifice, and taken up in 2X SDS-PAGE sample buffer (100mM Tris-HCl, pH 6.8, 200 mM Dithiothreitol (DTT) from Ampresco (Solon, Ohio), 4% Sodium Dodecyl Sulfate (SDS) from Ampresco (Solon, Ohio), 0.2% bromophenol blue from Ampresco (Solon, Ohio), 20% glycerol from Fisher Scientific (Pittsburgh, PA), 50 µL/retina). Proteins were separated on 12.5% SDS-PAGE (40 µg retinal protein/lane) and continued with Western blots using monoclonal mouse anti PKCγ antibodies (1:1000) from Sigma (Dallas, TX). Immunoreactive bands were detected by chemiluminescence (ECL; Pierce, Rockford, IL).

2.2.3 Light Microscopy

Eyes were dissected out of six to fourteen week old mice, fixed in 2% paraformaldehyde, 2.5% glutaraldehyde from Sigma (Dallas, Tx), 0.1M cacodylate (Electron Microscopy Science (EMS), Fort Washington, PA) then post-fixed with osmium tetroxide (EMS). This was followed by dehydration with 70% alcohol for 12 hours, then by 100% alcohol overnight and with 100% acetone for 12 hr then embedding in epon (LX112) (EMS.) Sectioning was done using a Reichter-Jung Ultracut E Ultramicrotome (Cambridge Instruments Inc., Buffalo, New York) at

room temperature. Sections were taken perpendicular to the optic nerve so that all of the layers of the retina could be observed. Eyes were sectioned to the point until the optic nerve was observed, so the depth was consistent in all of the sections. Thick sections (2-50 μm) were obtained using a diamond knife, then stained with 1% (w/v) toluidine blue (EMS) and viewed using a Nikon Eclipse E600 light microscope **(**Nikon Inc. Melville, New York) (4-100X). Exact locations were confirmed by low magnification photos (4-100X) and analyzed using analySIS software (Soft Imaging System GmbH; Munster, Germany). Statistical analyses were done using Origin 5.0 (MicroCal Software Inc., Northampton, MA).

2.2.4 Electron Microscopy

Ultra-thin silver and gold serial sections (80-95 nm) were cut using a diamond ultraknife (Diatome-US, Hatfield, PA) and placed on copper grids (Ted Pella, Redding, CA). Grids were stained with 2% (w/v) uranyl acetate (EMS) and 2% (w/v) lead citrate (EMS) in a humidified chamber. Pictures were taken using a Hitachi H-300 electron microscope (Schaumburg, IL). EM photos were taken on the right side of each retina for all the separate layers (approximately 250 μm, 550 μm and 880 μm away from the optic nerve).

2.2.5 Immunocytochemistry

Cryostat sections (100 μm) of retinas were fixed in 2% paraformaldehyde, washed 3 times with PBS .3%TritonX 100 buffer, blocked with 5% Normal Goat Serum (Santa Cruz Biotech, Ca, number 2043), labeled with primary antisera Mouse anti PKC gamma dilution 1 to 250 (Zymed San Francisco, CA, number 33-4300), then secondary Alexa Fluor 488 tagged antisera (Molecular Probes, Eugene, OR number A21042). Sections were stained with 4', 6' diamino-2 phenylindole dihydrochloride (DAPI) Hoechst dye (Molecular probes, Eugene, OR number D1306 (Blue stain) for 2 seconds, washed with PBS 0.3%TritonX 100 buffer, then viewed using a Nikon Eclipse E600 light microscope (Nikon Inc. Melville, New York).

2.2.6 Electroretinogram (ERG)

ERG's were performed on 4 week old control and knockout dark adapted mice. Mice were anesthesized using a single intraperitoneal injection of Telazol (40mg/kg) (Fort Dodge, Fort Dodge IA). Pupils were dilated with 1 drop of topical 1% tropicamide ophthalmic solution (Bausch & Lomb, Tampa FL). Mice were hand held during the experiment. A fine needle electrode was placed under the skin at the side of the face and back of the head. The wire electrode was placed in the conjunctival sac of the eye. Electrical recordings were taken on an Electroretinogram computer (ErtinoGraphics, Norwalk CT). ERG's were recorded at blue light (450 nm) in response to single flash averaged over 8 flashes. Settings were 5 msec/division and 10 microV/division. Statistical analysis was done using Origin 5.0 (MicroCal Software, Inc., Northampton, MA).

2.3 Results

2.3.1 Western Blot demonstrate no PKCγ in knockout mouse retina.

PKC gamma knockout mice are a well studied model that has been reported in multitude of publications. Still western blot analyses were performed to confirm a lack of PKCγ protein in the PKCγ knockout mouse retinas. Fig. 2.1 illustrates the results from retinas of a 6 week old control and knockout mouse. This result shows that knockout mice have no detectable PKCγ in the retina.

2.3.2 Light Microscopy demonstrates structural changes in knockout mouse retinas.

All eyes were sectioned perpendicular to the optic nerve, so that we were able to achieve the view of all 7 retinal layers. To keep all eyes at equal sectioning depth eyes were sectioned until the optic nerve was visible (Fig. 2.2). The widths of all the layers were determined at 250 µm, 550µm and 880 µm from the optic nerve. Average thicknesses for control retinas of all the layers: (RPE = retinal pigment epithelial layer, OS = outer segment, ONL = outer nuclear layer, OPL – outer plexiform layer, INL = inner nuclear layer, IPL = inner plexiform layer): is seen in the Table 2.1.

When comparing thicknesses of control vs. knockout mouse retinas, the INL in some retinas as can be seen in Fig. 2.2 in that particular retina was ~30% thicker (2.2C vs 2.2G), this was due to the formation of vacuoles (empty space) between the cells (shown as circles, Fig.2.2). These increases in thickness, when numbers were averaged among many retinas (n=12), were not significant, though vacuoles appeared in all INL of knock out retina. A count of the number of nuclei per area in the ONL demonstrated that total numbers of nuclei were reduced by ~20% at the central retina of knockout vs. control retina (Fig. 2.2 (B vs F) and Table 2.2). The vacuoles which were observed in the PKCγ knockout retina (Fig. 2.2) were responsible for the increase in thickness in some cases and reduction of total amount of nuclei in the INL, ONL, GCL (Table 2.2). The nuclei numbers among those layers were statistically different for control $p \leq 0.05$.

The ONL of the knockout retinas had 9-10 layers of nuclei vs. 10-11 layers of nuclei in the control retinas. This fact was not reflected in the thickness measurements, which was probably because of increased space (due to formation of vacuoles, resulting in overall reduction of nuclei per unit area) (Table 2.2).

The photoreceptor layers and the inner plexiform layers (IPL) were comparable in the control and knockout mouse retinas.

The greatest difference was observed in the OPL. This layer was completely un-defined in majority of the retinas (Fig 2.2); it had vacuoles and lacked any kind of organization or structure (Fig 2.2). The OPL of control retina appeared normal (Fig. 2.2). As OPL of the KOγ was much disorganized, OPL was further explored using electron microscopy (EM).

2.3.3 Electron Microscopy demonstrated additional disorganization of the OPL and IPL in KOγ retina

To explore the details of the disorganization of the IPL (Fig. 2.3) and OPL (Fig. 2.4) EM at 10,000x was done. The presence of unidentifiable structures in the OPL of the knockout retinas is apparent from Fig. 2.4 (U). These very dense structures could represent myelination of the cell, meaning that by knocking out PKCγ we disrupt normal functioning of several cells causing myelination. There were no myelinated cells found in the control retina (Fig 2.3 and Fig 2.4).

Rod bipolar and rod sphericules were present in both control and KOγ (Fig. 2.3 and Fig 2.4) (identified from Kolb, 1977), but rod bipolar cells in KOγ seem to be in disarray. In control retinas all the bipolar cells were correctly placed close to the cone pedicle and all the synapses could be clearly seen.

In Fig. 2.3 we can observe the ultra-structures in the IPL that were obtained using Electron Microscopy techniques. Results indicate that Control and KOγ ultrastructures are almost identical. Knocking out PKCγ does not seem to affect the quantity of amacrine cells. Ribbon and amacrine synapses were found both in control and KOγ mouse retinas.

Synaptic ribbons (identified from Rhodin, 1974) were present in both control and knock-out retinas (Fig 2.3). Presences of basal junctions (identified from Kolb and Jones, 1984) were detected in both OPLs from control and KOγ retina and were similar.

One of the more dramatic ultra structural differences was observed in horizontal cell arrangement and the synaptic organization within them. Horizontal cells were not found in the KOγ retina. OPL primarily consists of bipolar cells and horizontal cells, there were no horizontal cells in the KOγ retinas. Synaptic ribbons were still present (Fig. 2.4), but overall appearance of KOγ retinas was that of disarray (Fig. 2.4). The synaptic tetrads (as seen in Fig. 2.4 and marked as ST) in which bipolar and horizontal cells organize into a rosette structures was not seen in KOγ retina while it was normal in control retina.

2.3.4 PKCγ immunolocalizes in OPL, IPL and ganglion layer

Retinal localization of PKCγ was explored through immunolabeling with PKC gamma antibody. From Fig. 2.5 it can be observed that PKCγ had the highest immune-reactivity in the outer plexiform layer. The PKCγ was also detected in inner plexiform layer and ganglion layer (Fig. 2.5). PKCγ KO retinas were also stained with PKC antibodies to confirm what western blot analysis previously shown, that there is no detectable PKC gamma in the KO mouse retinas. There was no detectable PKC gamma present in inner and outer nuclear layers, the only layer that has nuclei that PKC γ was detected in was GCL. PKC gamma was primarily detected in plexiform layers where communication between cells takes place, indicating that PKC gamma possibly plays an important role in cellular communication.

2.3.5 Electroretinography (ERG) shows reduction in electrophysiological response in KOγ mice

ERG was performed to study the physiological functioning of the KOγ mice retina. ERG shows the intensity dependence and spectral sensitivity of the responses to light. In Fig. 2.6 we can demonstrate that the control retina has a normal **A** wave (wave #1), suggesting that rods have normal function. Wave #2 (**B**) bipolar cells ERG from control retina had a normal wave pattern. In KOγ mice there was no detectable **A** or **B** wave. This result showed from a functional standpoint that the presence of PKC gamma is essential for normal retinal functioning like e.g. light detection. This effect could be because PKC gamma plays a role in regulating cellular communication, which is achieved in retina primarily through gap junction proteins. Structural disruption that was noted in retina led to physiological functional change, this means that

presence PKC gamma which is a known regulator of gap junctions is needed for functional vision to occur. B-wave in part comes from cells in the OPL, lack of signal goes along with the structural data presented above. This result indicates that PKC gamma in part regulates cellular communication through gap junctions. Cx50 is of particular interest as it is the major connexin in the outer plexiform layer, the layer that was most structurally affected in PKCγ knockout mice.

2.4 Discussion

Results from this study clearly demonstrate that retina from the KOγ mice have altered structure (as shown by light and electron microscopy) and function (as shown by ERG). This result follows the path of several other studies where it was shown that KOγ alters normal functioning. Some of those studies indicate that mice show less pain sensitivity (Ohsawa et al., 2001; Mao et al., 1995) and that protection against brain ischemia is reduced (Aronowski et al., 2000; Asai 2009). Structural studies showing abnormal organization of the retina have not previously been shown.

PKCγ is an important enzyme in the signal transduction pathway. One of its functions is to regulate gap junction signaling (Das et.al., 2008; Newton, 2010). By knocking out such an important enzyme we disrupt the signal transduction communication pathway and, as this data shows, we also disrupt the normal structure and function of retina on a cellular level.

The outer plexiform layer consists of bipolar and horizontal cells. Although PKCγ has previously been noticed in ganglion and amacrine cells, we observed significant disorganization of the OPL (Fig 2.4) layer where ganglion and amacrine cells are absent. There were a reduced number of synapses, creation of new structures and lack of rosettes. Immunocytochemistry confirmed that PKCγ is present in the OPL (Fig. 2.5). This result indicates that PKCγ is found in more than just amacrine cells (as some of the previous studies suggested). Our data shows that PKCγ was heavily present in OPL layer which consist of both bipolar and horizontal cells.

All this indicates that PKCγ plays an important role in organization of retinal layers, in particular the cell communication layers, OPL and IPL. The inner nuclear layer, which consists of amacrine, bipolar and ganglion cells, surprisingly did not have detectable PKC gamma and was structurally only barely affected through formation of vacuoles in the KO model (Fig. 2.2), Analysis of most disrupted layers and its retinal location indicate that PKCγ primarily is involved in the cellular communication.

The function of the retina was clearly affected, which can be seen from Fig. 2.6 KOγ mice lost any kind of response to light which indicates that the functioning of the retina is disrupted. Both the **A-**wave and the **B-**wave responses were lost. **B-**wave represents bipolar cell responses. As previously stated, bipolar cells were present in the IPL, OPL layers of the retina, which coincidently are the exact same layers PKCγ is very prominent. Functional responses as

measured by ERG result, are consistent with the structural study measured by electron microscopy. A-wave represents photoreceptor responses, which are located in the outer segment. The outer segment does not seem to be disorganized so there is no structural explanation for loss of the A-wave but we can speculate that it was due to the disruption of the signal transduction pathway.

The result of this study clearly demonstrates that the presence of PKCγ is essential for normal functioning and organization of retina. PKCγ is a known regulator of gap junctions, so this regulation of connexins in part could be the reason for PKCγ needed presence for structural and functional integrity. In the next chapter we will explore how the presence of PKCγ has on the retina structure when retina is exposed to oxidative stress. Oxidative stress has been previously reported to have the ability to activate PKCγ , and role of PKC gamma will be explored in its ability to protect retina structure from oxidative stress. This neuroprotective effect is achieved in part due to PKCγ ability to control gap junctions. Cx50 is of particular interest as it is one of two connexins that are found in the OPL (most disrupted layer from our study). Oxidative stress caused by hyperbaric oxygen (in vivo), will be used to evaluate PKCγ neuroprotective affect, and what happens to Cx50 gap junctions after exposure to oxidative stress in PKCγ knock out and control mice.

2.5 Figures

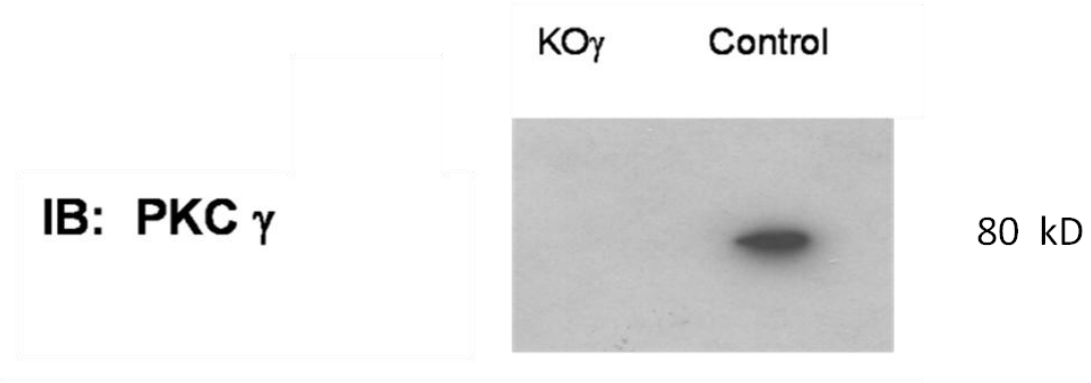

Figure 2-1 PKCγ in Retina Tissue

Whole retina from 6-week old control or PKCγ knockout (KOγ) mice were loaded in sample buffer at 40 μg protein/lane. Immunoblots using mouse anti-PKCγ antisera at 1:1000. Experiment was done in triplicate.

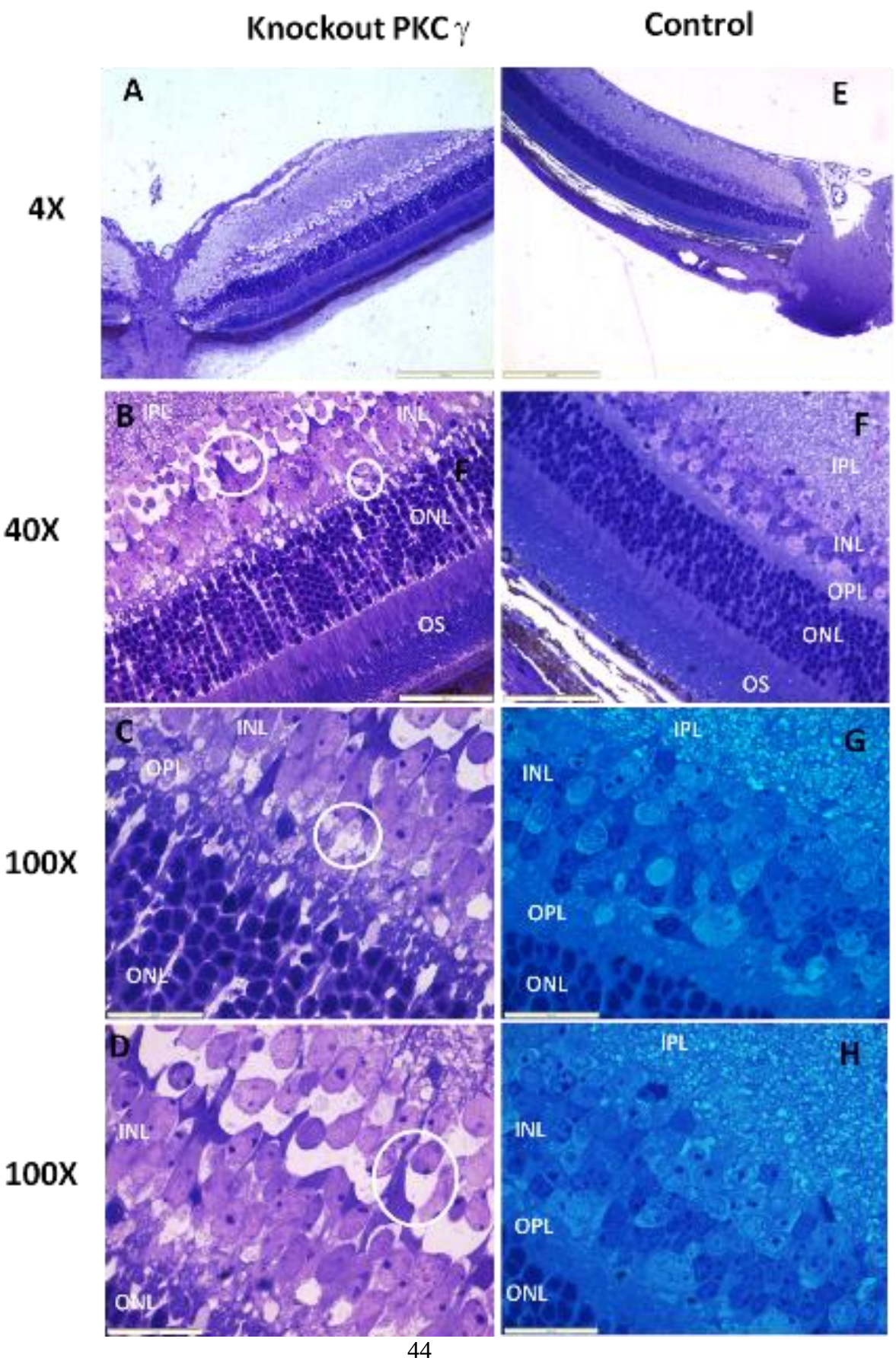
Knockout PKC γ
Control
4X
40X
100X
100X
A
E
B
IPL
INL
F
ONL
OS
F
IPL
INL
OPL
ONL
OS
C
INL
OPL
ONL
IPL
G
INL
OPL
ONL
D
INL
ONL
IPL
H
INL
OPL
ONL

Figure 2-2 Light microscopy structure of PKCγ Knockout Mice Retina

Boxes A and E, show the whole retina and optic nerve at 4X magnification. B and F show all the layers of Retina at 40 X magnification. C,D and G,H focus on the Inner Nuclear Layer (INL) and Outer Plexiform Layer (OPL) at 100X magnification. C and G are at approx 250 μm from optic nerve. D and H are approx 800 μm from the optic nerve. All mice were six weeks of age when they were euthanized. IPL = inner plexiform layer. OS = outer segments. ONL = outer nuclear layer. INL = inner nuclear layer. OPL = outer plexiform layer. A-E – PKCγ KO (knockout) knockout mice. E-H – control mice retinas.

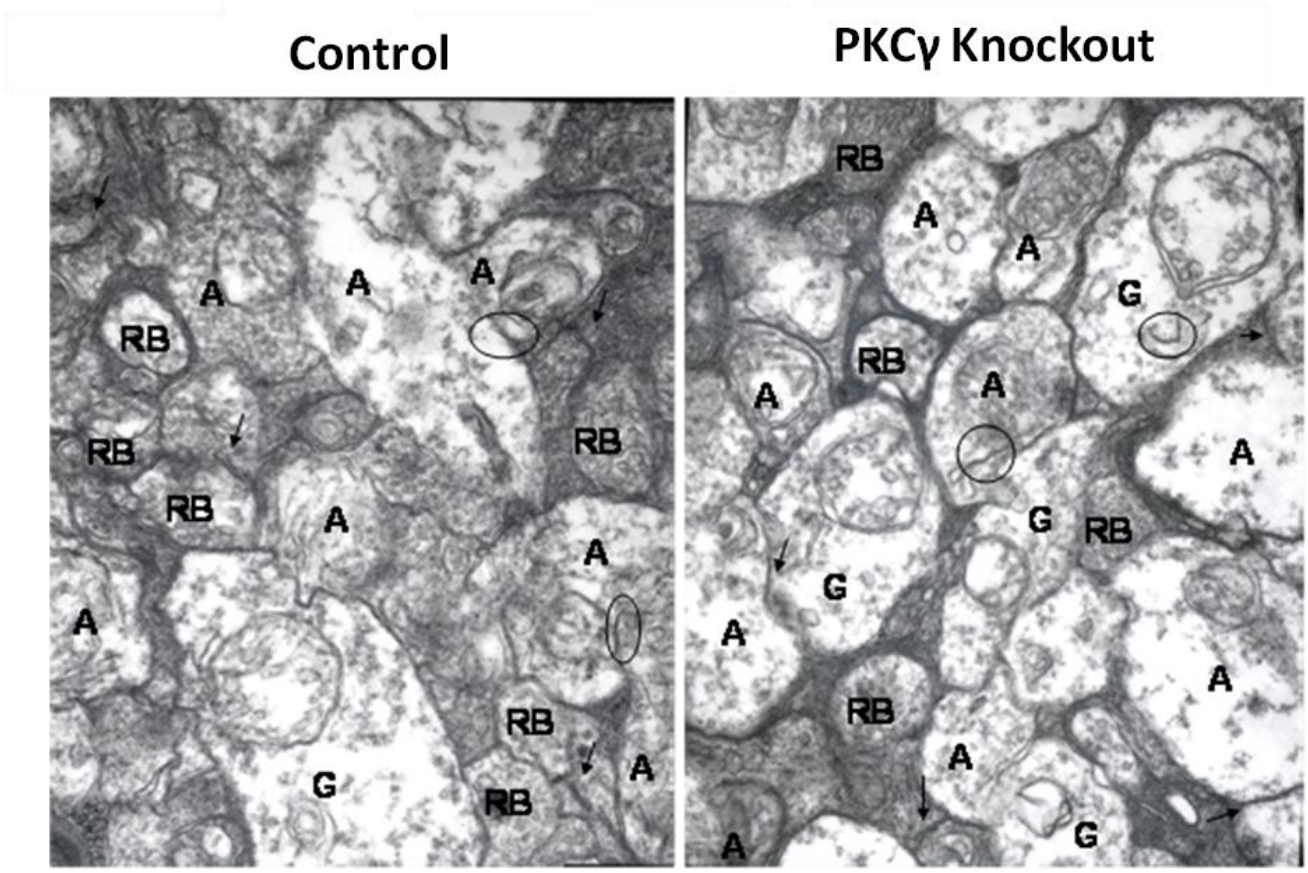

Figure 2-3 Electron Microscopy of Inner Plexiform Layer

Inner plexiform layer observed with Electron Microscope. 20,000X magnification, G = ganglion cell; A = amacrine cell; RB = Rod bipolar cell; Arrows are ribbon synapses; circles are amacrine synapses. Mice were 6-weeks of age at time of euthanasia..

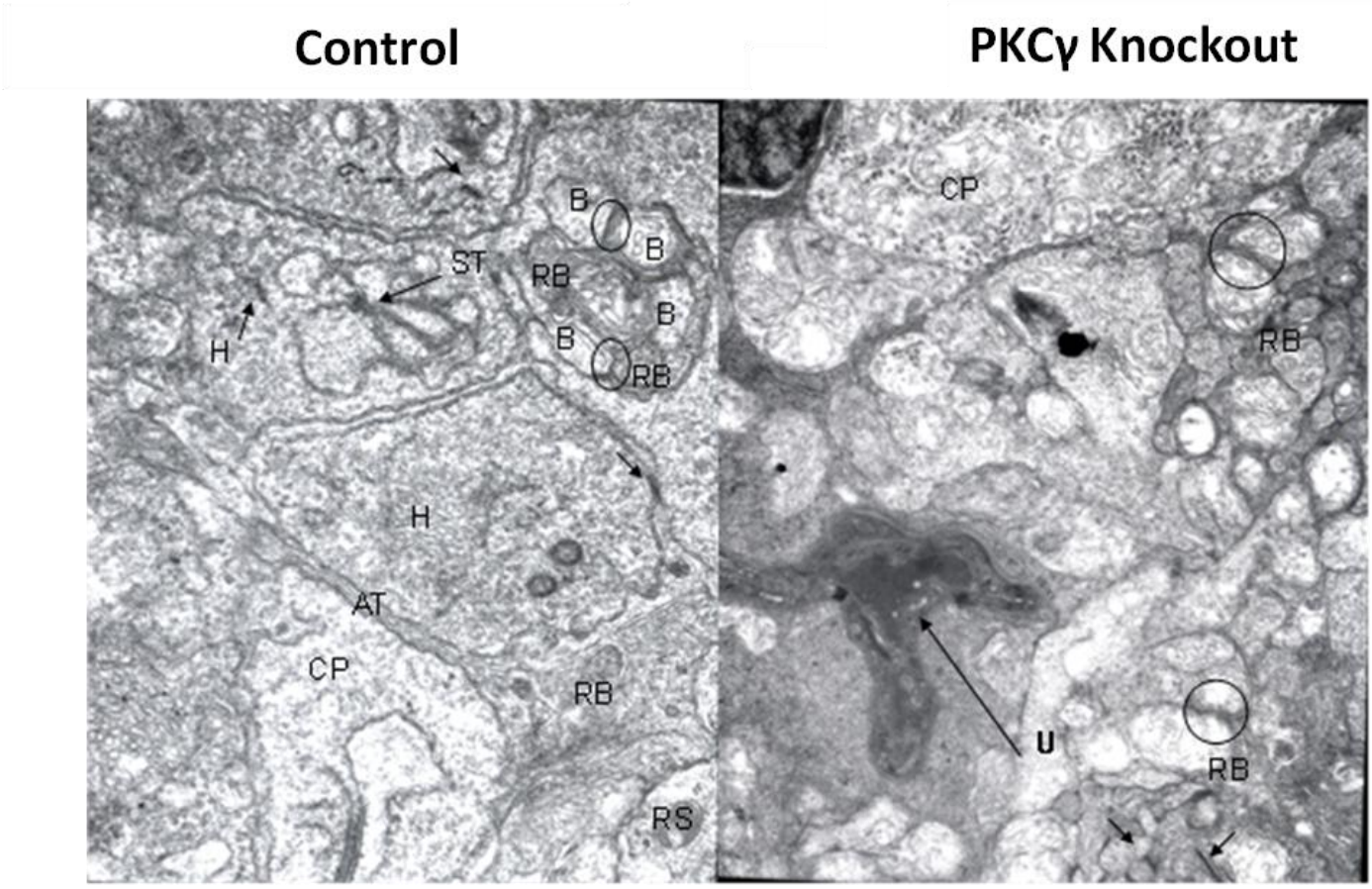

Figure 2-4 Electron Microscopy of Outer Plexiform Layer

20,000X magnification on 6 week old mice outer plexiform layer of retina. Arrows indicate synaptic ribbons. RB = rod bipolar cell, H = horizontal cell, CP- cone Pedicle, AT= axon terminals, B= bipolar cells, ST = bipolar process of synaptic tetrads, circles are basal junctions. U = unidentifiable structure.

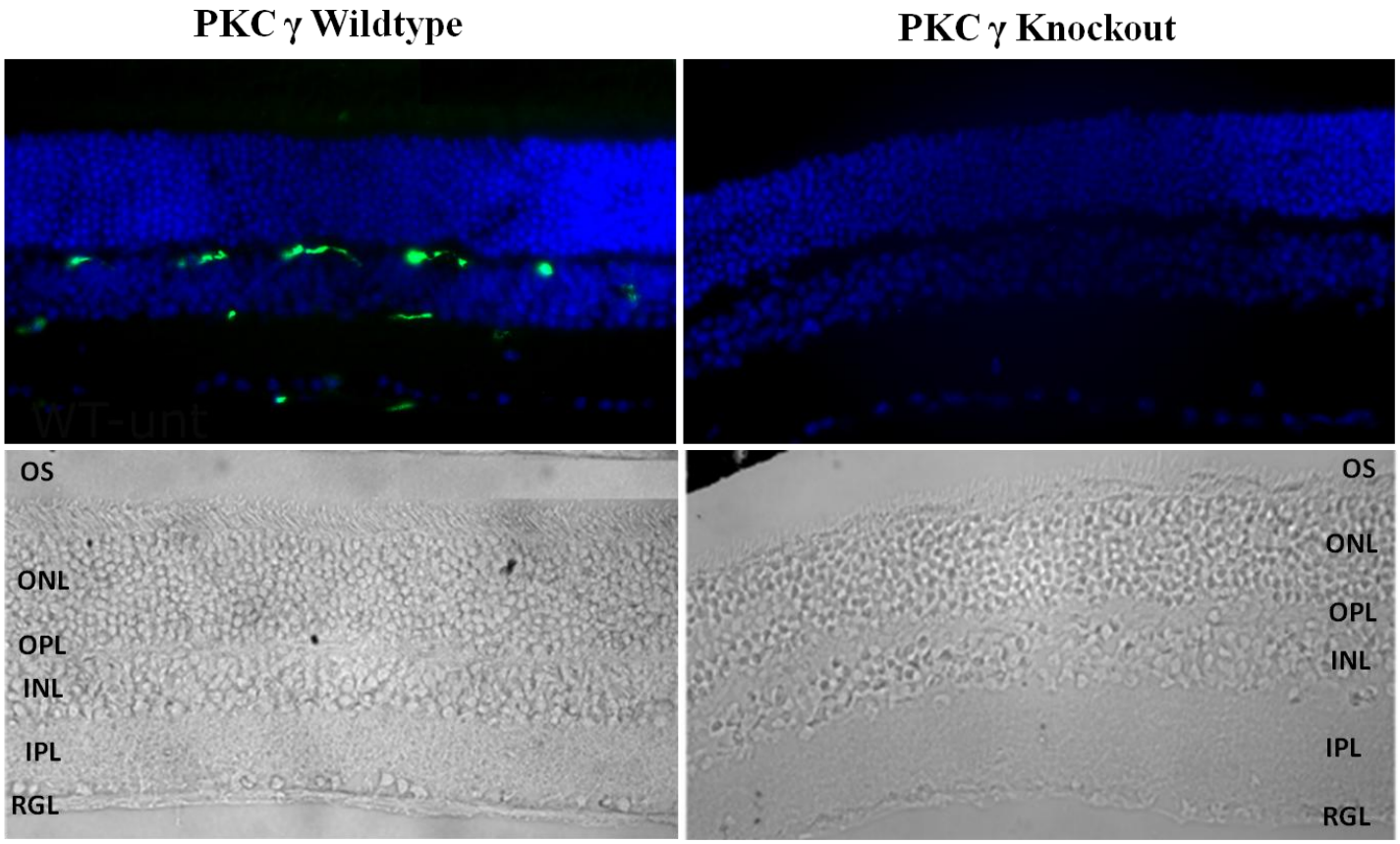

Figure 2-5 Retinal Localization of PKCγ

6-week old mice retinas were observed by fluorescent microscopy. Cell nuclei are colored blue with DAPI. Green Fluorescence from PKCγ is seen in the Outer Plexiform layer, Inner Plexiform layer and Retinal Ganglion layer. PKC gamma knockout retinas do not exhibit any fluorescence in response to PKCγ antibody. The two bottom images are a black and white picture of the same retinas as on top, to help with layer visualization. All layers can be clearly observed in Black and white images.

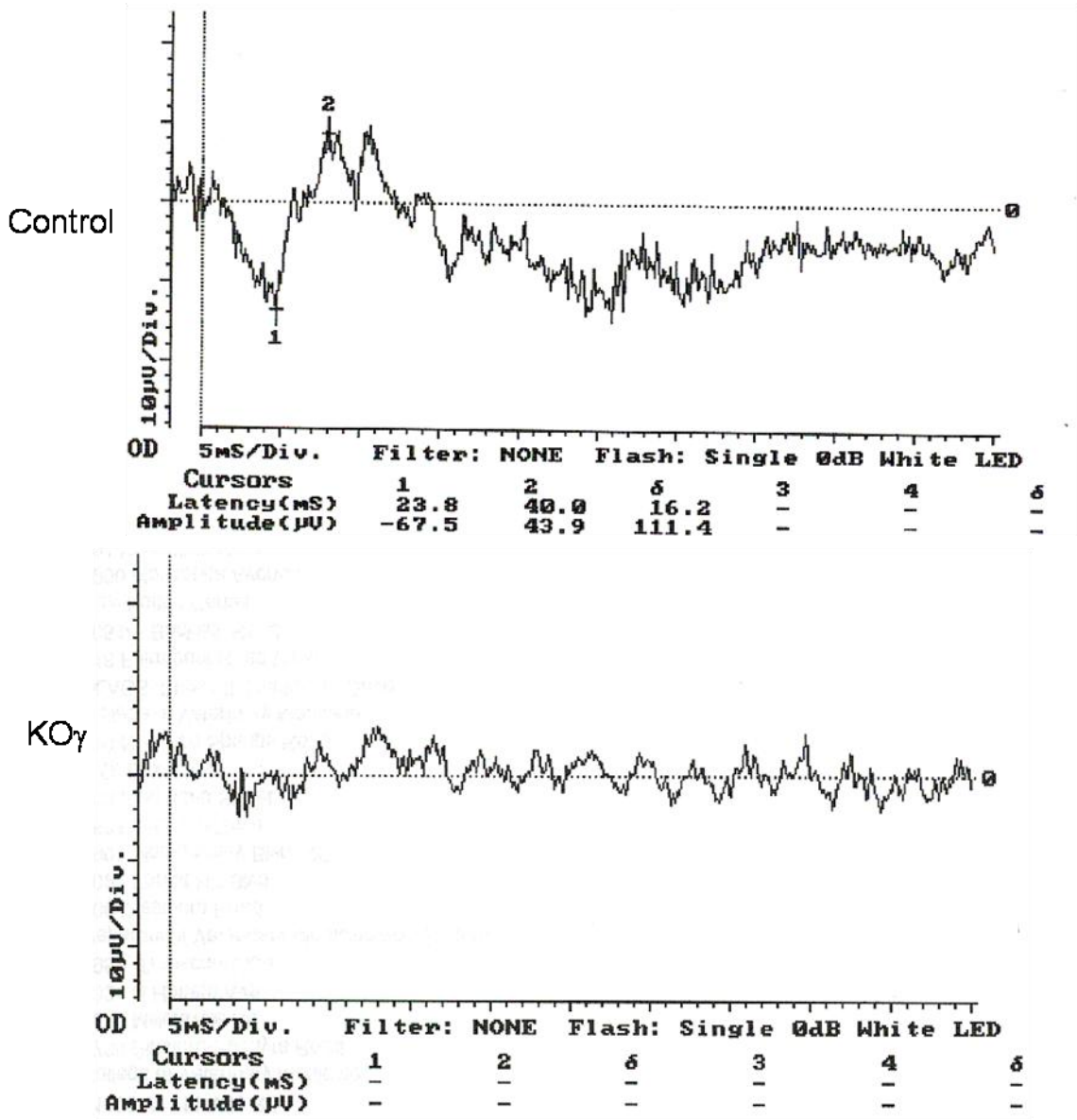

Figure 2-6 Functional response to light measured by Electroretinogram (in vivo)

ERG's were recorded at blue light 450 nm in response to single flash averaged over 8 flashes. Settings were 5 msec/division and 10 microV/division. Mice were 4 weeks old at the time of the procedure. Wave 1 – A-wave – tests the response of rod photoreceptor cells. Wave 2 –B-wave – tests the response for bipolar cells.

	~250µm	~559µm	~880µm
C RPE	6.65µm	4.76µm	5.06µm
KO γ RPE	5.51µm	5.85µm	5.85µm
C OS	23.1µm	20.6µm	19.82µm
KO γ OS	25.1µm	26.3µm	23.1µm
C ONL	35.6µm	32.09µm	30.64µm
KO γ ONL	37.2µm	34.64µm	32.64µm
C OPL	8.85µm	8.49µm	7.64µm
KO γ OPL			
C INL	33.47µm	32.83µm	29.1µm
KO γ INL	34.5µm	33.5µm	31.3µm
C IPL	46.93µm	46.15µm	41.41µm
KO γ IPL	50.95µm	49.71µm	45.33µm

Table 2-1 Thickness of Retinal layers

C = 6 week old control mice; KOγ = 6 week old knockout mice; RPE = retinal pigment epithelial layer; OS = outer segment; ONL = outer nuclear layer; OPL = outer plexiform layer; INL = inner nuclear layer; IPL = inner plexiform layer

Top numbers indicate distance from optic nerve where measurements were taken from

Results expressed as +/- SEM of 4 samples

~250 μm	INL	ONL	GCL
C	19±.68	57±2.6	12±1.8
KO	14±1.4**	43.6±3.1**	7.8±.9**
~880 μm			
C	18±1.7	48.0±2.0	10±1.2
KO	15±.6**	43.4±2.4	7.5±.8

Table 2-2 Amount of Nuclei in Inner, Outer, and Ganglion cell layers

Amount of nuclei is expressed as per 1000 μm^2 area. C – 6 week old control mice; KO – 6 week old PKCγ knockout mice; INL- inner nuclear layer; ONL – Outer nuclear layer, GCL – ganglion cell layer, Central – 250 μm away from optic nerve; Peripheral – 880 μm away from optic nerve; Results expressed as ± SEM of 4 sample retinas for each recording.

** Results are statistically different for control, $p \leq 0.05$

CHAPTER 3 - Loss of PKCγ in the Knockout Mouse Causes Increased Sensitivity to Hyperbaric Oxygen. Role of Gap Junction protein Cx50 is explored in this process.

Authors note: Figures and Data in this chapter are reprinted from the article:

Yevseyenkov VV, Das S, Lin D, Willard L, Davidson H, Sitaramayya A, Giblin FJ, Dang L, Takemoto DJ. (2009) Loss of protein kinase Cgamma in knockout mice and increased retinal sensitivity to hyperbaric oxygen. *Archives Ophthalmology.* Apr;127(4):500-6.

It can be found http://archopht.ama-assn.org/cgi/content/full/127/4/500 .

3.1 Introduction

Gap junctions have been called both "Good Samaritans" and "Executioners" (Ripps, 2002), terms which refer to their ability to pass both necessary metabolites and apoptotic signals from cell to cell. It has been suggested that this spread of cell death takes place through open gap junctions, a process referred to as the "Bystander Effect" (Ripps, 2002). The passage of apoptotic signals through gap junctions has been linked to oxidative cell death in retinal ischemia (Kamphuis et. al., 2007; Naus et. al., 2001, Frantseva et. al., 2002). Retinal gap junction proteins such as Connexin 43 (Cx43) or Cx50, play important roles in retinal function and defects in the control of these gap junction proteins may cause retinal cell death (Cusato et. al., 2003, Schutte et. al., 1998, Huang et. al., 2005, Massey et. al., 2003). In retinal and lens cells in culture the gap junction proteins, Cx43 and Cx50, are inhibited after phosphorylation by protein kinase C-γ (PKCγ), a process which is controlled by cell oxidative state (Lin et. al., 2003, 2004, 2005).

Previous studies of the PKCγ knockout mice showed reduced pain sensitivity and reduced protection against brain ischemia (Adachi et. al., 2008, Katsura et. al., 1999). However, no study has previously shown the affect on these knockout animals' retina, a tissue with known sensitivity to ischemia or changes in oxygen.

Spinocerebellar ataxias (SCAs) are heterogeneous, autosomal dominant neurodegenerative disorders clinically characterized by various symptoms, such as progressive ataxia of gait and limbs, cerebral dysarthria, and abnormal eye movement (Soong et. al., 2007). Currently, 28 genetic loci have been linked to the clinical phenotype of SCA and 14 causative genes have been identified (Soong et. al., 2007). SCA14 is caused by mutations in the PKCγ gene (Chen et. al., 2003) a classical PKC isoform expressed primarily in the CNS, peripheral nerves, retina and lens. SCA14 is a very slowly progressive ataxia mostly affecting gait and limb coordination with onset age as early as three years (Chen et. al., 2003, Vlak et. al., 2006). PKCγ consists of C1 and C2 regulatory domains and C3 and C4 catalytic domains. The C1 domain contains two tandem repeat, Cys-rich regions, C1A and C1B. In families with SCA14, more than 20 missense coding mutations have been identified in PKCγ. Although the SCA14 mutations occur throughout the PKCγ gene from the regulatory to catalytic domains and also include a six-pair in-frame deletion (ΔK100-H101); most mutations occur in the C1B regulatory domain (Seki et. al., 2005)

Humans with SCA-14 have point or truncation mutations in PKCγ, resulting in a non-functional enzyme (Asai et. al., 2009; Lin and Takemoto, 2007). Thus, the PKCγ KO mouse provides a model to determine physiological effects of loss of PKC gamma. We have previously demonstrated that lens epithelial cells with PKCγ SCA14 mutants (H101Y, S119P, or G128D) lack PKCγ enzyme activity even when endogenous PKCγ is present (Lin et. al., 2007). Effects are observed on gap junction proteins, Cx43 and Cx50, which are both found in retina (Srinivas et. al., 2005, Fugisawa et. al., 1992). PKCγ C1B mutants do not phosphorylate Cx43 or Cx50, cause increased Cx43 and Cx50 plaques, and disassembly of plaques does not occur after H_2O_2 stimulated activation of PKCγ ((Lin et. al., 2007). Hydrogen peroxide and TPA also failed to stimulate Cx57 phosphorylation in HT22 cells overexpressing PKCγ SCA14 mutants, but phosphorylation was achieved in the regular HT22 cells (Zhang et. al., 2009). This dominant negative effect on endogenous PKCγ has been linked to failure of control of gap junctions and causes cells to be more susceptible to H_2O_2-induced and caspase-3-dependent cell apoptosis (Lin et. al., 2007) and caspase-12-dependent apoptosis (Zhang et. al., 2009). In the PKCγ H101Y SCA14 mutant transgenic mouse model, Purkenje cells that are found in cerebella of central nervous system, showed altered morphology and significant reduction in numbers as early as 4 weeks of age (Zhang et. al., 2009).

Cx43 is found in retinal glial cells, myelinated fiber regions of neural retina, astrocytes and Müller cells (Johansson et. al., 1999, Janssen-Bienhold et. al., 1998). Cx50 another PKCγ target, is expressed in retinal Müller cells, astrocytes and in filamentous processes ensheathing the photoreceptors ((Schütte et. al.,1998, Huang et. al., 2005, Massey et. al., 2003). Cx50 also couples between A type horizontal cells (O'Brien, 2006), that are found outer plexiform layer. PKCs are found in the bow region and cortex of the lens and in cornea and retina (Greferath et. al., Negishi et. al., 1988).

Hyperbaric oxygen (HBO) also causes oxidative stress in the live mouse model and is thought to deplete cells of glutathione (Padgaonkar et. al., 2008). It induces several physiological effects such as increased blood pressure and hyperoxia. The HBO model is a non-invasive technique that is widely used for treatments of humans with stroke (Sinkovic et. al., 2006, Nighoghossian et. al., 1997). Treatment with HBO has also been used to ameliorate damage in the blood-retinal barrier during diabetic retinopathy (Chang et. al., 2006). There are

also adverse affects associated with HBO treatments such as damage to ears, increased oxygen toxicity and pulmonary barotraumas (Nighoghossian et. al., 1997).

The goal of this chapter is to determine if loss of PKCγ in the knockout mouse increases sensitivity of retina to HBO stress resulting in retinal cell damage and if this is linked to changes in gap junctions, especially Cx50.

3.2 Materials and Methods

3.2.1 Animals and Hyperbaric Oxygen Treatments

Control, 6 week old mice (B6129pf2/j100903) and 6 week old PKCγ knock-out mice (B6;129p-Prkcctm1St1) were purchased from Jackson Laboratory (Bar Harbor, MA); mice breed normally and were healthy. Control and knock-out mice were treated with elevated pressure of 100% oxygen, 3 times per week for 8 weeks. The procedure was as follows: treatment 1: 2.5 atm for 1hr; treatment 2-3: 2.5 atm for 2.5 hr; treatment 4-9: 2.5 atm for 3 hr; treatments 10-24: 3.0 atm for 3hr. The final age of the mice was 14 weeks at the time of sacrifice. Mice tolerated the HBO treatments well. Animals were sacrificed according to approved protocols. All experiments conformed to the ARVO Statement for Use of Animals in Ophthalmic and Vision Research and were performed under an institutionally approved animal protocol.

3.2.2 Western Blot

Retina tissues were collected within 5 min of mice sacrifice, taken up in 2X sample buffer (100mM Tris-HCl, pH 6.8, 200 mM Dithiothreitol (DTT) (Ampresco, Ohio), 4% Sodium Dodecyl Sulfate (SDS) (Ampresco, Ohio), 0.2% bromophenol blue (Ampresco, Ohio), 20% glycerol (Fisher Scientific, Pittsburgh), 50 µl/retina). Proteins were separated on 12.5% SDS-PAGE (40 µg retinal protein/lane) and continued with Western blots using monoclonal mouse anti PKCγ antibodies (1:1000) from Sigma (Dallas, TX)., mouse anti Cx50 antisera (1:500) from Zymed (San Francisco, CA) and/or mouse anti-β-actin antibody from Sigma (St. Louis, MO). Immunoreactive bands were detected by chemiluminescence (ECL; Pierce, Rockford, IL).

3.2.3 Light Microscopy

Eyes were dissected out of six to fourteen week old mice, fixed in 2% paraformaldehyde, 2.5% glutaraldehyde (Sigma), 0.1M cacodylate (Electron Microscopy Science (EMS), Fort Washington, PA) then post-fixed with osmium tetroxide (EMS). This was followed by dehydration with 70% alcohol for 12 hours, then by 100% alcohol overnight and with 100%

acetone for 12 hr then embedding in epon (LX112) (EMS.) Sectioning was done using a Reichter-Jung Ultracut E Ultramicrotome (Cambridge Instruments Inc., Buffalo, New York) at room temperature. Sections were taken perpendicular to the optic nerve so that all of the layers of the retina could be observed. Eyes were sectioned to the point until the optic nerve was observed, so the depth was consistent in all of the sections. Thick sections (2-50 μm) were obtained using a diamond knife, then stained with 1% (w/v) toluidine blue (EMS) and viewed using a Nikon Eclipse E600 light microscope (Nikon Inc. Melville, New York) (4-100X). Exact locations were confirmed by low magnification photos (4-100X) and layers were counted manually using analySIS software. (Soft Imaging System GmbH; Munster, Germany).

3.2.4 Fluorescent microscopy

Cryostat sections (100 μm) of retinas were fixed in 2% paraformaldehyde, washed 3 times with PBS, .3%Triton X 100 buffer, blocked with 5% Normal Goat Serum (Santa Cruz Biotech, Ca, number 2043), labeled with primary antisera, Mouse anti Connexin 50 dilution 1 to 100 (Zymed San Francisco, CA, number 33-4300), then secondary Alexa Fluor 488 tagged antisera (Molecular Probes, Eugene, OR number A21042). Sections were stained with 4',6-diamino-2 phenylindole dihydrochloride (DAPI) Hoechst dye (Molecular probes, Eugene, OR number D1306 Blue stain) for 2 seconds, washed with PBS, 3%Triton X 100 buffer, then viewed using a Nikon Eclipse E600 light microscope (Nikon Inc. Melville, New York).

3.2.5 Statistics

All experiments were performed at least in triplicates. Commercial software (Origin; Microcal Software Inc., Northampton, MA) was used for statistical analyses. Results were expressed as the mean ± SD. Differences at $P<0.05$ were considered to be statistically significant, and was determined by using paired T-test.

3.3 Results

3.3.1 Western Blots demonstrate no PKCγ in knockout mouse retinas.

Western Blot analyses were performed to confirm a lack of PKCγ protein in the PKCγ knockout mice retinas. Fig. 1 illustrates that knockout mice have no detectable PKCγ in the retina of 6 week old knockout mice. Western blots also demonstrated no change in Cx50 protein, used as a control, from knockout mice, when compared to control mice retinas indicating that normal levels of a possible PKCγ target (Cx50) remain intact in the knockout mice (Fig. 3.1). As this is a well-studied knockout model, we did not examine further protein levels. Extensive analyses in brain have already established validity of this model (Bowers et. al., 2001, Narita et. al., 2001)

3.3.2 Retinas from the PKCγ knockout mice are more sensitive to hyperbaric oxygen damage; this is more apparent in central retina.

After HBO treatments the thickness and structural differences between control and knockout retinas were more apparent in the PKCγ KO mouse retinas. In Figure 3.2 we show the results of treating six week-old mice with hyperbaric oxygen (100%), 3x a week for 8 weeks, 100% oxygen at 3 atm, for 3 hr/wk, 3 times per week, for 8 weeks, (14 weeks old, final age). (See Methods). Light microscopy of all retinal layers, in the central area of the retina near the optic nerve, demonstrated the most prevalent damage (Fig 3.2 and Table 3.1). As shown, the reduction of all layers was extensive in the PKCγ knockout mice whereas damage was much less severe in control mice. In particular, a severe loss of outer segment of the photoreceptor layers was observed. The average thickness was reduced by more than 50% (Table 3.1, Fig 3.2) in the knockout retina after HBO treatment vs. a 25% decrease in the control retina. In addition to reduction of thickness, the integrity of OS seemed completely collapsed (Fig 3.2). Vacuoles were observed between the inner and outer segments, and, outer segment fibers had no apparent direction when compared to control fibers that were organized in a very tight manner. Fig 3.2 demonstrates an extreme increase of structural damage to the outer segments of knockout retina when compared to control retina after HBO treatment.

The outer nuclear layer (ONL), which contains the nuclei of photoreceptor cells, decreased significantly in thickness after HBO treatment of knockout mice. The thicknesses of the ONL decreased by 45% in the HBO treated knockout mice (Table 3.1) when compared to no decrease in control retina. The number of layers of nuclei also decreased in the HBO treated knockout mice from 8-9 to 4-5 layers. This was not observed in control retinas.

Ganglion cell layers (GCL) were also damaged in the knockout retinas even after HBO treatment. Fig 2 shows many vacuoles in GCL resulting in an increase in thickness of this layer. The total number of nuclei decreased (Table 3.3), indicating that the increase in thickness was due to formation of vacuoles and not due to the extra nuclei. The HBO treated knockout GCL had the same thickness, but the number of nuclei was reduced significantly. The GCL from the HBO treated knockout mice had 11 valid nuclei, while the untreated knockout had 17 per 100 μm of GCL.

In contrast, to the central retina, results from Fig 3.3 and Table 3.2 demonstrate that the structural effects on peripheral retina were not as significant. The thickness of outer segments of photoreceptor layers were reduced to a lesser extent and other layers did not show any significant differences between the knockout and the control mice. This fact indicates that the knockout mice are much more sensitive to HBO damage in the central retina than in the peripheral retina. This could be due to the fact that practically all cone photoreceptors are located in the central retina, and the fact that the number of rod photoreceptors is half of that observed in the central retina, leading to more cellular communication in the central retina and making it more vulnerable to oxidative stress.

In conclusion, these data demonstrate that PKCγ knockout mice are more sensitive to retinal damage due to HBO than control mice, particularly in the central retina. The majority of signal transduction pathways that are involved in vision are in the central retina, thus indicating that PKC gamma plays an important role in that pathway, and it possibly does that, in part, through its downstream targets that such as Cx50.

3.3.3 Immunolocalization of Cx50 before and after HBO treatment

Immunolabeling with anti Cx50 antisera gave extensive localization of Cx50 in the inner segment, retinal ganglion layer, and inner plexiform layer in both control and knockout mice (Fig. 3.4). Cx50 labeling was significantly more pronounced in the OPL and ganglion layer control compared to that of KO. Oxidative stress supplemented by HBO treatment resulted in significant reduction of Cx50 immunolocalization in PKCγ mice control retinas, this can be seen when comparing Fig. 3.4 A to Fig. 3.4 B. Outer plexiform and inner plexiform layers had the largest reduction of Cx50 immunolabeling in the PKCγ mice control retinas. HBO treatment failed to produce decrease of Cx50 immunolabeling in the PKCγ mice KO retinas, if anything immunolabeling was actually increased after HBO treatment as evident in the junction of ganglion layer and inner plexiform layer as seen on Fig. 3.4 D. Cx50 immunolabeling in the PKC gamma knockout mice retinas was reduced, this could be due to the loss of cellular retina structure that PKC gamma knockout mice show as previously discussed in chapter 2. The most important fact is that retinas that had functional PKCγ protein and not the KO model, were shown to have a significant reduction of Cx50 immunolabeling, possibly indicating that PKCγ is in fact a protein through which Cx50 gap junction is in part regulated. This suggests that PKCγ could function as protector of these cells from oxidative stress, this is achieved by closure of Cx50 gap junction thus stopping the spread of apoptotic signals.

3.4 Discussion

The results from this study clearly demonstrate that retina from the PKCγ knockout mice is more sensitive to damage from HBO treatments. Previous findings suggest that PKCγ is required for protection of brain from ischemic stress damage (Aronowski et. al., 2000). The PKCγ knockout model is more sensitive to pain, has changes in long-term potentiation, increased alcohol consumption, an enhanced opioid response and decreased memory ((Bowers et. al., 2001, Narita et. al., 2001). PKCγ is involved in brain ischemic responses and it may serve a similar role in retina in cell regulation and developmental signaling.

PKCγ is an important enzyme in signal transduction pathways. One of its functions is to regulate gap junction signaling. Thus, by knocking out PKCγ, the signal transduction pathway and gap junction control may be disrupted in the retina. Gap junctions like those assembled from Cx50 or Cx43, although still present in the knockout mice (Fig 3.1), may be dependent upon PKCγ for closure in response to oxidative stress (i.e., the "Bystander Effect"). Gap junctions are observed throughout the retina and provide electrical coupling between retinal cells (Cuntz et. al., 2007). Cx50 has been shown to be tissue specific for the A-type horizontal cells, it localizes in outer plexiform layer and is responsible for providing neural connections with rod bipolar cell dendrites.

Besides gap junctions there are several other targets of PKCγ that are involved in neural protection and transmission of synaptic signals. Ionotropic glutamate receptors, which play a role in signal transduction in brain and are involved in learning and memory formation, are regulated by phosphorylation. PKCγ has been shown to phosphorylate GluR4 S482 alpha-amino-3-hydroxy-5-methyl-4-isoxazole propionate (AMPA)-type glutamate receptor (Correia et al., 2002). Calmodulin-binding RC3 (neurogranin) is phosphorylated through the activation of postsynaptic glutamate receptors by PKCγ (Ramakers et. al., 1999). PKCγ also has been shown to be associated with NMDA receptor-associated signal transduction, which is specifically associated with diacylglycerol levels (Giordano et. al., 2005). The exact biochemical effects in PKCγ knockout mice are yet to be identified. It provides an available model to study cerebella ataxia through PKC gamma SCA 14 mutants. In this study we explore its overall structural effect

on retina from the knockout mouse model and determine that retina shows increased damage after HBO treatments. This could be partly due to uncontrolled gap junctions.

The bystander effect occurs when a dying adjacent cell delivers a cellular apoptotic signal such as high Ca^{+2} to an adjacent cell through an open gap junction, causing spread of the death signal (Perez et. al., 2003; Farahani et. al., 2005). The process is well documented in brain injury caused by ischemia, where the expansion of the ischemic infarct results from transfer of apoptotic signal molecules through gap junctions of astrocytes and other cells. It is apparent that proper control of gap junctions is required for retinal cell survival and the identification of the gap junctions and their control mechanisms provide a challenge for future work. In this study we chose Cx50 because our previous data from Chapter 2, showed significant changes in outer plexiform layer, and Cx50 has been shown to be one of the gap junctions in that specific layer (O'Brian et. al., 2006). Effects on other gap junctions could occur, and, this would be a subject of future studies.

PKCγ is a member of the classical PKC family and has both a C1, diacylglycerol-binding domain and a C2, calcium-binding domain (Katsura et. al., 1999). Unlike other classical PKCs, PKCγ can be activated directly by an oxidative signal without elevated calcium (Lin and Takemoto, 2005). The C1 domain of PKCγ is exposed and becomes oxidized upon exposure of cells to hydrogen peroxide. This causes PKCγ enzyme activation, phosphorylation of Cx43 and Cx50, and inhibition of these gap junctions. PKCγ is found in control but not in knockout mouse retinas (Fig 1). Thus, normal control of Cx43 and/or Cx50 gap junctions in response to stress would not occur. This would be reflected in enhanced damage to retina in these mice.

A similar condition is observed in mutant PKCγs which mimic mutations found in humans with SCA-14. However, humans with this condition lack normal ERG's, humans do contain one normal PKCγ gene, a complete PKCγ knockout is lethal in humans. When these mutations are over expressed in neural HT22 cells, gap junctions are no longer controlled, the mutation causes less activity of the endogenous and normal PKC, and there is increased apoptosis and ER stress observed (Lin and Takemoto, 2005). Since HBO is sometimes used to treat a number of conditions, it may be critical to know if PKCγ is normal in these patients.

We have chosen HBO as a stress signal since it is non-invasive and unlike other treatments does not require anesthetics, which are PKC activators (Ohsawa et. al., 2001). This treatment has been extensively studied in cells in culture and in lens models, where cataracts

occur (Padgaonkar et. al., 2004). In Fig 3.2 and Table 3.1, we demonstrate that the retinas from the knockout mice show reduction in all retinal layers and a severe loss of outer segments and retinal ganglion cells. Significant structural damage in the knockout retinas was observed in the OPL, GCL, INL, while other layers showed less damage after HBO treatment.

In our study we noticed that the affects of HBO on the knockout were more apparent in the central retina. The retina is a highly specialized tissue that integrates light signal into the neural signal. In humans, this fact explains why some diseases affect different regions preferentially, as in age-related macular degeneration (AMD) and diabetic retinopathy (Zarbin 2004, Owsley et. al., 2000). This could be due to the fact that Glutathione peroxidase 3 (GPX3) catalyzes the reduction of hydrogen peroxide and functions in protection of cells against oxidative damage. Peripheral retina contains larger amounts of GPX3 than central retina, which could explain why depletion of glutathione by HBO affected central retina more than peripheral retina (Sharon et. al., 2002). Central retina is also more abundant in rods, practically all of the cones, neuronal axons, ganglion cells and neuron-filaments (Sharon et. al., 2002). This extra abundance in cellular organization of central retina, results in an increase in cellular communication, thus making it more vulnerable to oxidative stress. Electrical synaptic transmission via gap junctions is a primary mode of cellular communication in retina and central nervous system, suggesting that disruption of gap junctions could play a role in how retina responds to oxidative stress.

PKCγ ‘s ability to control gap junctions has been extensively studied. In this study we tried to see what the effect of lack of PKCγ would be on Cx50 gap junction localization in mouse retinal tissues, after exposure to hyperbaric oxygen. Immunocytochemistry results of Cx50 shows reduction of Cx50 in the PKCγ control mice in the outer-plexiform layer and inner-plexiform layers. HBO failed to produce reduction of Cx50 immunolabeling in the PKCγ knockout mice model, indicating that PKCγ is indeed needed for closure and disassembly of gap junctions. To our surprise there was even a slight increase in immunolabeling in the KO model after HBO treatment, especially as noticed in the junction of ganglion layer and inner plexiform layer, we hypothesize that this could be due to the fact that Cx50 gap junction formation was increased in response to oxidative stress, to help with promotion of cell death. Results from previous chapter showed PKCγ immunolocalization in outer plexiform, inner plexiform and ganglion cell layers, indicating that PKCγ and Cx50 localize in the same retina areas, coupled

with the fact that PKCγ control mice showed disruption of Cx50 immunolabeling in those layers, this result suggests that PKCγ might play a role in neuro-protective effect of stopping the progression of apoptotic signal through closure of Cx50 gap junctions.

In our study we observed a more prevalent loss of photoreceptor outer segments, after HBO, which was greater in the central region of the retina. Loss of outer segments plays an important role in age-related macular degeneration (AMD) pathophysiology (Ethen et. al., 2006). Human AMD provides a good example of how different areas of the retina contain different structures and may show different responses to stress.

At present, little is known of the specific function of individual gap junctions in retina. Earlier studies have shown that gap junctions are present between the rod bipolar cells and AII-type amacrine cells (Söhl et. al., 2000). Rod bipolar cells do not make direct connections with ganglion cells. Neural signals first pass to AII-type amacrine cells and AII-type cells make synapses with the ganglion cells. In a connexin 36 knockout model there were no AII/AII and AII/bipolar couplings, which demonstrated that the presence of connexin 36 was essential for normal coupling in rods (Feigenspan et. al., 2004).

PKCγ phosphorylates gap junction proteins which results in disassembly of gap junction plaques (aggregation of up to 10,000 gap junctions in one place, making it functional) and therefore in decreased gap junction activity. We have shown that the presence of PKCγ is essential for normal functioning and organization of retina and we speculate that some of the causes for the hyperbaric oxygen stress damage are due to the loss of control by PKCγ on gap junction activity and disassembly in response to stress. Cx50 plays an important role in retina cell communication, and in this study it shows disintegration of Cx50 immunolabeling in PKC gamma control retina after hyperbaric oxygen treatment, indicating that PKC gamma may play a part in Cx50 regulation in retina. Since PKCγ is vital to stress protection in retina, care should be given when treating patients with hyperbaric oxygen. Screening for SCA-14, for example, could prevent HBO-induced damage to retina. In conclusion, these data demonstrate that PKC γ-knockout mice are more sensitive to retinal damage due to HBO than control mice, particularly in the central retina.

3.5 Figures

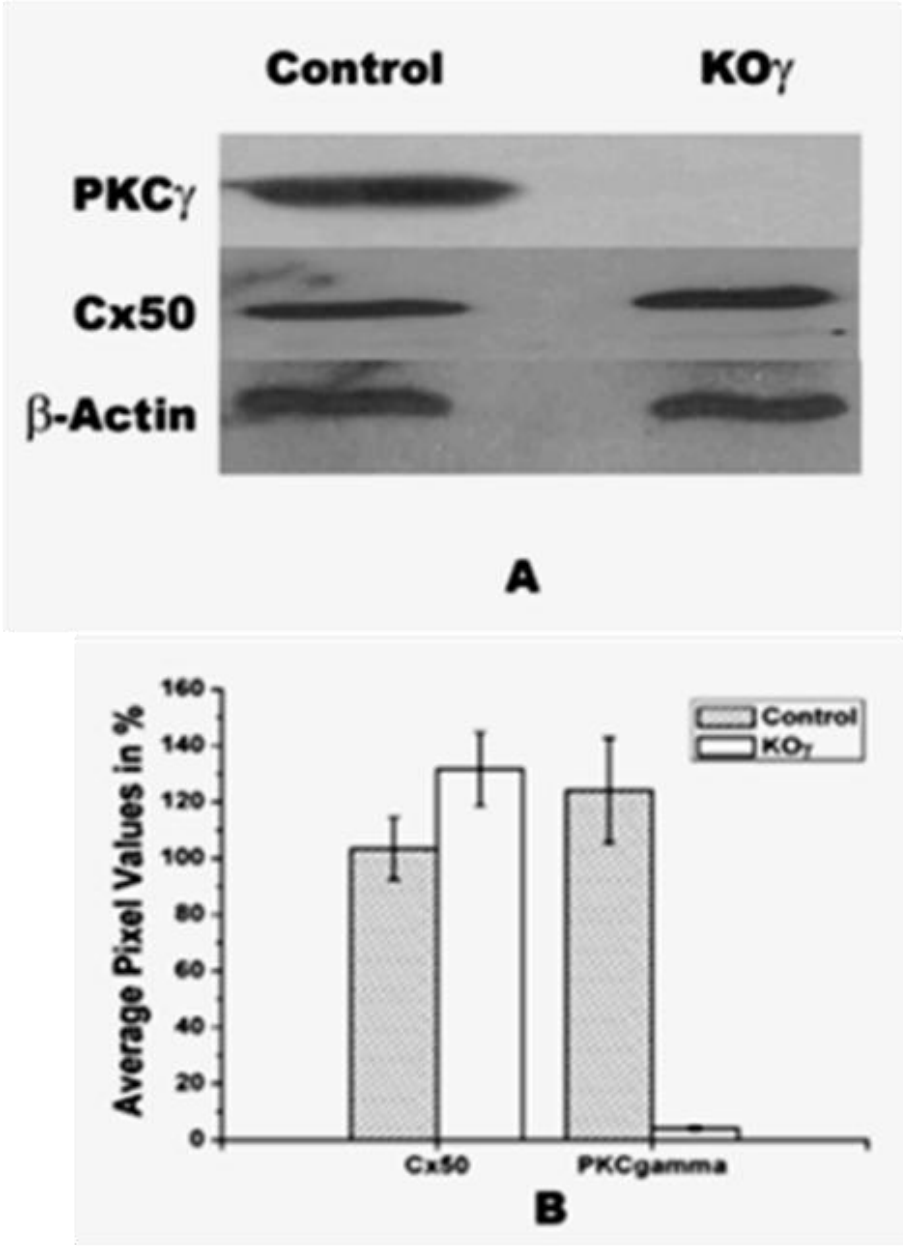

Figure 3-1Western Blots of Retina Tissue

Whole retina from 6-week old control or PKCγ knockout (KOγ) mice were loaded in sample buffer at 40 μg protein/lane. A) Immunoblots using mouse anti-PKCγ antisera at 1:1000, mouse anti-Cx50 at 1:500 and mouse anti-β-actin at 1:20,000. β-Actin is used as an internal loading control. B) Bar graph showing the average (%) pixel values of Cx50 and PKCγ protein/lane. A) γ knock-out mouse respectively. Data is plotted as percentage of control (Mean±SD, n=3).

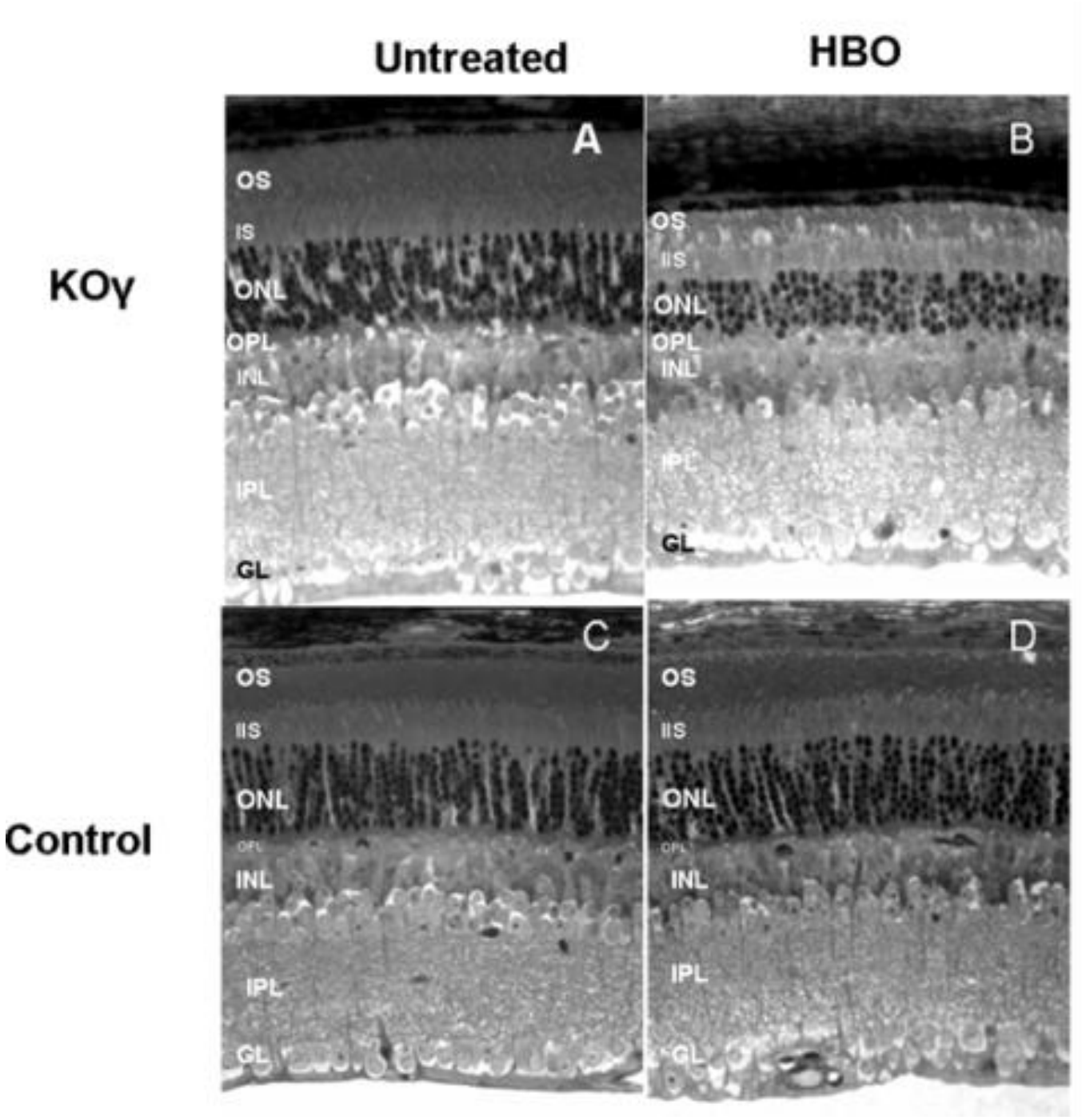

Figure 3-2 HBO Treatments of Central Retina

Structure of mouse retina (14 weeks old) before and after hyperbaric oxygen (HBO) treatment. Sections of fixed retina, about 250 μm away from the optic nerve are shown. A) PKCγ Knock Out; B) HBO-treated PKCγ knockout; C) Wild type retina; D) HBO-treated wild-type retina. IPL = inner plexiform layer, OS = outer segments, ONL = outer nuclear layer, INL = inner nuclear layer, OPL = outer plexiform layer, GL = ganglion cell layer, IS = inner segments.

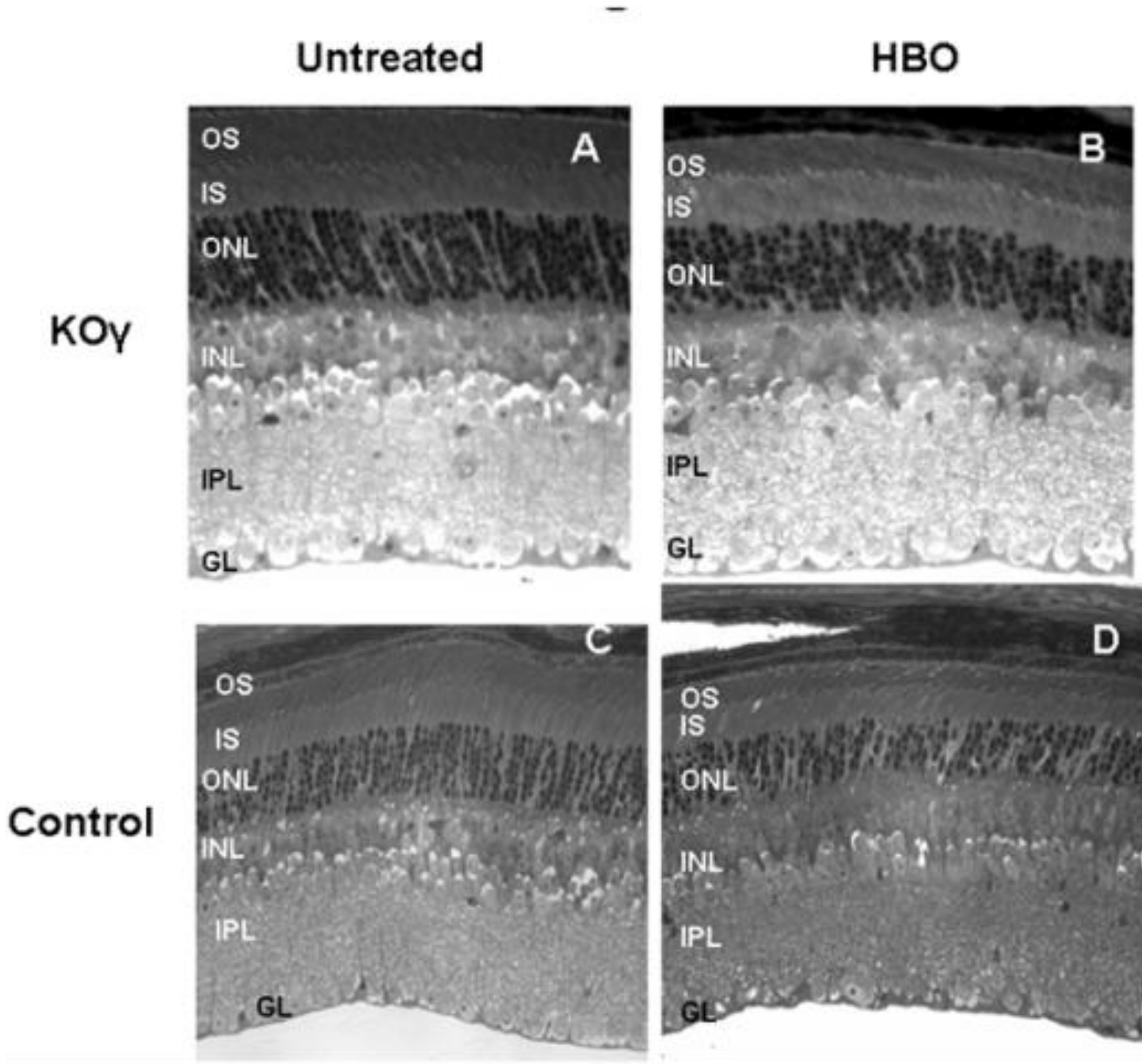

Figure 3-3 HBO Treatment of Peripheral Retina

Structure of mouse retina (14 weeks old) before and after hyperbaric oxygen (HBO) treatment. Sections of fixed retina, about 1100 μm away from the optic nerve are shown. A) PKCγ Knock Out; B) HBO-treated PKCγ knockout; C) Wild type retina; D) HBO-treated wild-type retina. IPL = inner plexiform layer, OS = outer segments, ONL = outer nuclear layer, INL = inner nuclear layer, OPL = outer plexiform layer, GL = ganglion cell layer, IS = inner segments.

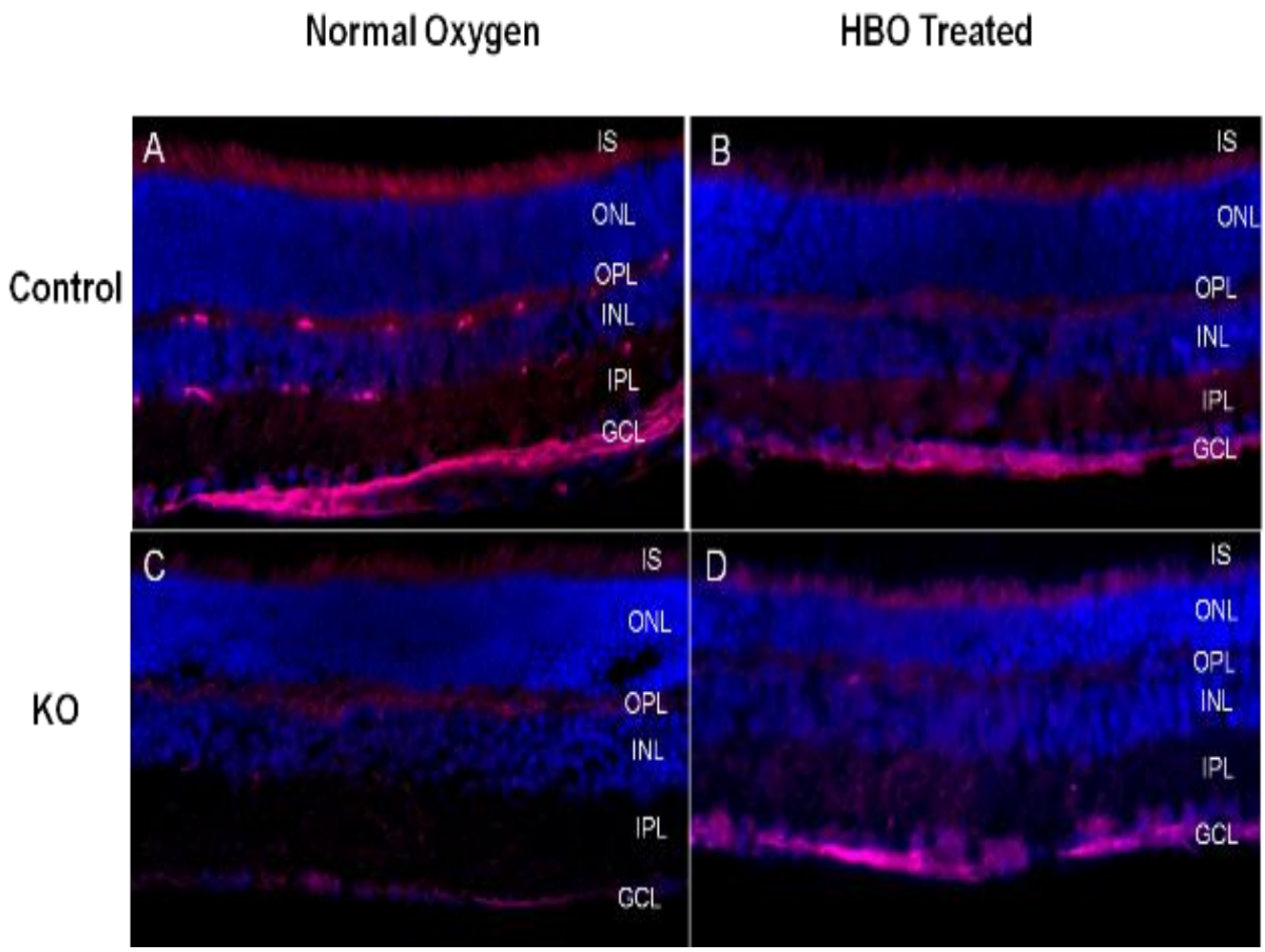

Figure 3-4 Cx50 immunolabeling decreases after HBO treatment in control but not in PKCγ Knockout Mice Retinas.

Immunolabeling with anti Cx50 antibody (Red Fluorescence) of Sections of fixed mouse retina (14 weeks old). Cell nuclei are colored blue with DAPI. Images are taken about 250 μm away from the optic nerve at 20X magnification. Control – retina from wild type mice, KO = PKCγ knockout mice are shown. HBO = hyperbaric oxygen treated for 8 weeks. View at 20X. GCL = retinal ganglion cell layer. KOγ = PKCγ knockout mice. Wild Type = control mice. IPL = inner plexiform layer, ONL = outer nuclear layer, INL = inner nuclear layer, OPL = outer plexiform layer, GCL = ganglion cell layer, IS = inner segments A) Wild type retina PKCγ Knock Out; B) HBO-treated wild-type retina C) PKCγ Knock Out type retina; D) HBO-treated PKCγ knockout mice retina.

	RPE		OS		IS		ONL		OPL		INL		IPL		GCL	
	C	KO	C	KO	C	KO	C	KO	C	KO	C	KO§	C	KO	C	KO
Unt.	5.4	5.1	22.2	20	17.1	16.9	35.7	35.8	9.8	-	34.3	41	44.4	45.3	13.4	18.7
HBO	5.9	5	15.7*	9.6*	16.7	11.4*	34.3	22.7*	8	-	31.7	30*	41.7	37.3*	19.8*	17.5*

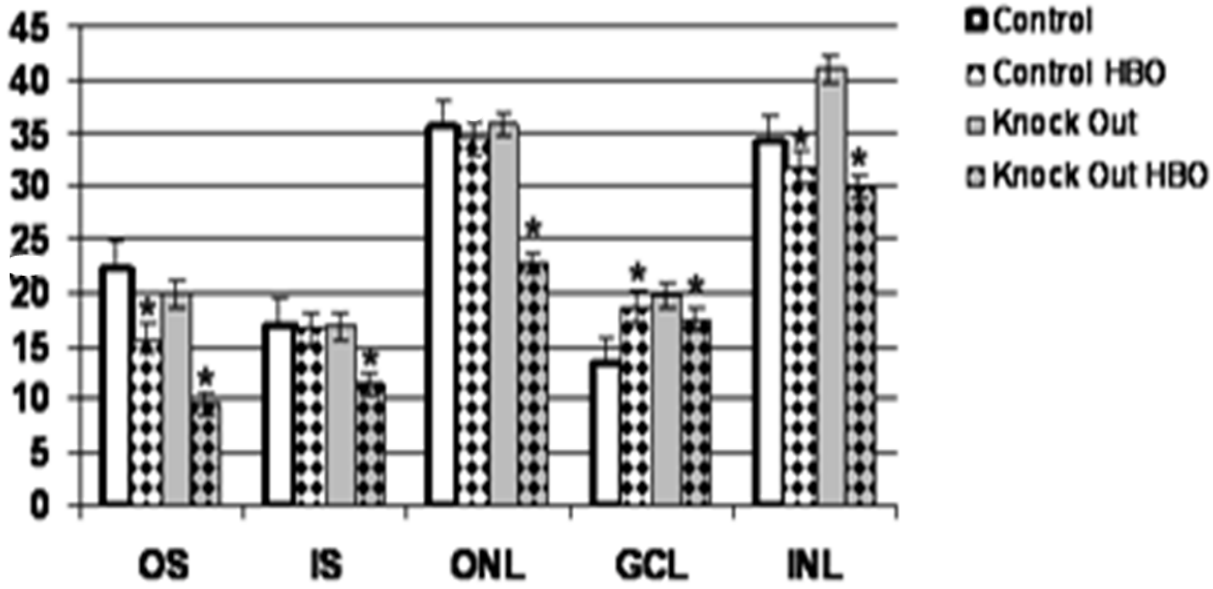

Table 3-1 Thickness of Control and PKCγ Knock Out Central Retinal Layers.

Unit= Micrometers, C – 14 week old control mice; KO – 14 week old PKC γ Knock-out mice; Central– 250 μm away from optic nerve, HBO – treated with Hyperbaric oxygen. Unt. – untreated. IPL = inner plexiform layer, ONL = outer nuclear layer, INL = inner nuclear layer, OPL = outer plexiform layer, GCL = ganglion cell layer, IS = inner segments, OS=outer segment

§ In Knockout thickness of Inner Nuclear Layer includes OPL as the border is undefined.

Results expressed as ± SEM of 5 sample retinas

*Results are statistically different for control, $p \leq 0.05$

	RPE		OS		IS		ONL		OPL		INL		IPL		GCL	
	C	KO	C	KO	C	KO	C	KO	C	KO	C	KO	C	KO	C	KO
Unt.	5.1	5.9	15.4	16.2	14.8	16.1	27.3	27.9	8.4	7.8	29.5	28.4	37.9	36.3	8.8	8.4
HBO	5.3	5.8	11.1*	10.8*	12.1*	13.2*	22.5*	25.2*	6.9	6.6	28.6	28.2	31.1	30.6	9.1	8.8

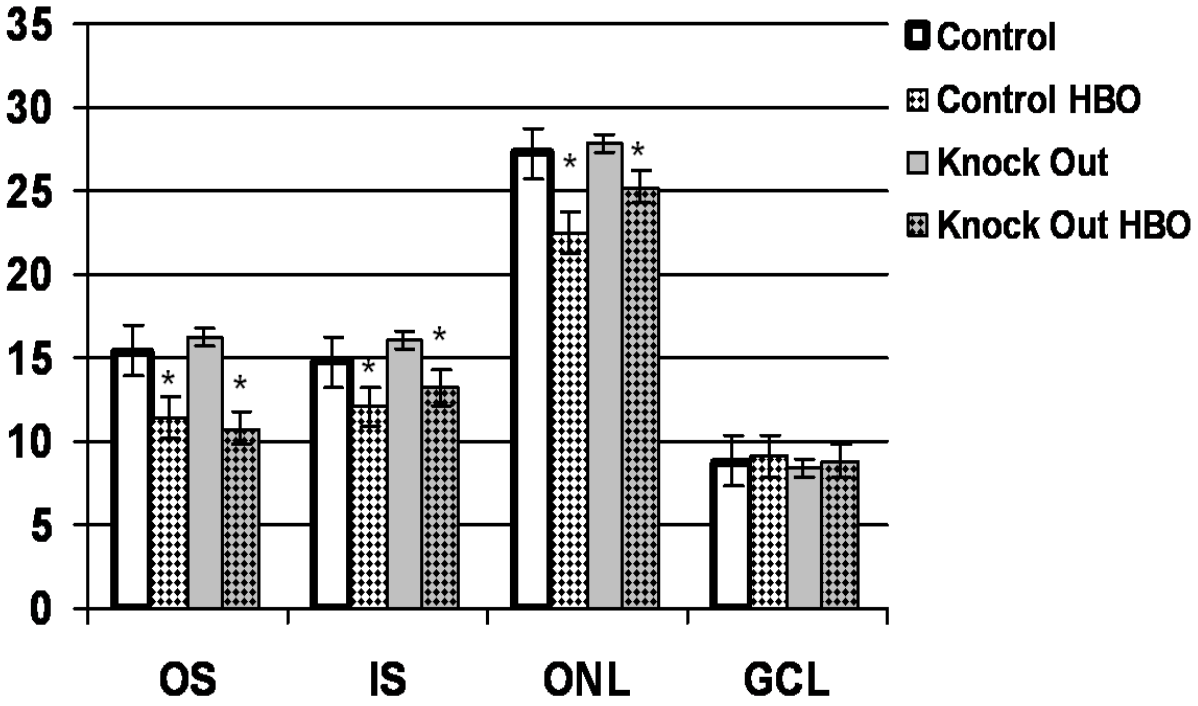

Table 3-2 Thickness of Control and PKCγ Knock Out Peripheral Retinal Layers.

Unit= Micrometers, C – 14 week old control mice; KO – 14 week old PKC γ Knock-out mice; Peripheral – 1100 μm away from optic nerve, HBO – treated with Hyperbaric oxygen. Unt. – untreated. IPL = inner plexiform layer, ONL = outer nuclear layer, INL = inner nuclear layer, OPL = outer plexiform layer, GCL = ganglion cell layer, IS = inner segments, OS=outer segment

Results expressed as ± SEM of 5 sample retinas

*Results are statistically different for control, $p \leq 0.05$

Central	INL	ONL	GCL
C	20±.58	59±2.1	13±1.5
C HBO	21±.75	50.5±3.6	9±.75
KO	15±1.2*	45.2±5.1*	7.5±.5*
KO HBO	18±1.5*	32.2±6.2*	6.5±.55*
Peripheral			
C	19±1.2	47.5±1.8	11±1.1
C HBO	19.5±1.4	47.5±3.1	10±1
KO	15±.75*	42.2±2.8	8±.5
KO HBO	16±1*	43.8±3.6	7±.75*

Table 3-3 Amount of Nuclei in Inner, Outer, and Ganglion cell layers of Control and KOγ Retina before and after HBO treatment.

Amount of nuclei is expressed as per 1000 μm^2 area. C – 14 week old control mice; KO – 14 week old PKC γ Knock-out mice; INL- inner nuclear layer, ONL – outer nuclear layer, GCL – ganglion cell layer; Central – 250 μm away from optic nerve; Peripheral – 1,100 μm away from optic nerve; HBO – treated with Hyperbaric oxygen, 3X/week for 8 weeks (see methods). Results expressed as ± SEM of 3 sample retinas for each recording.

*Results are statistically different for control, $p \leq 0.05$

CHAPTER 4 - Regulation of PKCγ and its target Cx50 in the neuronal R28 cell line

4.1 Introduction

PKCγ is an isoform of the conventional PKC group that is largely found in retina, lens and brain cells (Barnett et. al., 2007). Previous studies have shown that PKCγ plays a major role in pain sensitivity, protection against brain ischemia and as a target for ischemic preconditioning (Aranowski et. al., 2000, Adachi, 2008). It is proposed that PKCγ, once activated, moves to the synapse and affects neurotransmission and cell survival (Matsumoto et. al., 2004). The PKCγ has regulatory domains that contain C1 and C2 motifs. PKCγ binds calcium at a C2 domain and diacylglycerol (DAG) at a C1 domain (Newton, 2010). One unique property of the PKCγ isoform is that its C1B domain is always exposed and thus it does not require calcium for activation (Lin et. al., 2003). Phorbol esters (TPA) have been used in studies to mimic the effect of DAG as they both regulate PKCγ through the same mechanism, although TPA can continuously activate PKCγ because it is much harder to metabolize (Newton, 1995, Newton, 2010). PKCγ was previously shown to be activated by TPA, which, in turn, caused phosphorylation of Cx43 at serine and a decrease in gap junction dye transfer of Cx43 cell surface plaques (Rivedal et. al., 2001, Lin et. al., 2006).

PKCγ also is activated by oxidative stress in lens epithelial cells, it translocates to the membrane, and downregulates gap junction activity. The PKCγ C1B subdomain is oxidized after treatment with hydrogen peroxide, disulfide bonds are formed, and the enzyme becomes activated (Lin and Takemoto, 2005). Both Cx43 gap junction plaques and gap junction activity, were reduced after hydrogen peroxide activation of PKCγ, so the oxidation of the PKCγ C1B domain caused inhibition of the gap junction protein Cx43 (Lin and Takemoto, 2003, 2005). These results demonstrated that PKCγ is an oxidative stress-sensing protein that provides a protective effect for cells, by inhibition of gap junctions like Cx50. Oxidative and TPA activation of PKCγ were able to disrupt Cx50 gap junctions in dye activity assay in the lens epithelial cell line (Lin et al., 2004).

Spinocerebellar ataxias (SCA) are autosomal dominant neurodegenerative disorders. One of the disorders called SCA14, is caused by mutations in the PKCγ, with the majority of mutations occurring in the C1B regulatory domain (Seki et. al., 2005). It was previously shown

that lens epithelial cells with PKCγ SCA14 mutants (H101Y, S119P, or G128D) had no PKCγ enzyme activity and were more susceptible to H_2O_2-induced, caspase-3-dependent cell apoptosis (Lin et. al., 2007; Zhang, Snider, Willard, Takemoto and Lin, 2009). Effects were observed on the gap junction proteins, Cx43 and Cx50, which are both found in retina (Srinivas et. al., 2005, Fugisawa et. al., 1992). PKCγ C1B mutants do not phosphorylate Cx43 or Cx50, cause increased Cx43 and Cx50 plaques, and fail to disassemble after H_2O_2 stimulated activation of PKCγ in lens (Lin et. al., 2007). Thus, cell death was caused by the inability of PKCγ mutants to perform normal functions of PKC γ, by shutting down gap junction activity and preventing apoptotic signals from spreading.

Gap junctions allow the passage of ions and small molecules between adjacent cells and are composed of a family of proteins known as connexins (Ripps et. al., 2007). Cx50 is a potential PKCγ target that is expressed in retinal Müller cells, astrocytes and in filamentous processes ensheathing the photoreceptors ((Schütte et. al.,1998, Huang et. al., 2005, Massey et. al., 2003). Cx50 also couples between A type horizontal cells (O'Brien, 2006). As shown in Chapter 3, Cx50 antisera gave extensive localization of Cx50, in outer segments and in the outer plexiform layer. Cx50 gap junction immunolabeling was significantly reduced after exposure to hyperbaric oxygen in PKCγ control mice retinas, and not in the PKCγ knockout mice retina's.

In Yevseyenkov et. al. (2009) and Chapter 3, it was shown that retina of the PKC γ knockout mice are more susceptible to hyperoxia induced by hyperbaric oxygen. In Chapter 4 using R28 cells in culture PKCγ activation and downstream targets are the focus.

Retina is the innermost layer of the eye and it is an extension of the central nervous system. To study the effects of hyperoxia in cell culture, a neuronal cell line was chosen. Cell lines that are derived from CNS have been used to study neuronal cell growth and regulation. Y79 and WERI are, by far the most commonly used cell lines. But, for this study we chose R28 cells because, unlike the other neuronal cell lines, it is not tumor-derived, but comes directly from the rat retina. The R28 neuronal cell line, was developed by 12S E1A-induced immortalization of postnatal day 6 day Sprague-Dawley rat retinas (Seigel, 1996).

R28 is a stable line that can be maintained for over 200 passages, shows no signs of senescence, and has a doubling time of 24 hours. It is of heterogeneous population, so it cannot be purified further, but retina is itself a heterogeneous tissue so it is a suitable model for experiments to determine stimulation effects, since primary retinal tissue cannot grow in culture.

It contains several important growth factors such as Insulin like Growth Factor (IGF-1), (IGF-II), Transforming Growth Factor (TGF-beta2), Platelet derived growth factor (PDGF-alpha), Vascular Endothelial Growth factor (VEGF), Fibroblast derived growth factor (FGF), Brain Derived Growth factor (BDNF) and Schwannoma-derived factor (Seigel et. al., 2004). It is important to note that IGF-1 has been previously found to be important in the cascade of activation of PKCγ in lens epithelial cells, while FGF and EGF were not. It was reported that IGF-1 appeared to be a unique growth factor/activator of lens PKCγ (Lin et. al., 2003). It also has been shown that VEGF, in response to hypoxia, stimulated several PKC isozymes including PKCγ (Young et. al., 2005). This could be due to the production of reactive oxygen species (ROS) during hypoxia.

The R28 neuronal cell line is ideal for *in vitro* retinal studies because of its expression of retina-specific markers (transferring, retinol binding protein, retinol dehydrogenase, retinal protein RRG4, Cathepsins (B, C, S), beta-2 arrestin, green-sensitive opsin, blue cone opsin like pigment and retinoid X receptor gamma), neuronal genes (nestin), mature neuronal markers (clamodulin, P-glycoprotein, internexin, and calcineurin A), functional neurotransmitter responses and lack of tumorigenicity (Seigel et. al., 1996, Seigel et. al., 1998).

This is the first study of this kind to use the R28 retinal cell line for the purpose of establishing PKC γ ability to act as a stress sensor (through activation with hydrogen peroxide or TPA). This study will determine if PKCγ has neuroprotective properties through its downregulation of gap junctions, especially such an important retinal gap junction as Cx50.

In this final chapter, using the R28 neuronal cell line, we will show that PKC gamma gets activated by oxidative stress, translocates to the membrane, and causes loss of the Connexin 50 gap junction plaques. This study will also show that knocking down PKC gamma with si-RNA, results in increased cell death, showing that PKC gamma is essential in preventing the spread of apoptotic signals caused by oxidative stress.

4.2 Materials and Methods

4.2.1 Cell Culture

R28 cells, an immortalized retinal precursor cell line derived from the rat retina at postnatal day 6, were the kind gift of Gail M. Seigel (The State University of New York, Buffalo, NY). R28 cells were cultured in Dulbecco's modified Eagle's medium (DMEM, low glucose; Invitrogen, San Diego, CA) supplemented with 10% fetal bovine serum and 50 µg/mL gentamicin, 0.37% sodium bicarbonate, 0.05 U/mL penicillin, and 50 µg/mL streptomycin (pH 7.4) at 37°C in an atmosphere of 90% air and 10% CO_2.

4.2.2 Whole Cell Homogenate Preparations (WCH)

Whole cell homogenates were prepared (Lin et. al., 2003) from cells grown to 90% confluency, then collected by scraping from plates, sedimented and washed 2 times in cold phosphate-buffered saline (PBS). The cell pellets were lysed on ice with cell lysis buffer containing 20 mM Tris-HCl, pH 7.5, 0.5 mM EDTA, 0.5 mM EGTA, 0.5% Triton X-100, 0.1% protease inhibitor mixture cocktail, 5 mM NaF, and 2 mM PMSF. Lysates were sonicated for 20 seconds on ice. Protein concentration of each sample was measured using Bradford Coomassie Blue Colorimetric Assay (Bio-Rad, Hercules, CA) and samples were diluted to make concentrations equal in all samples to 2 mg/mL.

4.2.3 Western Blot

Western blot analyses were carried out as previously described in Wagner and Takemoto, 2001. R28 cells (6.0×10^6 cells/flask) were harvested in cold phosphate buffered saline (PBS). Whole cell Homogenate (WCH) was obtained and 12.5% SDS-PAGE gel containing 25 µg of total cell protein was loaded in each lane at all times (OPTI TRAN, Midwest Scientific, St. Louis, MO). The membrane was incubated for 12 h in primary antibody either in anti-PKCγ (BD, Transduction) or anti-Cx50 (Zymed, Invitrogen), in 3% powdered milk in water at 4 °C. The membranes were then washed for 10 min, 3 times, in PBS. Western blots were visualized

with SuperSignal West Femto Substrate kit supplied with Alexa Fluor 466 and 568 goat anti-mouse or anti-rabbit IgG (H+L) conjugated secondary antibodies. Anti-mouse or anti-rabbit IgG were conjugated with horseradish peroxidase (Pierce, Rockford, IL, cat no. 34095) and visualization was accomplished after exposure to X-ray film (Midwest Scientific, St. Louis, MO).

4.2.4 Transfection

Transient transfection of R28 cells took place when the cells reached approximately 60% confluency. The cells were transfected using Lipofectamine using manufacturer's instructions 2000 (Invitrogen). Cx50-EGFP was a kind gift from David Paul (Harvard, Boston, MA) and PKC γ-EGFP was a kind gift from Peggy Zelenka (National Institute of Health, Washington DC) 4 μg of DNA plasmid and 0.1 mg of Lipofectamine in 250 μL of serum and antibiotic free media were used for each transfection. The cells were incubated with the DNA plasmid and Lipofectamine for 24 h at 37 °C. After incubation, medium containing twice the amount of fetal calf serum (20%) was added for 24 h. Cx50-EGFP stable cell line was created by selection with 1 mg/mL G418 (Research Products International) for 6 weeks and grown in half that concentration of G418 thereafter.

4.2.5 PKCγ Activity Assay

Confluent cells were treated with 50 nM, 100 nM, 200 nM, 400 nM, or 800 nM of phorbol-12 myristate 13 acetate (TPA) for 30 min and 50 μM, 100 μM, 200 μM, 400 μM, 800 or μM of hydrogen peroxide for 30 min. After preparation of cells as previously described (Zhou et. al., 2003) whole cell homogenates (WCH) were incubated overnight with monoclonal mouse anti PKCγ antibodies (1:1000) from Sigma (Dallas, TX). After this, 20 μL protein-agarose beads (A/G Plus; Santa Cruz Biotechnology, Santa Cruz, CA) were added to the mixture and were further incubated for another 2 hours. The beads were collected by centrifugation at 2000 rpm for 1 min then washed with phosphate-buffered saline (PBS) four times. Specific PKCγ activity was analyzed by use of the PepTag® non-radioactive protein kinase C assay system (Promega Madison, WI). Beads were mixed with PepTag® PKC Reaction 5X Buffer (5 μL), PepTag® C1 Peptide (0.4 μg/μL, 5μL), PKC Activator 5X Solution, and incubated for 30 min in a 30 °C bath.

The reactions were stopped by heating at 100°C for 10 min and fluorescent phospho-PepTag peptides (phosphorylated by PKCγ) were resolved by 0.8 % agarose gel electrophoresis and visualized under UV light. Peptide bands were excised and their fluorescence intensities were quantified by spectrophotometry at 570 nm.

4.2.6 Translocation

R28 cells were grown until confluency, then 200 nM TPA or 100μM hydrogen peroxide was added for 30 min, then cells were collected by scraping from plates, sedimentation and washing 2 times in cold phosphate-buffered saline (PBS). Translocation was performed as described in Lin and Takemoto (2005). Translocation Buffer (1 mL) (50 mm Tris-HCl, ph7.5, 20 mm $MgCl_2$) was added to cells. Soluble and membrane fractions were separated by centrifugation at 100,000 × g for 1 h at 4 °C. The pellets were then resuspended with translocation buffer and incubated with monoclonal mouse anti PKCγ antibodies (1:1000) from Sigma (Dallas, TX). Western blot analyses of the pellets and supernatants were performed. Western blot bands were quantified by UN-Scan-It software (Silk Scientific, Orem, UT) and expressed as pixel intensities.

4.2.7 Translocation – Confocal Microscopy

Translocation to the membrane was measured by confocal microscopy. 90% confluent transfected R28 cells with PKCγ –EGFP were treated with 200 nM TPA or 100 μM hydrogen peroxide as described in the figure. The cells were fixed with 2.5% paraformaldehyde, quenched with 50 mM Glycine, washed with PBS, permeabilized with 0.05% Triton-X100 in PBS for 30 minutes, washed with PBS, cells were labeled with 1 μM TO-PRO-3 dye (to label the nuclei of cells) for 15 min (Molecular Probes, Eugene, Oregon) and were then washed in cold PBS, 2 times, and mounted onto coverslips using ProLong Gold antifade reagent (Molecular Probes, Eugene, Oregon). Confocal imaging was carried out at room temperature by Nikon confocal microscope model Nikon C1 scanning confocal microscope with a 2-laser units system: air-cooled argon laser (454 nm) and He–Ne laser (543). GFP tag was visualized through autofluorescence at 454nm (green), To-Pro3 was visualized at 543 nm. Images were taken using

Nikon Plan Fluor 40×/0.60 ELWD DIC oil objective, standardized pinhole (30 μm) and gain settings as indicated.

4.2.8 PKCγ siRNA

All siRNA transfection reagents: RNAiFect siRNA transfection reagent (cat no. 301605), negative non-silencing control siRNA (cat no. 102076), were purchased from Qiagen (Valencia, CA). Custom designed anti-PKC γ siRNAs, HPP grade, were designed and purchased from Qiagen by Dingbo Lin (Lin and Takemoto, 2006). To design siRNA, PKCγ amino acid sequence (NCBI access No. P05967 and Mus musculus protein kinase C, gamma (Prkcc), mRNA was used GeneID: 18752). Sequence #1 was sigma1 number 46172 against 639-659 sequence (5'-gctgtgtgcgcagcgtgccct-3') sequence coding for C2 domain)(Lin and Takemoto, 2006), Sequence #2 was sigma2 number 46173 targeting 181-201 sequence (5'- ggcatgaaatgttcctgttgc-3'), which is coded for C1B domain (Lin and Takemoto, 2006).

Control non-silencing siRNA and anti-PKC γ -siRNA were prepared according to Qiagen technical protocol in an RNAse-free environment. Transfection of adherent cells with siRNA was carried out according to the protocol in the Qiagen RNAiFect™ Transfection Handbook in 12-well plates using 2 μg siRNA per well (2.5 μg/mL per well). R28 cells were seeded and grown in 12-well plates and, when nearly 70% confluent, cells were transfected with siRNA with negative, non-silencing control siRNA and all three different types of PKC γ siRNA. After transfection, cells were grown for 48 hours. After that cells were collected, whole cell lysates were made, and western blot was done as previously described by using anti PKCγ antibodies (1:1000) from Sigma (Dallas, TX). Western blot bands were quantified by UN-Scan-It software (Silk Scientific, Orem, UT) and expressed as pixel intensities. The knockdown of PKCγ levels are expressed as % of the relative pixel intensities of PKCγ knockdown to the loading control.

4.2.9 Cell Viability Assay

R28 cells were grown to 70% confluency then transfected with 2μg siRNA type 1 and negative control siRNA for 48 hours in 12 well plates. 100 μM, 200 μM, 400 μM, 800 μM or 1600 μM of hydrogen peroxide was present for 12 hours to induce cell death. Cell viability

assays were performed as described by Narayanan et al. (2005). Cells were incubated for 5 minutes with 500 µl of 0.2% trypsin-EDTA after washing with PBS-EDTA; cells were scraped, and centrifugated at 1000 x *g* for 5 minutes. These were resuspended in 500 mL of serum free medium, and 100 µL of trypan blue to label non-viable cells (0.4% in 0.9% NaCI solution) was added to the solution. This mixture was allowed to stand at room temperature for 5 min in the dark prior to counting cells by use of a hemocytometer (Hausser Scientific, Horsham, PA). Experiment was repeated 4 times, every cell was counted in each well and expressed as a percentage of viable cell vs non-viable. Commercial software (Origin; Microcal Software Inc., Northampton, MA) was used for statistical analyses. Results were expressed as the mean ± SD. Differences at $p<0.05$ were considered to be statistically significant.

4.2.10 Caspase-3 Colorimetric Assay

Activation of caspase-3 in R28 cells was determined by caspase-3 colorimetric activity assay (Chemicon, Temecula, Calif.) as previously described in (Wang et.al., 2001). R28 cells were grown to 70% confluency then transfected with 10µg siRNA type 1 or negative control siRNA for 48 hours in 10 ml flasks, cells reached full confluency in 48 hours. Then cells were treated with 400 µM H_2O_2 for 30 min, 60 min or 2 hours. Cells were collected and pellets were prepared at 2,500 rpm for 5 min. Cells were then lysed in a provided lysis buffer (from the manufacturer). Protein levels in the lysates (cytosolic extract) were measured by the Bradford Coomassie blue colorimetric assay (Bio-Rad, Hercules, CA) and equalized accordingly to obtain 150 µg of cytosolic extract per sample. Samples were incubated with 300 mM caspase-3 substrate (*N*-acetyl-Asp-Glu-Val-Asp (DEVD)-*p*-nitroanilide) at 37°C for 2 hr. Samples were analyzed at 400 nm in a microtiter plate reader. Data are expressed as fold increase–decrease in caspase-3 activity compared with negative control siRNA and shown as the mean ± SEM. Values of $p \leq 0.05$ were considered to be statistically significant (*).

4.2.11 Gap Junction Activity Assay

R28 cell gap junction activity was measured by the scrape loading/dye transfer assay (SL/DT) as described previously (Lin and Takemoto, 2005). The SL/DT assay is a fast and simple measurement of the gap junction cellular communication between cultured cells in a

monolayer. Lucifer yellow is a very fluorescent 4-aminophthalimide and is used as a tracer dye. SL/DT is based on causing a cut in the plasma membrane to allow Lucifer Yellow to diffuse into the cell as it cannot penetrate intact membranes. Because of its low molecular weight (*M*r 457.2) the Lucifer yellow is able to be transmitted from one cell to another and it is assumed that this process takes place through gap junctions (El-Fouly et. al., 1987). Rhodamine dextran is a high molecular weight polymer (*M*r 10,000), not able to diffuse through intact plasma membranes, or cross the gap junctions; therefore, it is used as a control to differentiate dye transfer from dye leakage. (El-Fouly et. al., 1987)

R28 cells were grown until reaching 90% confluency, on glass slides, in six well plates, then, 200 nM TPA or 100 µM hydrogen peroxide was added for 20 min. After that cells were rinsed with phosphate-buffered saline (PBS) and then 2.5 µl of both 1% Lucifer Yellow and 0.75% Rhodamine Dextran (Molecular Probes, Oregon) were added at the center of the cover slip, and two cuts across the cover slip were made to form a transient tear in the plasma membranes of the cells to permit dye transfer through gap junctions. After incubation with the dye for 1 min at room temperature, these cells were rinsed with PBS and incubated with normal growth medium for an additional 10 min to allow dye transfer in the cell culture incubator. The cells were fixed with 2.5% paraformaldehyde, quenched with 50 mM Glycine, washed with PBS, permeabilized with 0.05% Triton-X100 in PBS for 30 minutes, washed with PBS and cell bodies were labeled with 1 µM 4',6-diamidino-2-phenylindole dihydrochloride (DAPI) for 15 min (Molecular Probes, Eugene, Oregon). Dye transfer was evaluated by Nikon Fluorescent microscope (Nikon Eclipse E600). For quantification, gap junction activity was expressed as the number of cells transferring Lucifer yellow minus cells with Rhodamine dextran per total number of DAPI stained cells. Cells were counted by using Image J software tools. Three different areas along each scrape were analyzed with at least 200 cells counted. The experiments were repeated three times, and data are mean ± S.E.M.

4.2.12 Cx50-EGFP Confocal Microscopy

R28 cells were grown on glass slides in 6 well plates, and transfected with Cx-50-EGFP as described in the transfection section. After the transfections, cells were treated with 200 nM TPA or 100µM hydrogen peroxide for 20 min, cells were fixed with 2.5% paraformaldehyde,

quenched with 50 mM Glycine, washed with PBS, permeabilized with 0.05% Triton-X100 in PBS for 30 minutes, washed with PBS, cells were labeled with 1 μM TO-PRO-3 dye (to label cell bodies) for 15 min (Molecular Probes, Eugene, Oregon), were then washed in cold PBS, 2 times, and mounted onto coverslips using ProLong Gold antifade reagent (Molecular Probes, Eugene, Oregon). Confocal imaging was carried out at room temperature with a Nikon (model Nikon C1) scanning confocal microscope with a 2-laser units system: air-cooled argon laser (454 nm) and He–Ne laser (543). GFP tag was visualized through autofluorescence at 454 nm (green), To-Pro3 was visualized at 543 nm. Images were taken using Nikon Plan Fluor 40×/0.60 ELWD DIC oil objective, standardized pinhole (30 μm) and gain settings. then viewed under on a laser scanning confocal microscope. The total number of cell surface plaques, the number of plaques on the outer edge of cells and on the border between cells, the number of plaques larger than 1 μm^2 per single cells in each image were counted manually by marking every spot of interest with Image J software tools. To find and count plaques with area more than 1 μm^2 a circle was drawn (1 μm^2) using Image J software tools which measures the area for every plaque. Four points per slide were photographed. The experiments were repeated three times, and data are mean ± S.E. Values of $p \leq 0.05$ were considered to be statistically significant (*).

4.2.13 Phosphorylation Assay

R28 cells were grown in 10 mL flasks, then transfected with EGFP empty vector and Cx50-EGFP grown until cells reached full confluency. After the transfection, cells were treated with 200 nM TPA or 100 μM hydrogen peroxide for 20 min then were collected and lysed on ice with 1 mL of lysis buffer followed by homogenization and sonication. The cell lysis buffer contains 20 mM Tris-HCl (pH 7.5), 0.5 mM EDTA, 0.5 mM EGTA, 0.5% Triton X-100, 25 μg/mL aprotinin, and 25 μg/mL leupeptin. After centrifugation at 13,000 rpm (20,000*g*) for 20 minutes, the supernatants were collected and used as whole cell extracts. Immunoprecipitation antibodies (5 μg/mL) anti-GFP antibody (BD Biosciences, Palo Alto, CA) were added to 1 mL whole-cell extracts containing 2 mg/ml total protein, and incubated at 4°C overnight with constant rotation. After this, 20 μL protein-agarose beads (A/G Plus; Santa Cruz Biotechnology, Santa Cruz, CA) were added to the mixture and were further incubated for another 2 hours. The beads were collected by centrifugation 10,000 rpm for 25 sec and washed with phosphate-

buffered saline (PBS) four times, extracted with 20 µL 1x sample loading buffer (containing 50 mM Tris-HCl [pH 6.8], 100 mM dithiothreitol [DTT], 2% sodium dodecyl sulfate [SDS], 10% glycerol, and 0.1% bromophenol blue), and boiled for 3 minutes. Then samples were loaded on to 12.5% SDS-PAGE and separated proteins were transferred to nitrocellulose membranes and probed with anti-phosphoserine antibodies (1:500; Chemicon) to try to detect any presence of phosphoserine in Cx50.

4.3 Results

4.3.1 PKCγ and Cx50 are present in R28 cell line

Western blot analyses confirmed the presence of both PKC gamma and Connexin 50 in R28 neuronal cell line. Signal for Cx50 was faint, but still was present, indicating that both PKCγ and Cx50 are present in R28 cell line (Fig. 4.1).

4.3.2 PKCγ activation by TPA and Hydrogen Peroxide

It was previously reported that hydrogen peroxide and TPA activates PKCγ through formation of disulfide bonds in the cysteine residues of the C1B domain (Lin et. al., 2003). To examine the effect of H_2O_2 and TPA on activation of PKCγ in R28 cells, PKC γ enzyme activity assays were performed. Endogenous PKCγ was immunoprecipitated and its enzyme activity was measured by use of the PKC peptide substrate. To determine the optimum concentration of H_2O_2 and TPA that is needed for PKC γ activation, a broad spectrum (50 nM, 100 nM, 200 nM, 400 nM, 800 nM of TPA and 50 µM, 100 µM, 200 µM, 400 µM, 800 µM of H_2O_2) of concentrations were used for these experiments. In Figure 4.2 it is shown that endogenous R28 cell PKCγ is activated after 30 min treatment with H_2O_2 and TPA. Results showed that optimal activation was with concentrations of 100 µM H_2O_2 (activity increased by 120%) and 200 µM of TPA (activity increased by 150%), thus, these concentrations were used in subsequent studies.

4.3.3 PKCγ is translocated to the membrane following treatment with TPA and Hydrogen Peroxide

In many types of mammalian cells, PKC is cytoplasmic and inactive as shown by comparing pellet (which is the membrane portion) and supernatant (cytoplasmic fraction). In Fig 4.3 majority of the untreated PKCγ was in the cytoplasmic fractions. PKCγ translocates from the cytosol to the membrane once it is activated by activators. Fig. 4.3 and Fig 4.4 shows the affect of 100 µM H_2O_2 and 200 µM of TPA on PKCγ translocation using two different methods.

Pellet and supernatant fractions (20 µg of protein per lane) were separated on 12% SDS-PAGE and probed by Western blotting. Fig.4.3 shows that PKCγ translocated to the membrane following treatment with TPA and hydrogen peroxide. TPA had a larger effect than hydrogen peroxide, judging from pixel intensities. About 34% of PKCγ of the total protein in untreated R28 cells was at the membrane (in the pellet fraction), while, after treatment with TPA, 87% of the total PKCγ protein was at the membrane (pellet fraction). Similarly, 35% of PKCγ total protein, in untreated R28 cells, was at the membrane, but following hydrogen peroxide treatment, 82% of the total PKCγ protein was in the membrane as can be observed in Fig. 4.3. This result indicates that PKCγ does indeed translocate from cytosol to membrane in R28 cell line upon activation.

To further show the ability of PKCγ to translocate to the membrane, confocal microscopy was performed. R28 cells were transfected with PKCγ –EGFP construct and, after the transfection, cells were treated with 200 nM TPA or 100 µM hydrogen peroxide. In Fig. 4.4 it can be observed that GFP tag (which lights up green) is primarily localized non- specifically throughout the cell in untreated cell. Following treatment with TPA or hydrogen peroxide, it can be observed that GFP tagged PKCγ translocated to the edges of the R28 cell, thus confirming that PKCγ does indeed respond to phorbol ester and hydrogen peroxide by translocating to the membranes.

4.3.4 Knockdown of PKCγ Reduces Protection of R28 Cells from Hydrogen Peroxide induced and Caspase-3 linked Apoptosis

PKCγ plays an important role in cell survival and its ability to sense oxidative stress, thus having a neuro-protective effect. To test this hypothesis in the R28 cell line, PKCγ levels were reduced with the use of PKCγ siRNA, then the cells were exposed to hydrogen peroxide to induce cell apoptosis and levels of cell survival were checked.

In order to show that PKCγ siRNA transfection decreased level of expression of PKCγ protein, whole cell homogenates from transfected cells were subjected to western blot analyses with PKCγ antibody. Fig. 4.5 shows that by transfecting cells with PKCγ sigma 1 siRNA protein levels decreased after 48 hours of transfection by approximately 80% (Fig. 4.5, sigma1 lanes), compared to the amount of PKCγ in control to cells transfected with negative control, non

silencing siRNA. Sigma 2 siRNA was not able to reduce the levels of PKCγ, so, for cell viability experiments, cells were transfected with sigma 1 PKCγ siRNA.

Hydrogen peroxide acts on many cells to induce apoptosis through activation of the caspase-3 pathway. Hydrogen peroxide was added for 12 hours to siRNA sigma 1 transfected cells to induce cell death at concentrations of 100 μM, 200 μM, 400 μM, 800 μM or 1600 μM. By knocking down levels of PKCγ with PKCγ siRNA, R28 cells were more susceptible to cell death after treatment with hydrogen peroxide. This held true for all levels of hydrogen peroxide (Fig. 4.6). At 400 μM of hydrogen peroxide the difference in the amount of viable cells was 25% between negative control transfected vs. sigma 1 PKCγ siRNA treated cells. These results show that PKC γ helps in protection against oxidative stress.

Reduction of endogenous PKCγ also resulted in less protection from hydrogen peroxide induced cell death as measured by active caspase-3 assay (Fig. 4.7). PKCγ siRNA treated cells were treated with 400 μM H_2O_2 for 0-120 min. In PKC gamma siRNA treated cells caspase-3 enzyme activity was detected as early as 30 min after initial treatment with hydrogen peroxide (Fig. 4.7), in negative control siRNA transfected cells caspase-3 enzyme activity was not measured until the cells were incubated with hydrogen peroxide for 2 hours. This result indicates that knocking down PKCγ enzyme in R28 cells causes the process of apoptosis to start earlier (as indicated by caspase 3 assay) and leads to statistically significant vulnerability to cell death resulting from prolonged exposure to hydrogen peroxide.

4.3.5 TPA and Hydrogen Peroxide inhibit gap junction activity in retinal R28 cells

Previous publications have documented that the activation of PKCγ decreases the gap junctional communications through phosphorylation of Cx43 in lens epithelial cells (Lin and Takemoto, 2003 and 2005). In the current study, TPA and hydrogen peroxide activated PKCγ which increased translocation of PKCγ to membranes. R28 cells were grown until 90% confluency on glass slides in six well plates, then 200 nM TPA or 100 μM hydrogen peroxide was added for 20 min. Gap Junction activity was measured using the scrape load/dye transfer method. In Fig. 4.8, the abilities of gap junctions to transfer Lucifer Yellow dye are shown. Photos were taken so they would show both Lucifer Yellow and Rhodamine Dextran as shown. In untreated cells green fluorescing Lucifer Yellow dye can be seen spreading away from the

scrape (Fig. 4.8). In both TPA treated and hydrogen peroxide treated samples, the amount of dye transfer was significantly reduced. For quantification, the extent of dye transfer was calculated by counting the number per square mm of Lucifer Yellow-labeled cells from the initial scrape with subtraction of Rhodamine Dextran label as a cell damage control. On average there were approximately 5 cells per square mm in untreated samples, both hydrogen peroxide and TPA showed reduction to around 1 cell per square mm (Fig. 4.8), average amount of dye transfer was reduced by approximately 85% in both TPA and hydrogen peroxide. Both TPA and Hydrogen peroxide affected the ability of gap junctions in R28 cell line to pass on Lucifer yellow dye, indicating that TPA and hydrogen peroxide have the ability to prevent gap junctions function. However, this assay cannot distinguish which exact gap junctions are affected.

4.3.6 Cx50-EGFP Gap Junction Plaques are reduced by TPA and Hydrogen Peroxide

GFP-Cx50 overexpression in R28 cell line allowed for an efficient way to visualize localization of Cx50 because of the GFP tag. Stable transfectants of the R28 cell line expressing the GFP-Cx50 or EGFP plasmids alone were selected using 1 mg/mL G418 antibiotic for 6 weeks. Confocal laser scanning microscopy (CLSM) was used to visualize successful transfection of the GFP plasmid through autofluorescence at 454 nm (green). Transfected cells with GFP-Cx50 were localized in distinguished plaques (Fig. 4.9, untreated). The EGFP empty plasmid appeared diffuse and nonspecific throughout the entire cell, (Fig. 4.10) it also lacked of any kind of change in localization in response to TPA or hydrogen peroxide, this experiment was done as a control.

90% confluent transfected cells then were treated with 200 nM TPA or 100 µM hydrogen peroxide for 20 min and fixed with 2.5% paraformaldehyde on glass slides, to see if TPA or hydrogen peroxide would have any effect on Cx50 plaque formation. Results shown in Fig. 4.9 demonstrates a 4-fold decrease in the number of plaques per cell in the presence of TPA or hydrogen peroxide. This result indicates that both hydrogen peroxide and phorbol ester have the ability to reduce the number of Cx50 plaques. Formation of gap junctional plaques is a prerequisite for the functional gap junctions, thus both TPA and hydrogen peroxide were able to make Cx50 gap junction less functional by disrupting plaque formation as indicated in Fig. 4.9.

This experiment, confirmed what was previously noted in gap junction activity assay, only it specifically shows direct effect of hydrogen peroxide and phorbol ester on Cx50.

4.3.7 Cx50 phosphorylation in response to TPA and Hydrogen Peroxide

Cx50 is a phospho-protein, which means that it regulates its gap junctional cell-to-cell communication through phosphorylation. It has been previously demonstrated that activated PKCγ caused phosphorylation of Cx43 which, in turn, decreased gap junction activity in lens epithelial cells in culture (Lin, et. al., 2003). This experiment was performed to see if TPA or hydrogen peroxide would stimulate phosphorylation of Cx50 in the R28 cell line.

Stable transfected R28 cell line with EGFP-Cx50 was treated with 200 nM TPA or 100μM hydrogen peroxide for 20 min, immunoprecipitated with the GFP antibody, and immunoblotted with anti-phosphoserine antibody. The results are shown in the Appendix A, as we were not able to duplicate it, thus its validity is under question.

Co-immunoprecipitation of PKC gamma and Cx50 and Phosphorylation of Cx50 experiments were not successful, this coupled with the previous results could mean that PKC gamma affects Cx50 indirectly. Previous studies have shown that PKCγ besides directly affecting Cx43, also is regulated through membrane protein ZO-1 and calmodulin (Akoev and Takemoto, 2007). Our results of gap junction Cx50 uncoupling due to TPA and oxidative stress, could be because Cx50 is a known Calcium ion channel dependent gap junction, PKC gamma is a known regulator of Calcium ion and this could be the reasoning for indirect PKC gamma control of Cx50 gap junction. See more in Appendix A.

4.4 Discussion

Exposure of cells to oxidative stress elicits cellular responses to avoid lethal damage through induction of necrosis or apoptosis. This is achieved by stimulating protective cellular functions as a compensatory response to stressful stimuli. We propose that in retina this is, in part, is achieved through a protein called PKC gamma. In Chapter 2, we showed that retinal structure is significantly affected especially in the plexiform layers, in the PKC gamma knockout mice. This was important because all the synapses occur in the plexiform layer, indicating that information is not getting passed down, which was confirmed by Electroretinogram, showing a total lack of functional response to the light stimulus in the PKC gamma knockout mice retina. Besides having a structural importance in the organization of the retina, PKC gamma knockout mice retina were more susceptible to oxidative stress induced by hyperbaric oxygen (Yevseyenkov, et.al., 2009) (Chapter 3). Thus, PKC gamma plays an important role in the retina's response to oxidative stress but the exact process of how it is achieved is still under investigation.

Exposure to oxidative stress leads to accumulation of reactive oxygen species (ROS). ROS include a group of molecules such as hydrogen peroxide (H_2O_2), superoxide anion (O_2^-), singlet oxygen (O_2), and hydroxyl radicals (OH^-). All cells have an endogenous antioxidant enzyme that protects against ROS, but when cells undergo oxidative stress, ROS levels have the ability to exceed the counter-regulatory antioxidant capacity, resulting in cell death by apoptosis.

Activation of PKCγ by oxidative stress has been shown to take place in the lens and PKCγ knock mice lenses were more susceptible to H_2O_2 induced oxidative stress damage that led to lens opacities and formation of cataract (Lin et. al., 2006). This study attempts to evaluated PKCγs response and its ability to have neuro-protective function in response to oxidative stress in the retina using the retinal neuronal R28 cell line as a model.

PKC gamma enzyme was previously shown to be activated by hydrogen peroxide and phorbol esters in the NN lens epithelial cell line (Lin et. al., 2004). In this study PKCγ activity is also activated by hydrogen peroxide and phorbol ester in the retinal neuronal R28 cell line (Fig. 4.2). Before PKCγ can be activated it first needs to translocate to the membrane of the cell where the rest of PKC activation takes place (Newton, 2010). PKCγ has the ability to translocate

to the membrane in retinal R28 cells, in response to phorbol ester and hydrogen peroxide. This result can be observed both on western blot and by confocal analyses in Fig.3 and Fig. 4.

In this study, we also demonstrate that the activation of PKCγ by H_2O_2-induced oxidative stress in the R28 retinal cell line, protects from H_2O_2-induced cell apoptosis. Suppression of PKCγ protein synthesis by siRNA, rendered R28 cells more sensitive to oxidative stress-induced cell apoptosis. Results from our study showed that the process of apoptosis started earlier (as indicated by caspase 3 assay) and lead to statistically significant increased vulnerability to cell death after prolonged exposure to hydrogen peroxide (Fig. 6 and 7). Therefore, our study demonstrates an important role of PKCγ in the protection of oxidative stress-induced damage and cell death.

Our study suggests that this process of neuro-protection from oxidative stress by PKCγ is achieved through its ability to regulate one of its downstream targets called gap junctions. Several studies implicated PKCγ dependent closure of gap junction channels as a protective/survival mechanism. The induced channel closure and disruption of gap junction plaques prevents the intercellular transmission of apoptotic signals in lens epithelial cells and whole lens culture by phosphorylation of Cx43 (Lin and Takemoto, 2005; Solan and Lampe, 2009; Laird, 2006). It was also shown that PKCγ has the ability to regulate Cx50, and disrupt functional Cx50 gap junction plaques in lens tissue (Zampighi et.al, 2005).

Oxidative stress (hydrogen peroxide) resulted in activation of PKCγ in R28 cells and this led to the reduction of dye transfer activity, indicated by a reduction of gap junction's ability to pass on Lucifer yellow among cells. Specifically reduced coupling of Cx50 gap junctions plaques in R28 cell line were observed, indicating that PKCγ in part may regulate Cx50 either through direct phosphorylation or through indirect regulation e.g. ZO-1, Calmodulin, disorganization of lipid rafts or altering interaction with other gap junctions. Finding the exact way PKC gamma regulates Cx50 is part of our future studies.

In summary, the results presented in this chapter, indicate a critical role of PKCγ activation in response to oxidative stress, and suggests a role in stopping the spread of apoptotic signal through its regulation of gap junctions, specifically Cx50 in retinal R28 cells. Oxidative stress is implicated in a variety of retinal disorders that includes : diabetic retinopathy, retinitis pigmentosa and retinopathy of prematurity. Understanding how retina responds to oxidative

injury can lead to new and exciting treatments. In fact there are several ongoing clinical trials involving Protein Kinase C for diabetic retinopathy (Shah et. al., 2008).

4.5 Figures

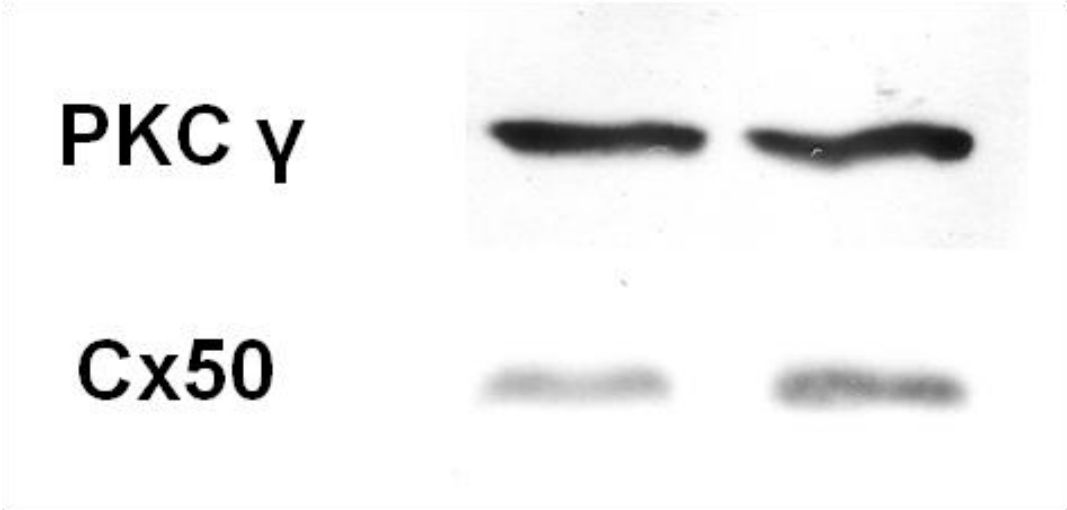

4-1 PKCγ and Cx50 are present in R28 cells

Whole cell lysates from R28 cells, were loaded at 2 µg/lane, blotted with anti-PKC gamma antibody (2 µg/mL) and anti-Cx50 antibody (5 µg/mL). Results show presence of both PKC gamma and Cx50 in the R28 cell line. Lanes are duplicates. Experiments were done in triplicate.

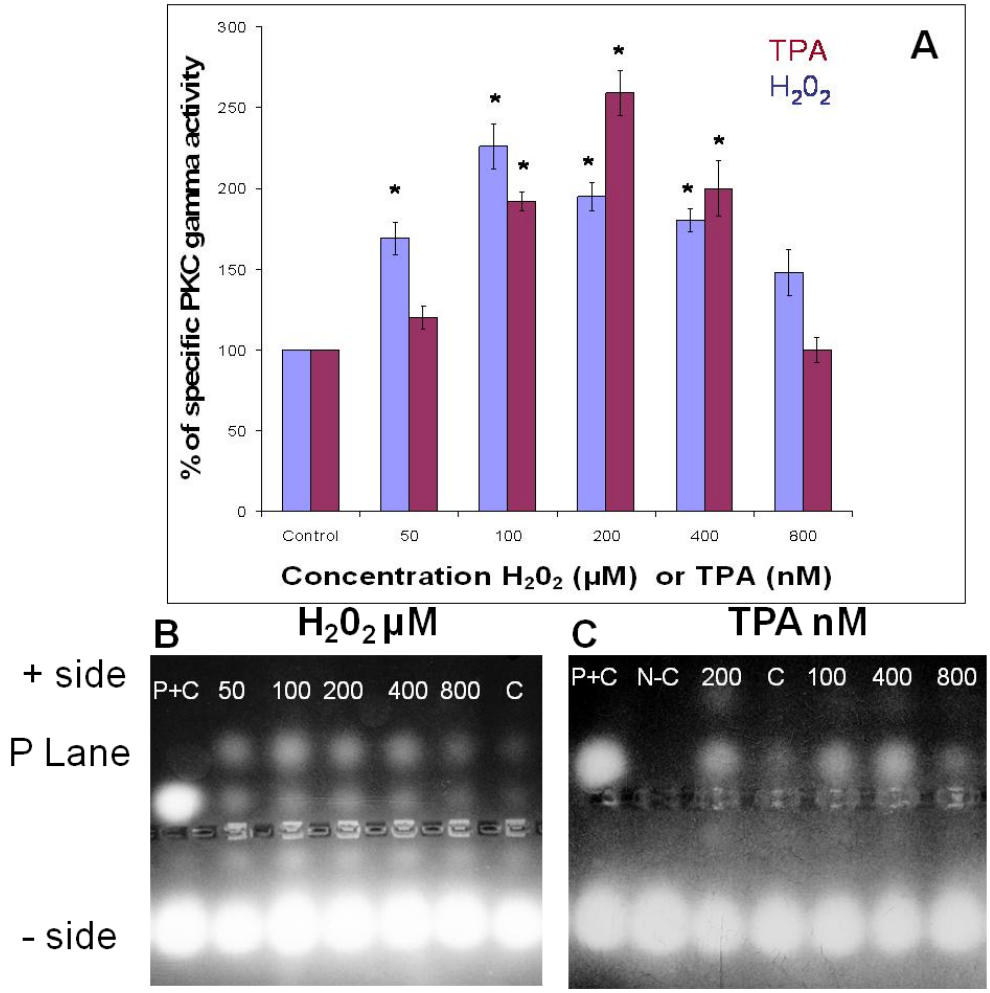

4-2 PKCγ Activity Assay after TPA and H_2O_2 stimulation

R28 cells were treated with TPA and H_2O_2 for 20 min. Enzyme activity was measured using PepTag non-radioactive protein kinase assay. Fluorescence intensities were quantified by spectrophotometry after cutting out the bands (from P Lane) at 570 nm.

A) Graph was plotted as % relative to the untreated Control R28 cells. As ± SEM of three experiments in % difference to control. TPA is shown in Magenta, H_2O_2 is in blue.

*Results are statistically different from control $p \leq 0.05$.

B) Photo of the agarose gel demonstrating PKCγ activity after treatment by H_2O_2. Numbers indicate µM concentration C) Photo of the agarose gel demonstrating PKCγ activity after TPA treatment. Numbers indicate nM concentration.

P+C= Positive PKC control (provided by PepTag), N-C=Negative PKC control (provided by PepTag), C = Untreated Control R28 cells, + side = indicates positive side, - side =indicates negative side, P lane = indicates Phosphorylated PKCγ bands that were cut out for analyses.

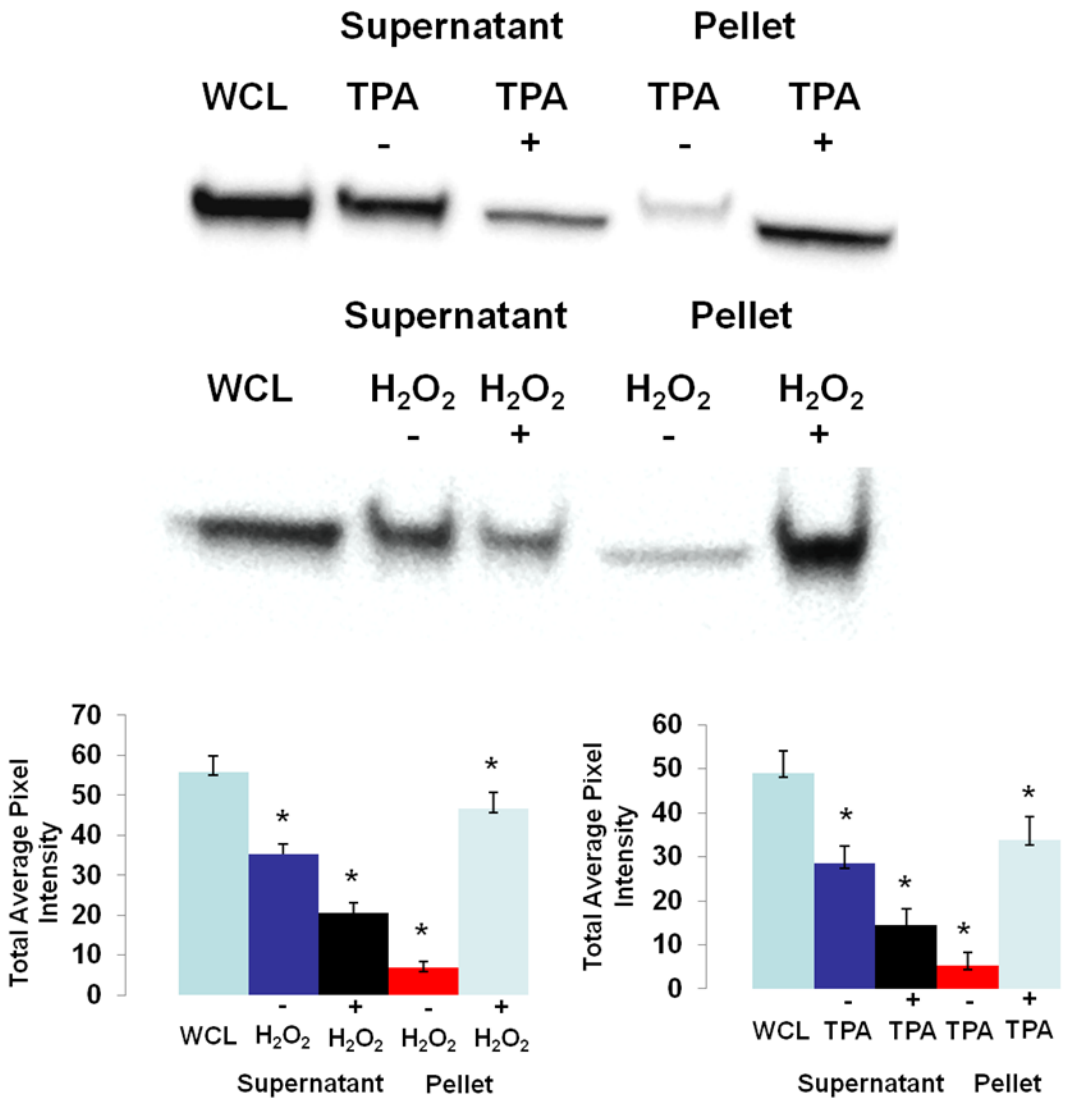

4-3 PKCγ Translocation by Western Blot Analyses.

R28 cells were treated with 100 µM H_2O_2 or 200 µM of TPA for 20 min and samples were subjected to translocation studies and probed with PKCγ antisera at 1:100. For Quantitative analyses bands were digitized using UN-Scan-It software and expressed as pixel intensities of ± SEM of three (separate gels, separate experiments). Results were graphed

* indicates significant difference when comparing levels of protein in treated and untreated samples as compared to changes when going from supernatant to pellet, with $p \leq 0.05$.

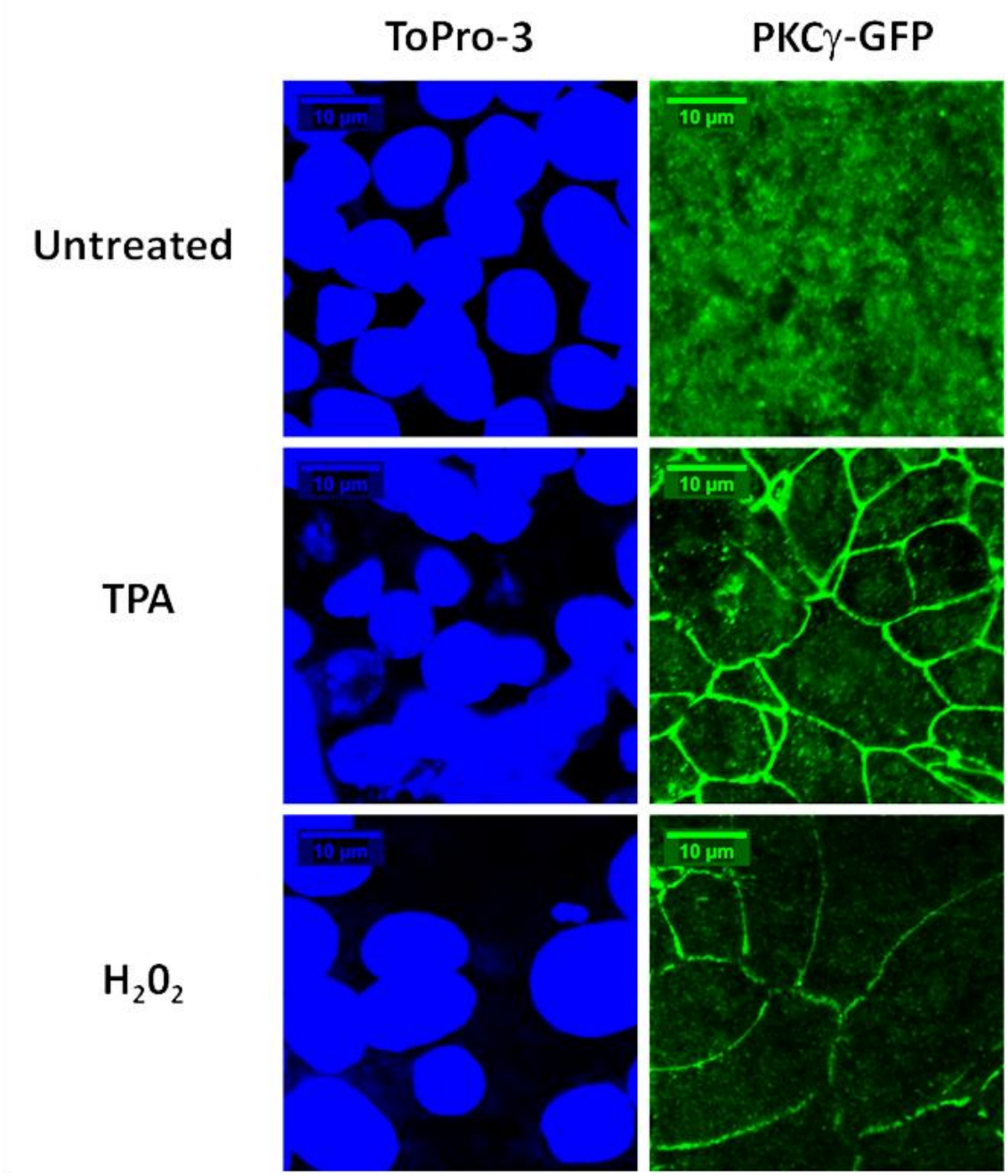

4-4 PKCγ Translocation by Confocal Microscopy

R28 stable cells that contain transfect PKCγ –EGFP construct, were treated with 200 nM TPA or 100 µM hydrogen peroxide for 20 min. Imaging of translocation of EGFP fusion proteins was carried out at room temperature by use of model Nikon C1 scanning confocal microscope. Cells were fixed with 2.5% paraformaldehyde and treated with ToPro-3 for 15 min (to label Cell nuclei). ToPro-3 is depicted in Blue. PKC γ –EGFP construct is labeled in green.

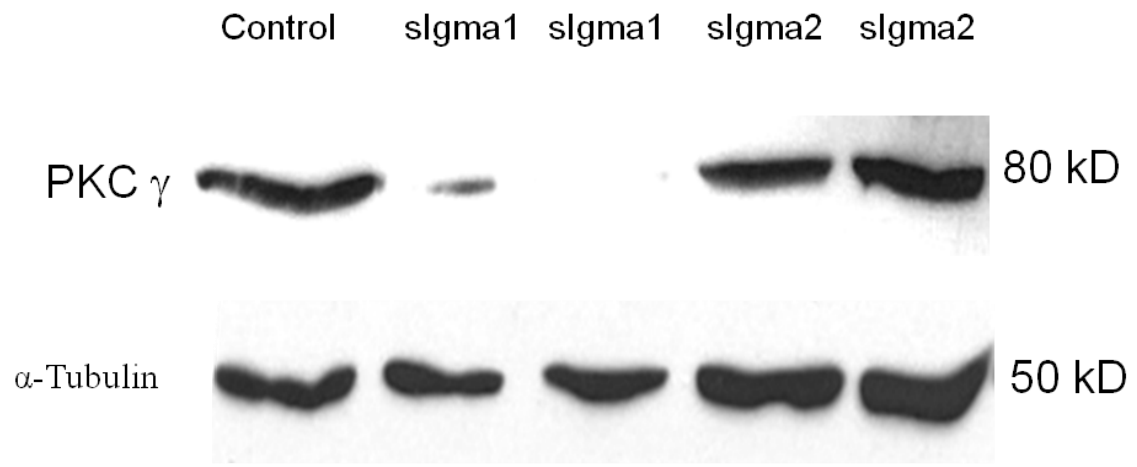

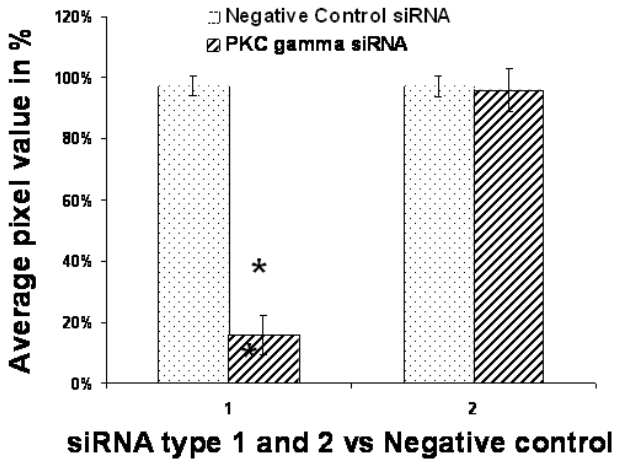

4-5 Levels of PKCγ protein are reduced by siRNA

Western blots analyses of whole cell homogenates (WCH) after siRNA PKC γ transfection 60% confluent R28 cells with 2.5 μg/mL of siRNA for 48 hours. Control cells were transfected with negative control siRNA. Sigma 1 and Sigma 2 – PKCγ siRNA were transfected into the cell line and PKCγ protein levels are shown in these blots as to PKCγ antibody. Bands were digitized by UN-SCAN-It gel software. The average pixel value for all other bands was normalized to tubulin loading controls and expressed in percentage of loading control for ± SEM of three (separate gels, separate experiments).

*Results are statistically different for control $p \leq 0.05$.

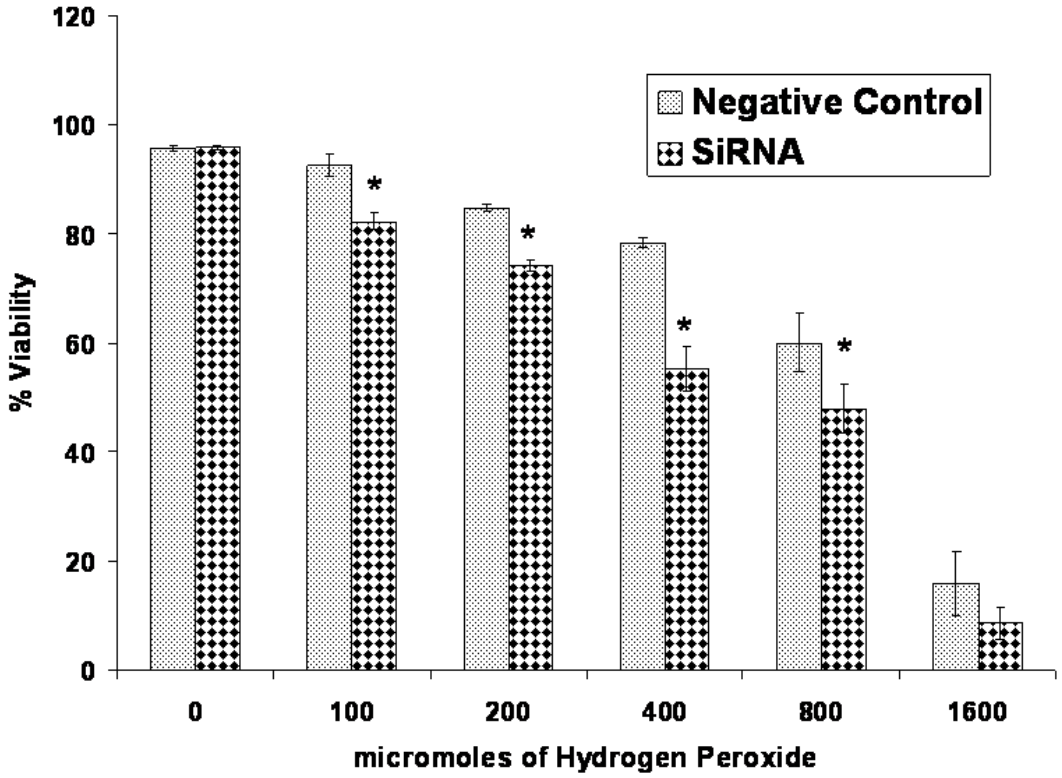

4-6 PKCγ Knockdown with siRNA decreases cell viability after hydrogen peroxide challenge

60% confluent R28 cells were transfected with 2.5 µg/mL sigma 1 PKCγ siRNA for 48 hours in 12 well plates. Control cells were transfected with negative control siRNA. Then incubated with H_2O_2 for 12 hours. Cell death was recorded using the Trypan Blue dye exclusion method. Amounts of viable and dead cells (which stained blue), were counted using hematocymeter and graphed as % of Viability (viable (non-stained cells) divided by the total amount of cells (dead cells, which were Trypan Blue stained plus the non stained cells). There were 2 wells of siRNA transfected cells for each of H_2O_2 concentrations. There were 3 separate experiments. Checkered bars are sigma 1 transfected siRNA and lightly spotted bars are transfected cells with negative control siRNA. The experiments were carried out in triplicate.

*Results are statistically different for negative control transfected siRNA among each concentration of H_2O_2 treatment $p \leq 0.05$.

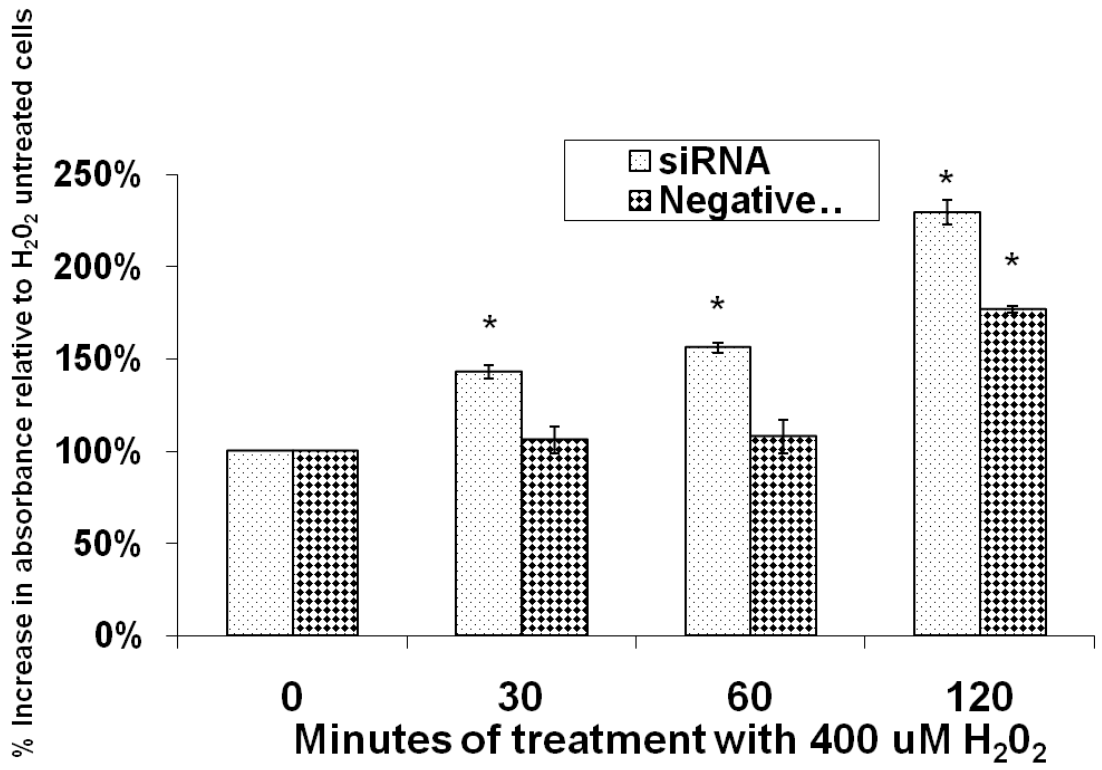

4-7 PKCγ Knockdown with siRNA increases Caspase-3 a pro-apoptotic cell signal after hydrogen peroxide challenge as measured by Caspase-3 Colorimetric Activity.

R28 cells were transfected with 10µg sigma 1 PKCγ siRNA and negative control siRNA for 48 hours in 10 mL flasks then incubated with 400 µM H_2O_2 for periods of 30 min, 60 min and 120 min. Caspase-3 enzyme activity was detected by Caspase-3 Colorimetric activity assay kit (Chemicon), in a microtiter plate reader at 400 nm. Lightly spotted bars are sigma 1 transfected siRNA and checkered bars are transfected cells with siRNA negative control. The experiments were carried out in triplicate on different days and there was 1 flask of cells per each concentration of H_2O_2 on each day of experiments.

Data is expressed as fold increase–decrease in caspase-3 activity compared with H_2O_2 untreated cells, treated sigma siRNA is compared only to treated sigma siRNA, and negative control treated is compared with negative control to find fold increase.

*Results are statistically significant as compared to H_2O_2 untreated cells, $p \leq 0.05$.

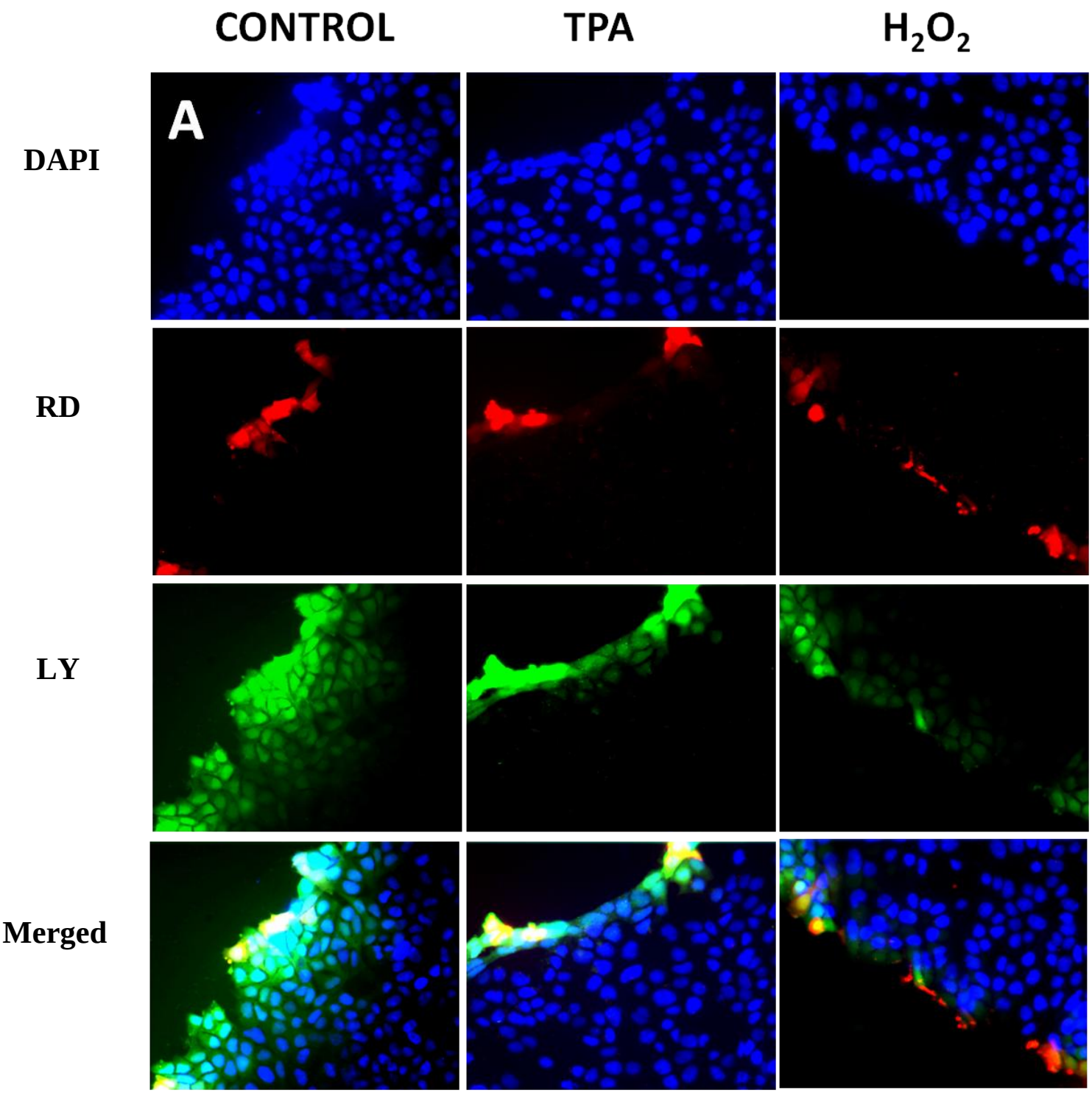

4-8 A. Fluorescent Representation of the scrape load/dye transfer (SL/DT) method

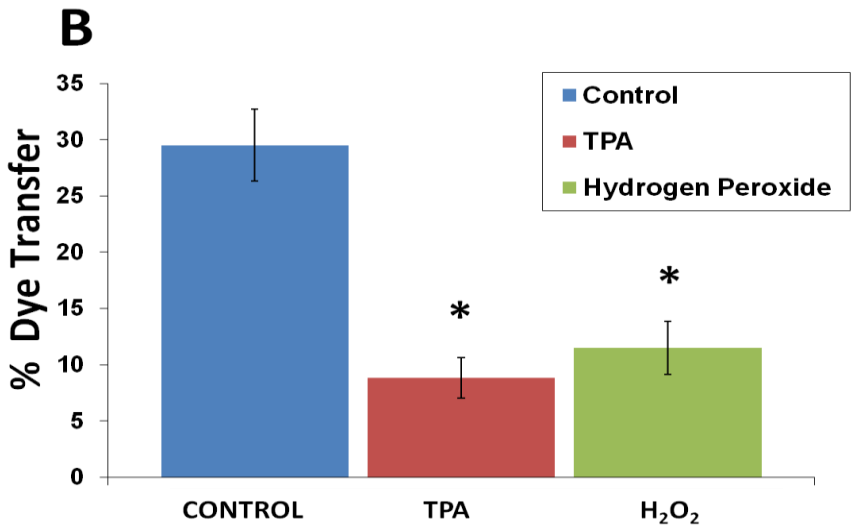

4-8 B. Graphical Representation of the scrape load/dye Transfer (SL/DT) method Peroxide

A. R28 cells were grown until 90% confluency on glass slides in six well plates, then 200 nM TPA or 100 µM hydrogen peroxide was added for 20 min, and level of gap junction activity was measured using the scrape load/dye transfer (SL/DT) method. The images are from fluorescently labeled cells in the microscopic field under 40 x magnifications with a cut showing in each image. 1st row is DAPI labeled cell bodies as showing in blue, 2nd row is (RD) Rhodamine Dextran transfer showing damaged cells by the cut and is shown in Red, 3rd row is (LY) Lucifer Yellow transfer, showing actual transfer among gap junctions, 4th row showing the merged field of all transfers.

Control column – is untreated cells, TPA and H_2O_2 columns are treated samples.

B. For quantification, gap junction activity was expressed as the number of cells transferring Lucifer yellow minus cells with Rhodamine dextran per total number of DAPI stained cells. Three different areas along each scrape were analyzed with at least 200 cells counted by utilizing Image J software tools. The experiments were repeated three times, and data are mean ± S.E.M. The average percentages were graphed and are shown in as control (Blue), TPA (Red), H_2O_2 (Green).

*Results are statistically different for control $p \leq 0.05$.

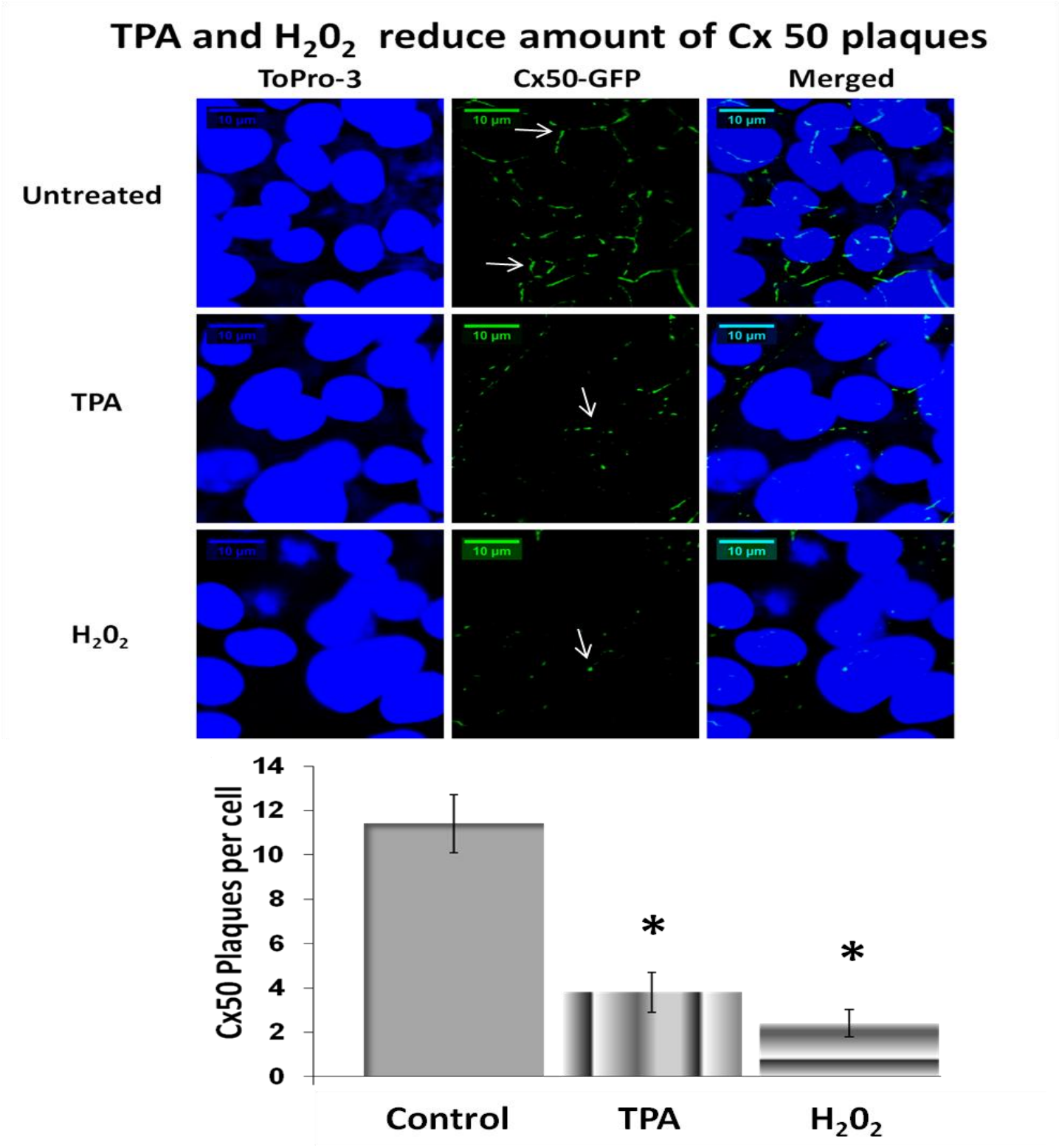
TPA and H_2O_2 reduce amount of Cx 50 plaques
ToPro-3
Cx50-GFP
Merged
Untreated
TPA
H_2O_2
10 µm
Cx50 Plaques per cell
14
12
10
8
6
4
2
0
*
*
Control
TPA
H_2O_2

4-9 TPA and Hydrogen peroxide reduce the amount of Cx50 plaques

R28 cell stable Cx50 –EGFP construct, was activated with 200 nM TPA or 100 μM H_2O_2 for 20 min. Cells were fixed with 2.5% paraformaldehyde and treated with ToPro-3 for 15 min (to label Cell nuclei). ToPro-3 is depicted in Blue. Cx50–EGFP construct is depicted in green. Imaging of EGFP fusion proteins was carried out at room temperature by use of model Nikon C1 scanning confocal microscope. To find and count plaques with area more than 1 μm^2 a circle was drawn (1 μm^2), using Image J software tools which measures the area for every plaque. Arrows depict a 1 μm^2 plaque. Four points per slide were analyzed. The experiments were repeated three times, and data are mean ± S.E.M and was graphed as depicted below confocal images.

* Values of $p \leq 0.05$ were considered to be statistically significant for control untreated.

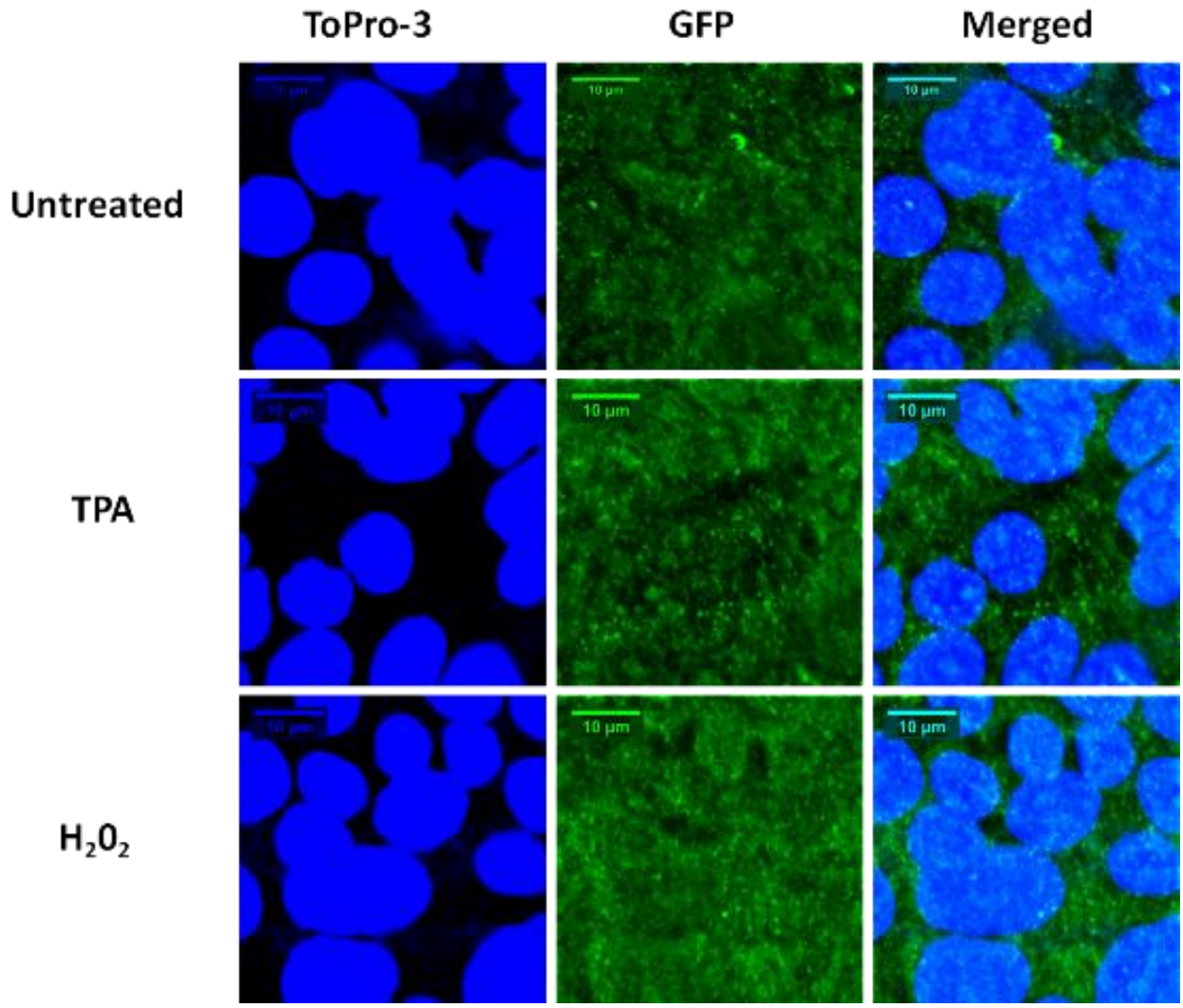

4-10 GFP empty Vector and Effect of TPA and H_2O_2 on it

R28 cell stable empty vector EGFP construct, was activated with 200 nM TPA or 100 µM H_2O_2 for 20 min. Cells were fixed with 2.5% paraformaldehyde and treated with ToPro-3 for 15 min (to label Cell nuclei). ToPro-3 is depicted in Blue. EGFP construct is depicted in green. Imaging of EGFP proteins was carried out at room temperature by use of model Nikon C1 scanning confocal microscope. This was done as control to show that TPA and H_2O_2 have no effect on empty vector.

CHAPTER 5 - Conclusion

Exposure to oxidative stress leads to accumulation of reactive oxygen species and this stimulates protective cellular functions as a compensatory response to prevent the spread of apoptotic signal and prevent cell death. The purpose of this dissertation was to understand the importance of PKCγ activation and regulation of the retinal gap junction protein Cx50, and what role PKCγ plays in this neuro-protective effect.

In Chapter 2, we explored the importance of the presence of PKCγ for retinal structural integrity. Immuno-fluorescence showed presence of PKCγ in outer plexiform (OPL), inner plexiform (IPL) and ganglion cell layers (GCL). Light microscopy of PKCγ knockout mice (KO) retina's showed disorganization of retinal layers, biggest difference was appreciated in the OPL synaptic layer of the retina. INL, GCL of the PKCγ KO showed formation of vacuole like structures, thus in part resulting in decreased nuclei density. Structural damage was further investigated by use of Electron Microscopy to identify the ultra structures (synaptic connections, axon terminals, bipolar cells terminals) and how they were affected in the PKCγ knockout (KO) mice retinas. Lack of PKCγ in mice retinas resulted in disruption of tetrads synaptic vesicles', increased unidentifiable structures; we hypothesize that this structures could be due to the increased in demyelination of the neural tissue in the outer plexiform layer. Electro-Retinogram (ERG), which measures functional response of the retina, showed a marked decrease in both photoreceptor and bipolar cells functional response to light stimuli. This functional result alongside structural damage as shown by microscopy, suggests that presence of PKCγ is essential for normal retinal structure and function.

In Chapter 3, we evaluated whether PKCγ KO mice retinas were more susceptible to oxidative damage caused by hyperbaric oxygen treatment (HBO). Our results showed that PKCγ KO mice retinas were more susceptible to damage after exposure to HBO. Thickness of the ONL, which contains cell bodies of the photoreceptors was drastically reduced following exposure to HBO in the PKCγ KO mice retinas, this effect was more evident in the central part of the retina. This result suggests that PKCγ plays a vital role in protecting photoreceptor cells from oxidative damage. Photoreceptors besides being the light sensors of the eye, are also responsible for the protein metabolism of the outer retina. HBO treatment caused significant reduction of the photoreceptor outer segments, thus disrupting normal retinal organization at the

basal level. INL thickness was significantly reduced in the HBO treated central PKCγ KO mouse retinas. This layer contains cell bodies of rod bipolar, amacrine and horizontal cells. OPL in the HBO treated PKCγ KO mouse retina was disrupted as well. PKCγ was previously shown to be present in the OPL and IPL (Ch.2), our results from Ch.3 indicate that absence of PKCγ in the synaptic layers that connect photoreceptors to bipolar cells (OPL), and bipolar cells to ganglion cells (IPL) resulted in significant decrease in photoreceptor, bipolar, amacrine cells after exposure to HBO. Thus, it is possible to conclude that PKCγ plays a role in regulating synaptic connections and this regulation is vital for protecting retinal cells from oxidative damage.

Our hypothesis is that PKCγ in part achieves this neuro-protective effect through gap junctions. We decided to look specifically at gap junction protein Cx50, because as previous studies have shown it is one of two major connexins in the OPL (the layer most effected by PKCγ KO), it is also a layer that is responsible for interconnections of two cellular layers (ONL and INL) that were most prone to oxidative damage after HBO treatment. Immunolabeling of Cx50 showed that it was present in inner segments, OPL, IPL and GCL), in the PKCγ KO model, immunolabeling was reduced but still was detectable in all the three layers. This, in part, could be due to the fact that was previously shown in Chapter 2, PKCγ KO retina's reduction of cell nuclei density of INL, ONL and GCL. Indicating, in part, that reduction of nuclei results in reduction of connections (provided by Cx50) that are needed. Exposure to HBO in PKCγ control retinas resulted in significant reduction in Cx50 immunolabeling, while exposure to HBO in PKCγ KO mouse retinas resulted in no reduction of Cx50 immunolabeling. This result in part indicates that PKCγ might be responsible for closure of Cx50 gap junctions after exposure to HBO.

Retina tissues cannot be cultured, thus to investigate further how PKCγ responds to oxidative stress, we decided to use retina derived neuronal R28 cells. Our results indicated that PKCγ does indeed get activated (phosphorylated) in response to oxidative stress (mimicked by H_2O_2) as shown by PKCγ activity assay. As previously discussed PKCγ needs to be translocated to the membrane to have the effect on its downstream targets, our results showed that PKCγ is indeed translocated to the membrane as shown both by western blot and confocal microscopy. R28 cells were transfected with PKCγ siRNA and resulted in decrease of PKCγ levels, this cells were then exposed to oxygen challenge by exposure to H_2O_2, this resulted in increased cell death

as measured by PKCγ cell viability test and increased expression of pro-apoptotic signal (Caspase 3) in the PKCγ siRNA treated cells when compared to negative control siRNA treated R28 cells. Therefore, our study demonstrates an important role of PKCγ in the protection of oxidative stress-induced damage and cell death in the retinal R28 cells.

Effect of TPA and H_2O_2 on R28 cells gap junction activity was measured by scrape load/dye transfer (SL/DT) method. Our results indicate that gap junction activity was reduced in response to TPA and H_2O_2; this indicates that gap junctions in R28 cells close in response to phorbol esters and oxidative stress. For connexins to have full functional ability they arrange into plaques, which are clusters of up to 10,000 connexons. Cx50-GFP R28 stable cell line was created to demonstrate whether phorbol ester or oxidative stress would have any effect on Cx50 ability to form plaques. Our results showed that TPA and H_2O_2 caused a reduction in Cx50 plaques in R28 cell line. This result indicates that oxidative stress has the ability to reduce gap junction activity and specifically reduce formation of Cx50 gap junction plaques.

In summary, results from this dissertation indicate that PKCγ does indeed have a neuro-protective function in the retina and it is possible that in part this effect is achieved through control of Cx50 gap junction protein.

CHAPTER 6 - Bibliography

Adachi N, Kobayashi T, Takahashi H, Kawasaki T, Shirai Y, Ueyama T, Matsuda T, Seki T, Sakai N, Saito N. (2008) Enzymological analysis of mutant protein Kinase C gamma causing spinocerebellar ataxia type 14 and dysfunction in Ca2+ homeostasis. *J Biol Chem.* 283:19854-63.

Akoyev V, Takemoto DJ. (2007) ZO-1 is required for protein kinase C gamma-driven disassembly of connexin 43. *Cell Signal.* 19:958-67.

Ananthanarayanan B, Stahelin, RV, Digman MA, Cho W. (2003) Activation mechanisms of conventional protein kinase C isoforms are determined by the ligand affinity and conformational flexibility of their C1 domains. *J Biol Chem.* 278:46886-94.

Aronowski J, Grotta JC, Strong R, Waxham MN. (2000) Interplay between the gamma isoform of PKC and calcineurin in regulation of vulnerability to focal cerebral ischemia. *J Cereb Blood Flow Metab.* 20:343-349.

Asai H, Hirano M, Shimada K, Kiriyama T, Furiya Y, Ikeda M, Iwamoto T, Mori T, Nishinaka K, Konishi N, Udaka F, Ueno S. (2009) Protein kinase C gamma, a protein causative for dominant ataxia, negatively regulates nuclear import of recessive-ataxia-related aprataxin. *Hum Mol Genet*. 18:3533–43.

Baldo GJ, Gong X, Martinez-Wittinghan FJ, Kumar NM, Gilula NB, Mathias RT. (2001) Gap junctional coupling in lenses from alpha (8) connexin knockout mice. *J Gen Physiol.* 118:447–456.

Balendran A, Casamayor A, Deak M, Paterson A, Gaffney P, Currie R, Downes CP, Alessi DR. (1999) PDK1 acquires PDK2 activity in the presence of a synthetic peptide derived from the carboxyl terminus of PRK2. *Curr Biol.* 9:393–404.

Banks EA., Yu XS., Shi Q., Jiang JX. (2007) Promotion of lens epithelial-fiber differentiation by the C-terminus of connexin 45.6 a role independent of gap junction communication. *J Cell Sci.* 120:3602–3612.

Barnett ME, Madgwick DK, Takemoto DJ. (2007) Protein Kinase C as a stress sensor. *Cellular Signaling*. 19:1820-1829.

Battaini F, Mochly-Rosen D (2007) Happy birthday protein kinase C: past,present and future of a superfamily. *Pharmacol Res.* 55:461–466.

Bazan HE, Dobard P, Reddy STK. (1987) Calcium and phospholipid-dependent protein kinase C, and phosphatidylinositol kinase: two major phosphorylations systems in the cornea. *Curr Eye Res.* 6:667-673.

Beahm D, Hall J. (2002) Hemichannel and Junctional Properties of Connexin 50. *Biophysical Journal* 82:2016–2031.

Beatty S, Koh HH, Phil M, Henson D, Boulton M. (2000) The role of oxidative stress in the pathogenesis of age-related macular degeneration. *Surv Ophthalmol.* 45:115-34.

Behn-Krappa A, Newton AC. (1999) The hydrophobic phosphorylation motif of conventional protein kinase C is regulated by autophosphorylation. *Curr Biol.* 728–737.

Blumberg PM, Kedei N, Lewin NE, Yang D, Czifra G, Pu Y, Peach ML, Marquez VE. (2008) Wealth of opportunity—the C1 domain as a target for drug development. *Curr Drug Targets.* 9:641–652.

Bowers BJ, Wehner JM. (2001) Ethanol consumption and behavioral impulsivity are increased in protein kinase Cgamma null mutant mice. *J Neurosci*. 21:RC180.

Campochiaro PA. (2000) Retinal and choroidal neovascularization. *J Cell Physiol.* 184:301–310.

Cha DR, Kim NH, Yoon JW, Jo SK, Kim HK, Won NH. (2000) Role of vascular endothelial growth factor in diabetic nephropathy. *Kidney Int Suppl.* 77:104–S112

Chang YH, Chen PL, Tai MC, Chen CH, Lu DW, Chen JT. (2006) Hyperbaric oxygen therapy ameliorates the blood-retinal barrier breakdown in diabetic retinopathy. *Clin Experiment Ophthalmol.* 34:584-589.

Chen B, Cepko CL. (2009) HDAC4 regulates neuronal survival in normal and diseased retinas. *Science*. 323:256-9.

Chen DH, Brkanac Z, Verlinde CL. (2003) Missense mutations in the regulatory domain of PKC gamma: a new mechanism for dominant nonepisodic cerebellar ataxia. *Am J Hum Genet.* 72:839-849.

Cho W, Stahelin R. (2005) Membrane-Protein Interactions in Cell Signalling and Membrane Trafficking. *Annual Review of Biophysics and Biomolecular Structure* 34:119-151.

Clemens MJ, Trayner I, Menaya J. (1992) The role of protein kinase C isoenzymes in the regulation of cell proliferation and differention. *J Cell Sci*. 103:881-7.

Condorelli DF, Parenti R, Spinella F, Salinaro AT, Belluardo N, Cardile V, Cicirata F. (1998) Cloning of a new junction gene (Cx36) highly expressed in mammalian brain neurons. *European Journal of Neuroscience*. 10:1202-1208.

Correia SS, Duarte CB, Faro CJ, Pires EV, Carvalho AL. (2002) Protein kinase C gamma associates directly with the GluR4-alpha-amino-3hydroxy-5-methyl-4-isoxazole

propionate receptor subunit. Effect on receptor phosphorylation. *J Biol Chem*. 278:6307-6313.

Cooper CD, Lampe PD. (2002) Casein kinase 1 regulates connexin43 gap junction assembly. *J Bioch Chem.* 277:44962–44968.

Cuntz H, Haag J, Forstner F, Segev I, Borst A. (2007) Robust coding of flow-field parameters by axo-axonal gap junctions between fly visual interneurons. *Proc Natl Acad Sci U S A.* 104:10229-10233.

Cusato K, Bosco A, Rozenthal R. (2003) Gap junctions mediate bystander cell death in developing retina. *J Neurosci.* 23:6413-6422.

Dacey DM. (1993) The mosaic of midget ganglion cells in the human retina. *J Neurosci.* 13:5334-5355.

Das S, Lin D, Jena S, Shi A, Battina S, Hua DH, Allbaugh R, Takemoto DJ. (2008) Protection of retinal cells from ischemia by a novel gap junction inhibitor. *Biochem Biophys Res Commun.* 373:504-8.

Deans MR, Volgyi B, Goodenough DA, Bloomfield SA, Paul DL. (2002) Connexin 36 is essential for transmission of rod-mediated visual signals in the mammalian retina. *Neuron.* 36:703-12.

Decrock E, Vinken M, De Vuyst E, Krysko DV, D'Herde K, Vanhaecke T, Vandenabeele P, Rogiers V, Leybaert L. (2009) Connexin-related signaling in cell death: to live or let die? *Cell Death Differ.*16:524-3.

Dedek K, Schultz K, Pieper M. (2006) Localization of heterotypic gap junctions composed of connexin45 and connexin36 in the rod pathway of the mouse retina. *Eur J Neurosci.* 24:1675-1686.

DeRosa AM., Meşe G., Li L., Sellitto C., Brink PR., Gong X, White TW. (2009) The cataract causing Cx50-S50P mutant inhibits Cx43 and intercellular communication in the lens epithelium. *Exp Cell Res.* Apr 1;315:1063-7.

Duda DG. (2006) Antiangiogenesis and drug delivery to tumors: bench to bedside and back. *Cancer Res.* 66:3967–3970.

Dutil EM, Newton AC. (2000) Dual role of pseudosubstrate in the coordinated regulation of protein kinase C by phosphorylation and diacylglycerol. *J Biol Chem.* 275:10697–10701.

Ehrlich R, Harris A, Ciulla TA, Kheradiya N, Winston DM, Wirostko B. (2010) Diabetic macular oedema: physical, physiological and molecular factors contribute to this pathological process. *Acta Ophthalmol*. 88:279-91.

El-Fouly MH, Trosko JE, Chang CC. (1987) Scrape-loading and dye transfer. A rapid and simple technique to study gap junctional intercellular communication. *Exp Cell Res.* 168:422-30.

Ethen CM, Reilly C, Feng X, Olsen TW, Ferrington DA. (2006) The proteome of central and peripheral retina with progression of age-related macular degeneration. *Invest Opthalmol Vis Sci*. 47:2280-2290.

Farahani R, Pina-benabou MH, Kyrozis A. (2005) Alterations in metabolism and gap junction expression may determine the role of astrocytes as "good Samaritan" or executioner. *Glia*. 50:351-361.

Feigenspan A, Janssen-Bienhold U, Hormuzdi S. (2004) Expression of connexin 36 in cone pedicles and OFF-cone bipolar cells of the mouse retina. *J Neurosci.* 24:3325-3334.

Feigenspan A, Teubner B, Wilecke K, Weiler R. (2001) Expression of neuronal connexin 36 in AII amacrine cells of the mammalian retina. *J Neurosci*. 21:230-9.

Feigl B, Stewart I, Brown B. (2007) Experimental hypoxia in human eyes: implications for ischaemic disease. *Clin Neurophysiol*. 118:887–895.

Feigl B, Stewart IB, Brown B, Zele AJ. (2008) Local neuroretinal function during acute hypoxia in healthy older people. *Invest Ophthalmol Vis Sci*. 49:807-13.

Frantseva MV, Kokarovtseva L, Perez Velazquez JL. (2002) Ischemia-induced brain damage depends on specific gap-junctional coupling. *J Cerebral Bood Flow Metab.* 22:453-462.

Fugisawa N, Ogita K, Saito N, Nishizuka Y. (1992) Expression of protein kinase C subspecies in rat retina. *FEBS Lett.* 309:409-412.

Gallegos LL, Newton AC. (2008) Spatiotemporal dynamics of lipid signaling: protein kinase C as a paradigm. *IUBMB Life.* 60:782–789.

Gao T, Toker A, Newton AC. (2001) The carboxyl terminus of protein kinase C provides a switch to regulate its interaction with the phosphoinositide-dependent kinase, PRK-1. *J Biol Chem.* 276:19588–19596.

Gariano RF, Gardner TW. (2005) Retinal angiogenesis in development and disease. *Nature.* 438:960–966.

Giordano G, Sanchez-Perez AM, Burgal M, Montoliu C, Costa LG, Felipo V. (2005) Chronic exposure to ammonia induces isoform-selective alterations in the intracellular distribution and NMDA receptor-mediated translocation of protein kinase C in cerebellar neurons in culture. *J Neurochem.* 92:143-57.

Goldberg M, Steinberg S. (1996) Tissue-specific developmental regulation of protein kinase C isoforms. *Biochem Pharmacol*. 51:1089-1093.

Gong X, Cheng C, Xia, CH. (2007). Connexins in lens development and cataractogenesis. *J Membr Biol. 218*:9–12.

Gonzalez K, Udovichenko I, Cunnick J, Takemoto D. (1993) Protein kinase C in galactosemic and Tolrestat-treated lens epithelial cells. *Curr Eye Res*. 12:373-377.

Gould CM, Newton AC. (2008) The life and death of protein kinase C. *Curr Drug Targets*. 9:614-25.

Greferath U, Grunert U, Wassle H. (1990) Rod bipolar cells in the mammalian retina show protein kinase C-like immunoreactivity. *J Comp Neurol.* 301:433-442.

Grodsky N, Li Y, Bouzida D, Love R, Jensen J, Nodes B, Nonomiya J, Grant S. (2006) Structure of the catalytic domain of human protein kinase C beta II complexed with a bisindolylmaleimide inhibitor. *Biochemistry.* 45:13970–13981.

Hommel U, Zurini M, Luyten M. (1994) Solution structure of a cysteine rich domain of rat protein kinase C. *Nat Struct Biol.* 1:383-387.

House C, Kemp BE. (1987) Protein kinase C contains a pseudosubstrate prototope in its regulatory domain. *Science.* 238:1726-8.

Huang H, Li H, He S. (2005) Identification of connexin 50 and 57 mRNA in A-type horizontal cells of the rabbit retina. *Cell Res*. 15:207-211.

Hunt RJ. (2004) The Reproduction of Colour (6th ed.). Chichester UK: Wiley–IS&T Series in Imaging Science and Technology. 11–2.

Hurley JH, Misra S. (2000) Signaling and subcellular targeting by membrane-binding domains. *Annu Rev Biophys Biomol Struct.* 29:49-79.

Hurley JH, Newton AC, Parker PJ, Blumberg PM, Nishizuka Y. (1997) Taxonomy and function of C1 protein kinase C homology domains. *Protein Sci.* 6:477-80.

Ishii H, Koya D, King GL. (1998) Protein kinase C activation and its role in the development of vascular complications in diabetes mellitus. *J Mol Med*. 76:21–31.

Jacobs GH, Williams GA, Cahill H, Nathans J. (2007) Emergence of novel color vision in mice engineered to express a human cone photopigment. *Science*. 315:1723-5.

Janssen-Bienhold U, Dermietzel R, Weiler R. (1998) Distribution of connexin 43 immunoreactivity in the retinas of different vertebrates. *J Comp Neurol.* 396:310-321.

Johansson K, Bruun A, Ehinger B. (1999) Gap junction protein connexin 43 is heterogeneously expressed among glial cells in the adult rabbit retina. *J Comp Neurol.* 407:395-403.

Johnson JE, Giorgione J, Newton AC. (2000) The C1 and C2 domains of protein kinase C are independent membrane targeting modules, with specificity for phosphatidylserine conferred by the C1 domain. *Biochem.* 39:11360-11369.

Kalesnykas G, Tuulos T, Uusitalo H, Jolkkonen J. (2008) Neurodegeneration and cellular stress in the retina and optic nerve in rat cerebral ischemia and hypoperfusion models. *Neuroscience.* 155:937-47.

Kamphuis W, Dijk F, Bergen AA. (2007) Ischemic preconditioning alters the pattern of gene expression changes in response to full retinal ischemia. *Mol Vis.* 13:1892–1901

Kang DJ, Linsenmeier R. (2000) Effects of hypoxemia on the a- and b-waves of the electroretinogram in the cat retina. *Invest Ophthalmol Vis Sci*. 41:3634–3642.

Kargi SH, Altin R, Koksal M, Kart L, Cinar F, Ugurbas SH, Ayoglu F. (2005) Retinal nerve fibre layer measurements are reduced in patients with obstructive sleep apnoea syndrome. *Eye.* 19:575-9.

Katsura K, Kurihara J, Siesjo BK, Wieloch T. (1999) Acidosis enhances translocation of protein kinase C but not Ca^{+2}/calmodulin-dependent protein kinase II to cell membranes during complete cerebral ischemia. *Brain Res.* 849:119-127.

Kaur C, Sivakumar V, Foulds WS, Luu CD, Ling EA. (2009) Cellular and vascular changes in the retina of neonatal rats after an acute exposure to hypoxia. *Invest Ophthalmol Vis Sci.* 50:5364-74.

Kistler J, Evans C, Donaldson P, Bullivant S, Bond J, Eastwood S, Roos M, Dong Y, Gruijters T, Engel A. (1995) Ocular lens gap junctions: protein expression, assembly, and structure-function analysis. *Microsc Res Tech.* 31:347-56.

Klemp K, Lund-Andersen H, Sander B. (2007). The effect of acute hypoxia and hyperoxia on the slow flash multifocal lectroretinogram in healthy subjects. *Invest Ophthalmol Vis Sci*. 48: 3405–3412.

Knighton DR, Zheng J, Ten Eyck LF, Ashford VA, Xuong NH, Taylor SS, Sowadski JM. (1991) Crystal structure of the catalytic subunit of cyclic adenosine monophosphate-dependent protein kinase. *Science*. 253:407–414.

Kojima, I, Kitaoka, M, Ogata, E. (1990) Insulin-like growth factor-I stimulates diacylglycerol production via multiple pathways in Balb/c 3T3 cells. *J Biol Chem* 265:16846-16850.

Kolb H. (1991) The neural organization of the human retina. In "Principles and Practices of Clinical Electrophysiology of Vision" (Eds. Heckenlively, J.R. and Arden, G.B.) *Mosby Year Book Inc.* 25-52.

Kolb H. (1977) The organization of the outer plexiform layer in the retina of the cat: electron microscopic observations. *J Neurocytol.* 6:131-153.

Kolb H, Jones J. (1984) Synaptic organization of the outer plexiform layer of the turtle retina: an electron microscope study of serial sections. *J Neurocytol.* 13:567-591.

Kolb H, Linberg KA, Fisher SK. (1992) The neurons of the human retina: a Golgi study. *J Comp Neurol.* 318:147-187.

Kolb H, Nelson R. (1993) Off-alpha and off-beta ganglion cells in the cat retina. II. Neural circuitry as revealed by electron microscopy of HRP stains. *J Comp Neurol* 329:85-110.

Kolb H. (2003) How the Retina Works. Much of the construction of an image takes place in the retina itself through the use of specialized neural circuits. *American Scientist.* 91:28-35.

Lamark T, Perander M, Outzen H, Kristiansen K, Overvatn A, Michaelsen E, Bjorkoy G, Johansen T. (2003) Interaction codes within the family of mammalian Phox and Bem1p domain-containing proteins. *J Biol Chem.* 278:34568–34581.

Lampe PD, Lau AF. (2004) The effects of connexin phosphorylation on gap junctional communication. *Int J Biochem Cell Biol.* 36:1171–1186.

Le AC, Musil LS. (1998) Normal differentiation of cultured lens cells after inhibition of gap junction-mediated intercellular communication. *Dev Biol*. 204:80-96.

Le Good JA, Ziegler WH, Parekh DB, Alessi DR, Cohen P, Parker PJ. (1998) Protein kinase C isotypes controlled by phosphoinositide 3-kinase through the protein kinase PDK1. *Science.* 281:2042–2045.

Leung CK, Cheung CY, Weinreb RN, Qiu Q, Liu S, Li H, Xu G, Fan N, Huang L, Pang CP, Lam DS. (2009) Retinal nerve fiber layer imaging with spectral-domain optical coherence tomography: a variability and diagnostic performance study. *Ophthalmology.* 116:1257-63.

Leslie NR, Biondi RM, Alessi DR. (2001) Phosphoinositide-regulated kinases and phosphoinositide phosphatases. *Chem Rev.* 101:2365–2380.

Li GY, Lin HH, Tu ZJ, Kiang DT. (1998) Gap junction Cx26 gene modulation by phorbol esters in benign and malignant human mammary cells. *Gene*. 209:139-47.

Lin D, Boyle DL, Takemoto DJ. (2003) IGF-I-induced phosphorylation of connexin 43 by PKCgamma: regulation of gap junctions in rabbit lens epithelial cells. *Invest Ophthalmol. Vis. Sci.* 44:1160-1168.

Lin D, Lobell S, Jewell A, Takemoto DJ. (2004) Differential phosphorylation of connexin 46 and connexin 50 by H_2O_2 activation of protein kinase Cγ. *Mol Vis.* 10:688-695.

Lin D, Shanks D, Prakash O, Takemoto DJ. (2007) Protein kinase C gamma mutations in the C1B domain cause caspase-3-linked apoptosis in lens epithelial cells through gap junctions. *Exp Eye Res.* 85:113–122.

Lin D, Takemoto DJ. (2005) Oxidative activation of protein kinase Cγ through the C1 domain. *J Biol Chem*. 80:13682-13693.

Lin D, Takemoto DJ. (2007) Protection from ataxia-linked apoptosis by gap junction inhibitors. *Biochem Biophys Res Commun.* 362:982-987.

Makowske M, Rosen OM. (1989)Complete activation of protein kinase C by an antipeptide antibody directed against the pseudosubstrate prototope. *J Biol Chem.* 25:16155-9.

Massey S, O'Brien J, Trexler E. (2003) Multiple neuronal connexins in the mammalian retina. *Cell Comun. Adhes*. 10:425-430.

Mellor H, Parker PJ. (1998) Theextended protein kinase C superfamily. *Biochem. J.* 332:281–292.

Meier C, Dermietzel R. (2006) Electrical synapses—gap junctions in the brain. Results. *Probl Cell Differ.* 43:99 –128.

Meşe G, Richard G, White TW. (2007) Gap junctions: basic structure and function. *J Invest Dermatol.* 127:2516-24.

Mochly-Rosen D, Gordon AS. (1998) Anchoring proteins for protein kinase C: a means for isozyme selectivity. *FASEB J.* 12:35–42.

Morley GE, Taffet SM, Delmar M. (1996) Intramolecular interactions mediate pH regulation of connexin43 channels. *Biophys J.* 70:1294–1302.

Munoz B, West SK. (2002) Blindness and visual impairment in the Americas and the Caribbean. *Br J Ophthalmol.* 86:498–504.

Nalefski EA, Falke JJ. (1996) The C2 domain calcium-binding motif: structural and functional diversity. *Prot Sci.* 5:2375–2390.

Narayanan R, Kenney MC, Kamjoo S, Thuan-Hau T, Trinh GM, Seigel GP (2005). Trypan Blue: Effect on Retinal Pigment Epithelial and Neurosensory Retinal Cells. *Investigative Ophthalmology and Visual Science.* 46:304-309.

Narita M, Mizoguchi H, Suzuki T. (2001) Enhanced mu-opioid responses in the spinal cord of mice lacking protein kinase Cgamma isoform. *J Biol Chem*. 276:15409-15414.

Naus C, Ozog M, Bechberger J, Nakase T. (2001) A neuroprotective role for gap junctions. *Cell Commun Adhes.* 8:325-328.

Negishi K, Kato S, Teranishi T. (1988) Dopamine cells and rod bipolar cells contain protein kinase C-like immunoreactivity in some vertebrate retinas. *Nerosci Lett*. 94:247-252.

Negishi K, Sugawara K. (1973) Evidence for the anoxia sensitivity of the synaptic region at the outer plexiform layer in the fish retina. *Vision Res.* 13:983-987.

Neri LM, Borgatti P, Capitani S, Martelli AM. (1998) Nuclear diacylglycerol produced by phosphoinositide-specific phospholipase C is responsible for nuclear translocation of protein kinase C-gamma. *J Biol Chem.*273:29738-44.

Newton AC, Johnson JE. (1998) Protein kinase C: a paradigm for regulation of protein function by two membrane-targeting modules. *Biochem Biophys Acta.* 1376:155-72.

Newton AC. (2001) Protein Kinase C: Structural and spatial regulation by phosphorylation, cofactors, and macromolecular interactions. *Chem Rev* 101:2353-2364.

Newton A. (1995) Protein Kinase C: Structure, Function, and Regulation. *J Biol Chem.* 270:28495-28498.

Newton AC. (2010) Protein kinase C: poised to signal Am. *J Physiol Endocrinol Metab.* 298:395-402.

Newton AC. (2003) Regulation of the ABC kinases by phosphorylation: protein kinase C as a paradigm. *Biochem J.* 370:361–371.

Nighoghossian N, Trouillas P. (1997) Hyperbaric oxygen in the treatment of acute ischaemic stroke: an unsettled issue. *J Neurol Sci*. 150:27-31.

Nishizuka, Y. (1995) Protein kinase C and lipid signaling for sustained cellular responses. *FASEB J*. 9:484–496.

Nishizuka Y. (1986) Studies and perspectives of protein kinase C. *Science*. 233:305-12.

Oancea E, Meyer T. (1998) Protein kinase C as a molecular machine for decoding calcium and diacylglycerol signals. *Cell.* 95:307–318.

O'Brien JJ, Li W, Pan F, Keung J, O'Brien J, Massey SC. (2006) Coupling between Atype horizontal cells is mediated by connexin 50 gap junctions in the rabbit retina. *J Neurosci*. 26:11624-11636.

Ohsawa M, Narita M, Mizoguchi H, Cheng E, Tseng LF. (2001) Reduced hyperalgesia induced by nerve injury, but not by inflammation in mice lacking protein kinase C gamma isoform. *Eur J Pharmacol*. 429:157-160.

Orr JW, Keranen LM, Newton AC. (1992) Reversible exposure of the pseudosubstrate domain of protein kinase C by phosphatidylserine and diacylglycerol. *J Biol Chem*. 267:15263-6.

Orr JW, Newton AC. (1994) Intrapeptide regulation of protein kinase C. *J Biol Chem.* 269: 8383–8387.

Osborne NN, Barnet NL, Morris NJ. (1992) The occurance of three isoenzymes of protein kinase C (α,β,γ) in retinas of different species. *Brain Research*. 570:161-166.

Owsley C, Jackson GR, Cideciyan AV. (2000) Psychophysical evidence for rod vulnerability in age-related macular degeneration. *Invest Opthalmol Vis Sci*. 41:267-273.

Padgaonkar VA, Leverenz VR, Dang L, Chen S, Pellicciccia S, Giblin FJ. (2004) Thioredoxin reductase may be essential for the normal growth of hyperbaric oxygen-treated human lens epithelial cells. *Exp Eye Res*. 79:847-857.

Pahujaa M, Anikin M, Goldberg GS. (2007) Phosphorylation of connexin43 induced by Src: regulation of gap junctional communication between transformed cells. *Exp Cell Res*. 313:4083-90.

Perez Velazquez JL, Frantseva MV, Naus CC. (2003) Gap junctions and neuronal injury: Protectants or executioners? *Neuroscientist.* 9:5-9.

Ponting CP. Parker PJ. (1996) Extending the C2 domain family: C2s in PKCs d, e, h, q, phospholipases, GAPs and perforin. *Protein Sci*. 5:162–166.

Ramakers GM, Gerendasy DD, de Graan PN. (1999) Substrate phosphorylation in the protein kinase Cgamma knockout mouse. *J Biol Chem*. 274:1873-1874.

Ramkumar HL, Zhang J, Chan CC. (2010) Retinal ultrastructure of murine models of dry age-related macular degeneration (AMD). *Prog Retin Eye Res*. 29:169-90.

Rutkowski R, Kosztyła-Hojna B, Kańczuga-Koda L, Sulkowska M, Sulkowski S, Rutkowski K. (2008) Structure and physiological function of connexin proteins. *Postepy Hig Med Dosw*. 62:632-41.

Reichenbach A, Faude F, Enzmann V. (1997) The Müller (glial) cell in normal and diseased retina: a case for single-cell electrophysiology. *Ophthalmic Res.* 29:326–40.

Rhodin AG. (1971) *HISTOLOGY*: A Text and Atlas. *Oxford University Press*. 764-777.

Riddle RC, Khatri R, Schipani E, Clemens TL. (2009) Role of hypoxia-inducible factor-1alpha in angiogenic-osteogenic coupling. *J Mol Med.* 87:583-90.

Ripps H. (2002) Cell death in retinitis pigmentosa: Gap junctions and the "Bystander" effect. *Exp Eye Res.* 74:327-336.

Rivedal E, Opsahl H. (2001) Role of PKC and MAP kinase in EGF-and TPA-induced onnexin43 phosphorylation and inhibition of gap junction intercellular communication in rat liver epithelial cells. *Carcinogenesis*. 22:1543–1550.

Saez JC, Nairn AC, Czernik AJ, Fishman GI, Spray DC, Hertzberg EL. (1997) Phosphorylation of connexin 43 and the regulation of ne-natal rat cardiac myocytes gap junctions. *J Mol Cell Cardiol.* 29:2131-45.

Salameh A. (2006) Life Cycle of Connexins:Regulation of Connexin Synthesis and Degradation. *Adv Cardiol*. 42:57-70.

Saleh S, Takemoto D. (2000) Overexpression of protein kinase Cγ inhibits gap junction intercellular communication in the lens epithelial cells. *Exp Eye Res*. 71:99-102.

Sánchez-Bautista S, Corbalán-García S, Pérez-Lara A, Gómez-Fernández JC. (2009) A comparison of the membrane binding properties of C1B domains of PKCgamma, PKCdelta, and PKCepsilon. *Biophys J.* 96:3638-47.

Schütte M, Chen S, Buku A, Wolosin J. (1998) Connexin 50, a gap junction protein of macroglia in the mammalian retina and visual pathway. *Exp Eye Res*. 66:605-613.

Seigel GM. (1996) Establishment of an E1A-immortalized retinal cell culture. *In Vitro Cell Dev Biol Anim.* 32:66-68.

Seigel GM, Mutchler AL, Imperato EL. (1996) Expression of glial markers in a retinal precursor cell line. *Molecular Vision*. 2:2.

Seigel GM, Sun W, Wang J, Hershberger DH, Campbell LM, Salvi RJ. (2004) Neuronal gene expression and function in the growth-stimulated R28 retinal precursor cell line. *Current Eye Reasearch.* 28:257-269.

Seigel GM, Takahashi M, Adamus G, McDaniel T. (1998) Intraocular transplantation of E1A-immortalized retinal precursor cells. *Cell Transplantation.* 7:559-566.

Seki T, Adachi N, Ono Y, Mochizuki H, Hiramoto K, Amano T, Matsubayashi H, Matsumoto M, Kawakami H, Saito N, Sakai N. (2005) Mutant protein kinase Cgamma found in

spinocerebellar ataxia type 14 is susceptible to aggregation and causes cell death. *J Biol Chem.* 280:29096–106.

Shah CA. (2008) Diabetic retinopathy: A comprehensive review. *Indian J Med Sci.* 62:500-19.

Sharon D, Blackshaw S, Cepko CL, Dryja TP. (2002) Profile of the genes expressed in the human peripheral retina, macula, and retinal pigment epithelium determined through serial analysis of gene expression (SAGE). *Proc Natl Acad Sci U S A.* 99:315-320.

Shakespeare TI, Sellitto C, Li L, Rubinos C, Gong X, Srinivas M, White TW. (2009). Interaction between Connexin50 and mitogen-activated protein kinase signaling in lens homeostasis. *Mol Biol Cell.* 20:2582-92.

Shi Q, Banks EA, Yu XS, Gu S, Lauer J, Fields GB, Jiang JX. (2010) Amino acid residue Val362 plays a critical role in maintaining the structure of C terminus of connexin 50 and in lens epithelial-fiber differentiation. *J Biol Chem.*285:18415-22.

Shoji S, Titani K, Demaille JG, Fischer EH. (1979) Sequence of two phosphorylated sites in the catalytic subunit of bovine cardiac muscle adenosine 3´:5´-monophosphate-dependent protein kinase. *J Biol Chem.* 254:6211–6214.

Sinkovic A, Smolle-Juettner FM, Krunic B, Marinsekz M. (2006) Severe carbon monoxide poisoning treated by hyperbaric oxygen therapy--a case report. *Inhal Toxicol*. 18:211-214.

Snell R, Lemp M. (1998) Clinical Anatomy of the Eye. *Blackwell Science*. 132-214.

Solan JL, Lampe PD. (2005) Connexin phosphorylation as a regulatory event linked to gap junction channel assembly. *Biochim Biophys Acta.* 1711:154–163.

Sonnenburg ED, Gao T, Newton AC. (2001) The phosphoinositide dependent kinase, PDK-1, phosphorylates conventional protein kinase C isozymes by a mechanism that is independent of phosphoinositide-3-kinase. *J Biol Chem.* 276:45289–45297.

Söhl G, Güldenagel M, Traub O, Willecke K. (2000) Connexin expression in the retina. *Brain Res Brain Res Rev.* 32:138-145.

Söhl G, Willecke K. (2004) Gap junctions and the connexin protein family. *Cardiovasc Res.* 62:228-32.

Soong BW, Paulson HL. (2007) Spinocerebellar ataxias: an update. *Curr Opin Neurol.* 20:438–446.

Spitaler M, Cantrell DA. (2004) Protein kinase C and beyond. *Nat Immunol.* 5:785-90.

Srinivas M, Kronengold J, Bukauskas FF, Bargiello TA, Verselis VK. (2005) Correlative studies of gating in Cx46 and Cx50 hemichannels and gap junction channels. *Biophys J.* 88:1725-1739.

Stahl A, Connor KM, Sapieha P, Chen J, Dennison RJ, Krah NM, Seaward MR, Willett KL, Aderman CM, Guerin KI, Hua J, Löfqvist C, Hellström A, Smith LE. (2010) The mouse retina as an angiogenesis model. *Invest Ophthalmol Vis Sci.* 51:2813-26.

Steinberg SF. Structural basis of protein kinase C isoform function. (2008) *Physiol Rev.* 88:1341-78.

Strettoi E, Raviola E, Dacheux RF. Synaptic connections of the narrow-field, bistratified rod amacrine cell (AII) in the rabbit retina. (1992) *J Comp Neurol*. 325:152-68.

Taylor SS, Radzio-Andzelm E. (1994) Three protein kinase structures define a common motif. *Structure.* 2:345–355.

Toker A, Newton A. (2000) Cellular signalling: pivoting around PDK-1. *Cell.* 103:185–188.

Vlak MH, Sinke RJ, Rabelink GM, Kremer BP, van de Warrenburg BP. (2006) Novel PRKCG/SCA14 mutation in a Dutch spinocerebellar ataxia family: expanding the phenotype. *Mov Disord.* 21:1025-1028.

Wagner L, Saleh SM, Boyle DL, Takemoto DJ. (2002) Effect of protein kinase C_ on gap junction disassembly in lens epithelial cells and retinal cells in culture. *Mol Vis.* 8:59–66.

Wagner L, Saleh S, Boyle D, Takemoto D. (2002) Effect of protein kinase Cγ on gap junction disassembly in lens epithelial cells and retinal cells in culture. *Mol Vis.* 8:59-66.

Walia S, Fishman GA, Edward DP, Lindeman M. (2007) Retinal nerve fiber layer defects in RP patients. *Invest Ophthalmol Vis Sci.* 48:4748-52.

Wang D, De la Fuente C, Deng L, Wang L, Zilberman I, Eadie C, Healey M, Stein D, Denny T, Harrison L, Meijer L, Kashanchi F. (2001) Inhibition of Human Immunodeficiency Virus Type 1 Transcription by Chemical Cyclin-Dependent Kinase Inhibitors. *Journal of Virology*. 75:7266-7279.

Wang Z, Schey KL. (2009) Phosphorylation and truncation sites of bovine lens connexin 46 and connexin 50. *Exp Eye Res.* 89:898-904.

Warn-Cramer, B, Lampe, P, Kurata, W. (1996) Characterization of the mitogen-activated protein kinase phosphorylation sites on the connexin 43 gap junction protein. *J Biol Chem.* 271:3779-3786.

Wolosin M, Schutte M, Chen S. (1997) Connexin Distribution in the Rabbit and Rat Ciliary Body A Case for Heterotypic epithelial Gap Junctions. *Invest Ophthalmol Vis Sci.* 38:341-348.

Wood JP, McCord RJ, Osborne NN. (1997) Retinal protein kinase C. *Neurochem Int.* 30:119-36.

Xia CH, Liu H, Cheung D, Cheng C, Wang E, Du X, Beutler B, Lo WK, Gong X. (2006) Diverse gap junctions modulate distinct mechanisms for fiber cell formation during lens development and cataractogenesis. *Development.* 133:2033–2040.

Xu RX, Pawelczyk T, Xia TH, Brown SC. (1997) NMR structure of a protein kinase C-gamma phorbol-binding domain and study of protein-lipid micelle interactions. *Biochemistry*. 36:10709-17.

Yevseyenkov VV, Das S, Lin D, Willard L, Davidson H, Sitaramayya A, Giblin FJ, Dang L, Takemoto DJ. (2009) Loss of protein kinase Cgamma in knockout mice and increased retinal sensitivity to hyperbaric oxygen. *Arch Ophthalmol.* 127:500-6.

Yu DY, Cringle SJ. (2002) Outer retinal anoxia during dark adaptation is not a general property of mammalian retinas. *Comp Biochem Physiol A Mol Integr Physiol*. 132:47-52.

Yu DY, Cringle SJ, Yu PK, Su EN. (2007) Intraretinal oxygen distribution and consumption during retinal artery occlusion and graded hyperoxic ventilation in the rat. *Invest Ophthalmol Vis Sci.* 48:2290-6.

Zahs KR, Ceelen PW. (2006) Gap junctional coupling and connexin immunoreactivity in rabbit retinal glia. *Vis Neurosci.* 23:1-10.

Zampighi GA. (2003) Distribution of connexin 50 channels and hemichannels in lens fibers: a structural approach. *Cell Commun Adhes*. 10:265-270.

Zampighi GA, Loo DD, Kreman M, Eskandari S, Wright EM. (1999) Functional and morphological correlates of connexin50 expressed in *Xenopus laevis* oocytes. *J Gen Physiol.* 113:507–524.

Zarbin MA. (2004) Current concepts in pathogenises of age-related macular degeneration. *Arch Opthalmol*. 122:598-614.

Zhang G, Kazanietz MG, Blumberg PM, Hurley JH. (1995) Crystal structure of the cys2 activator-binding domain of protein kinase C delta in complex with phorbol ester. *Cell* 81:917-924.

Zhang Q, Wang D, Kundumani-Sridharan V, Gadiparthi L, Johnson DA, Tigyi GJ, Rao GN. (2010). PLD1-dependent PKC{gamma} activation downstream to Src is essential for the development of pathological retinal neovascularization. *Blood.* 116:1377-1385.

Zhang Y, Snider A, Willard L, Takemoto DJ, Lin D. (2009) Loss of Purkinje cells in the PKCgamma H101Y transgenic mouse. *Biochem Biophys Res Commun.* 378:524-8.

Zhou J, Fariss RN, Zelenka P S. (2003) Regulation of c-fos Induction in Lens Epithelial Cells by 12(S)HETE-Dependent Activation of PKC. *J Biol Chem.* 278:5388-598.

Appendix A - Phosphorylation of Cx50

Appendix Figure 1 shows bands at 75 kD mark, it is the EGPF-Cx50 construct band (50kD for Cx50 and 25 kD for GFP). This shows that Cx50 was already slightly phosphorylated even in untreated samples. However samples that were treated with TPA showed an increase of phosphorylation levels in four fold compared to the untreated EGFP-Cx50 cells. Hydrogen peroxide did not have any effect on the phosphorylation levels of Cx50, this could be due to the fact that TPA is a constant activator and hydrogen peroxide activates PKC gamma transiently. It is important to note that this experiment only worked once, as co-immunoprecipitation with GFP antibody is very unpredictable, I was not able to duplicate this experiment, thus the validity of this data is questionable and if desired by committee, this data can be completely removed. Co-immunoprecipitation with PKCγ antibody is not possible as manufacture had an infected line and stopped making it.

Finally, these figures shows that TPA caused increased immunoreactions of phospho-serine in immunoprecipitated Cx50, even though this result could not be duplicated it is probable to say based on general understanding of how gap junctions work, PKC gamma possibly caused gap junction disassembly through phosphorylation either direct or indirect.

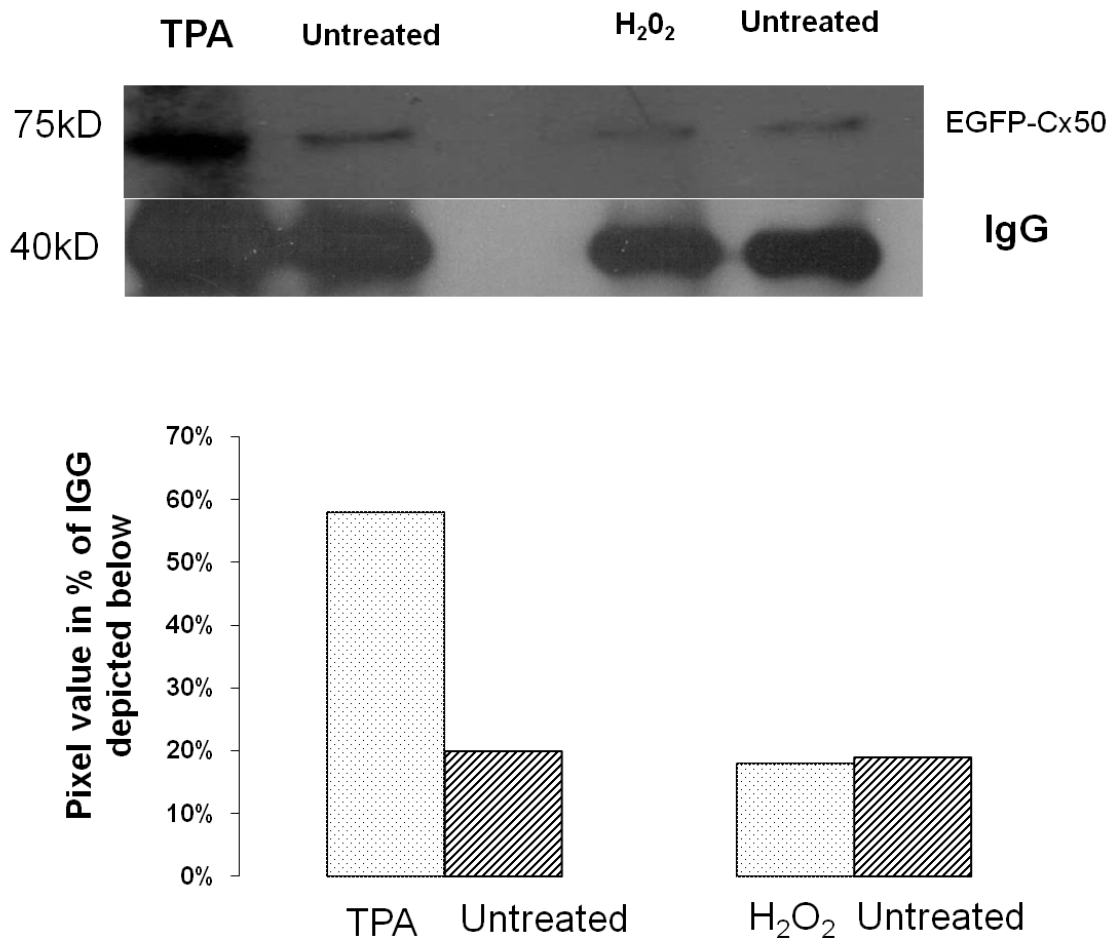

6-1 Phosphorylation of Cx50 by TPA

Cx50-EGFP stable line construct cells were activated with 200 nM TPA or 100µM hydrogen peroxide then were immunoprecipitated and immunoblotted with anti-phosphoserine ab. The intensity of phosphorylated bands was digitalized and graphed. Phosphorylation of Cx50 bands was normalized to IGG band which was used to check sample for loading control. Untreated control band is the EGFP-Cx50 stable line construct that was not treated with TPA or Hydrogen peroxide.